RSC Sustainability

Supporting Information (SI)

Synthesis, Biocompatibility and Antibacterial Properties of Glucose-based Ionic Liquids

Stefan Jopp,[*,#,a] Tabea Fleischhammer,[b] Antonina Lavrentieva,[b] Selin Kara[b] and Johanna Meyer[*,#,b]

[a] Institute of Chemistry, University of Rostock, Albert-Einstein-Str. 3a, 18059, Rostock, Germany.

[b] Institute of Technical Chemistry, Leibniz University Hannover, Callinstraße 5, 30167 Hannover, Germany.

[#] Authors contributed equally.

E-mails: stefan.jopp@uni-rostock.de
johanna.meyer@iftc.uni-hannover.de

Table of Contents

1. NMR Spectra

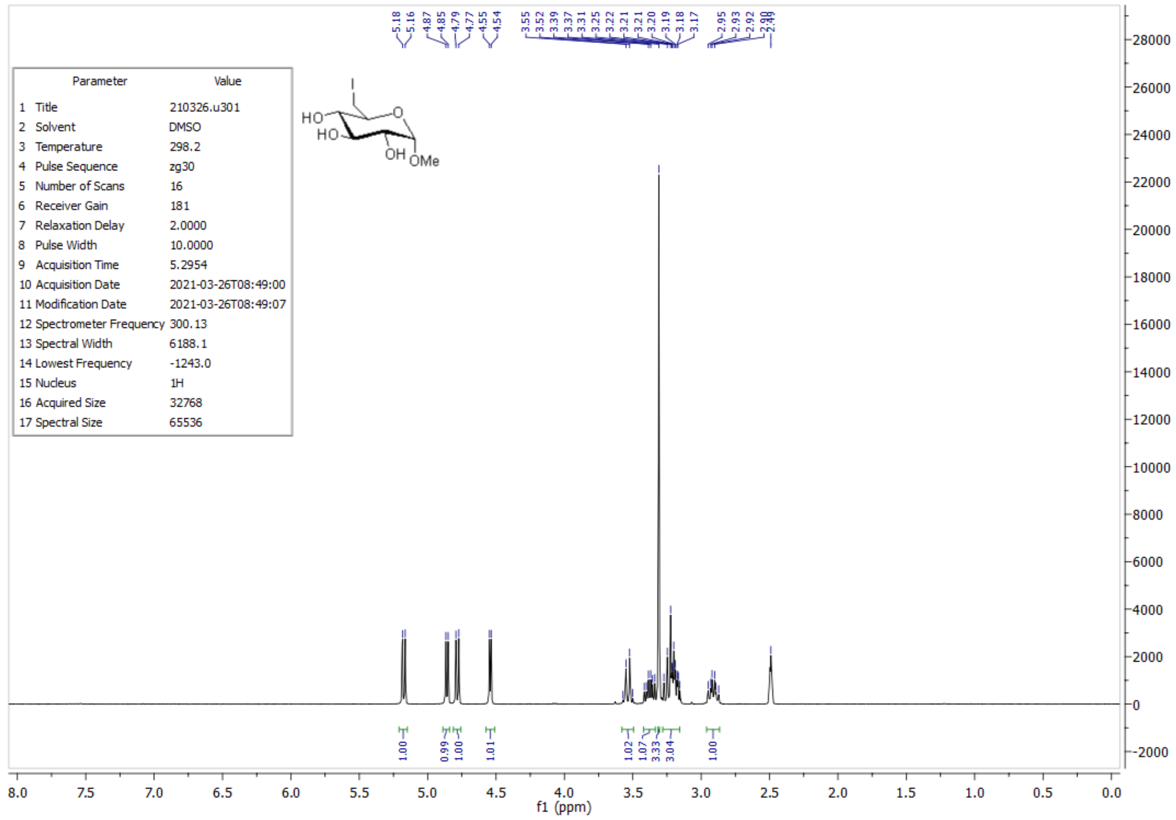

Figure S1. ^{1}H-NMR (DMSO) spectrum of compound Methyl-6-iodo-α-D-glucopyranoside **2a**.

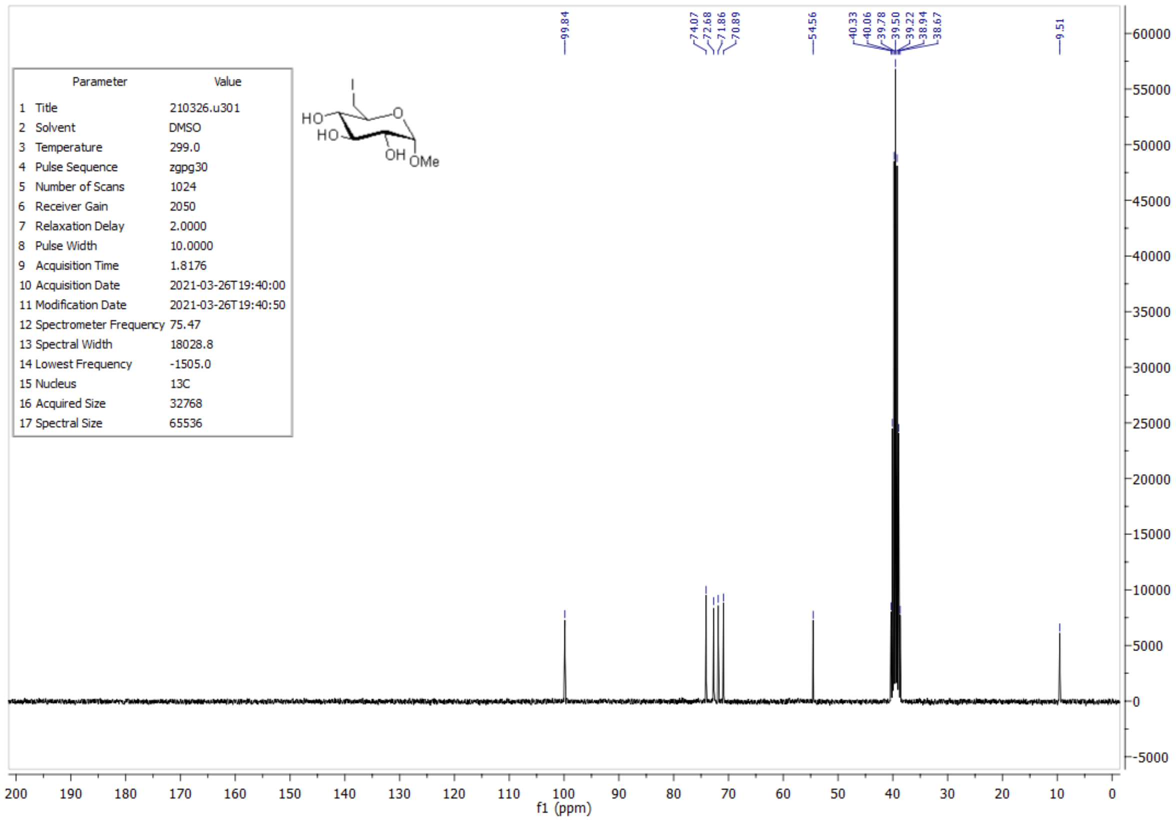

Figure S2. ^{13}C-NMR (DMSO) spectrum of compound Methyl-6-iodo-α-D-glucopyranoside **2a**.

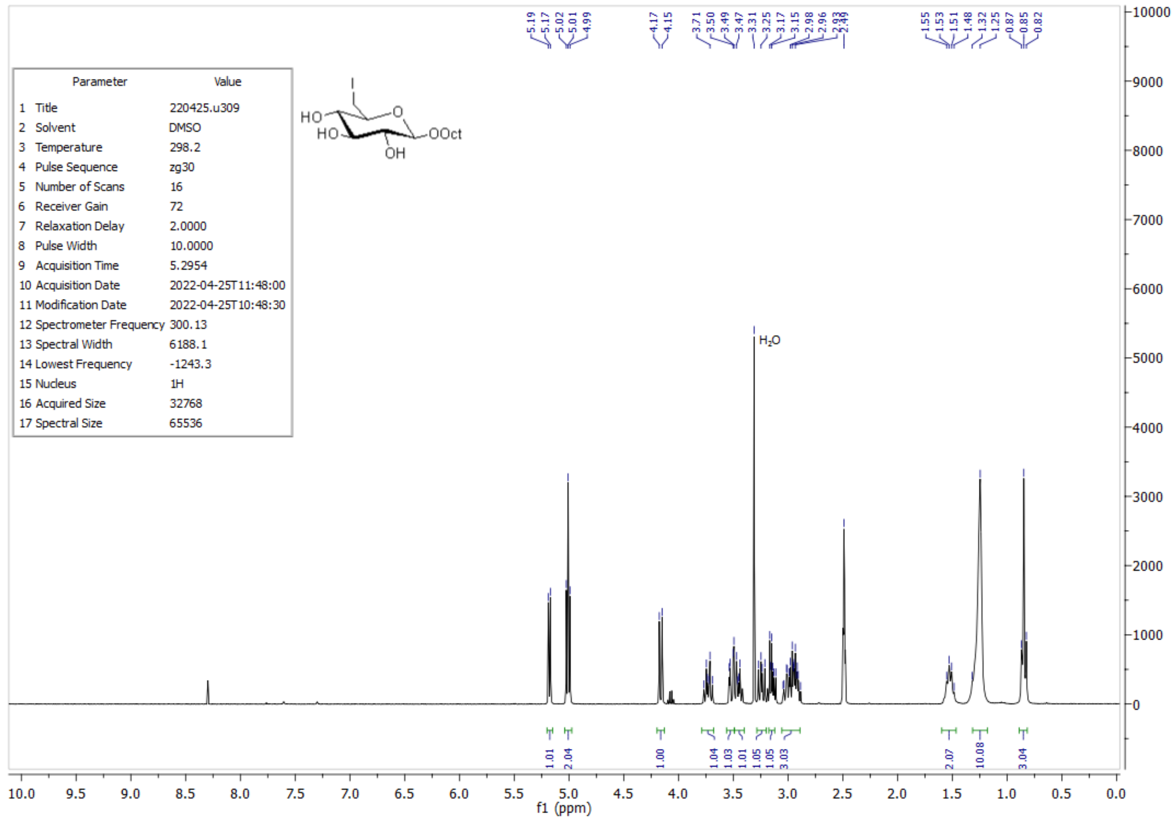

Figure S3. ^{1}H-NMR (DMSO) spectrum of compound *n*-Octyl-6-iodo-ß-D-glucopyranoside **2b**.

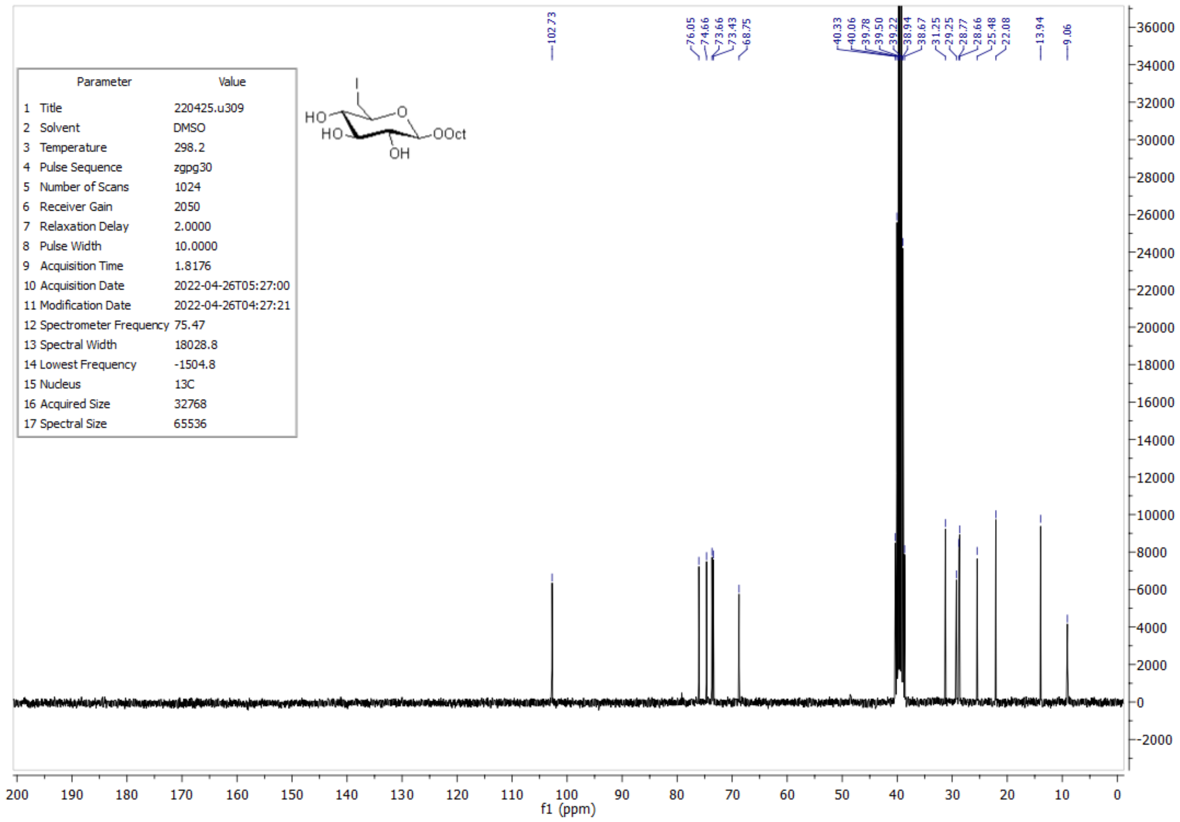

Figure S4. ^{13}C-NMR (DMSO) spectrum of compound *n*-Octyl-6-iodo-ß-D-glucopyranoside **2b**.

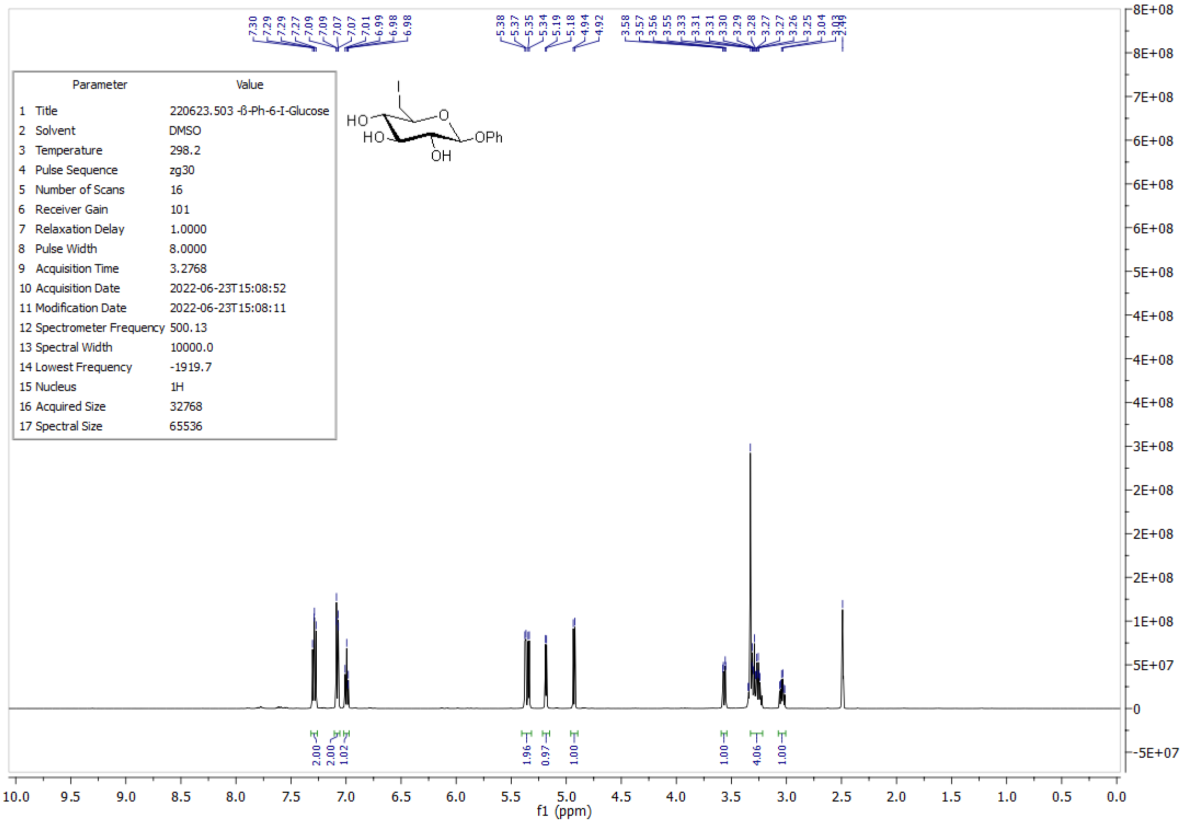

Figure S5. ^{1}H-NMR (DMSO) spectrum of compound Phenyl-6-iodo-ß-D-glucopyranoside **2c**.

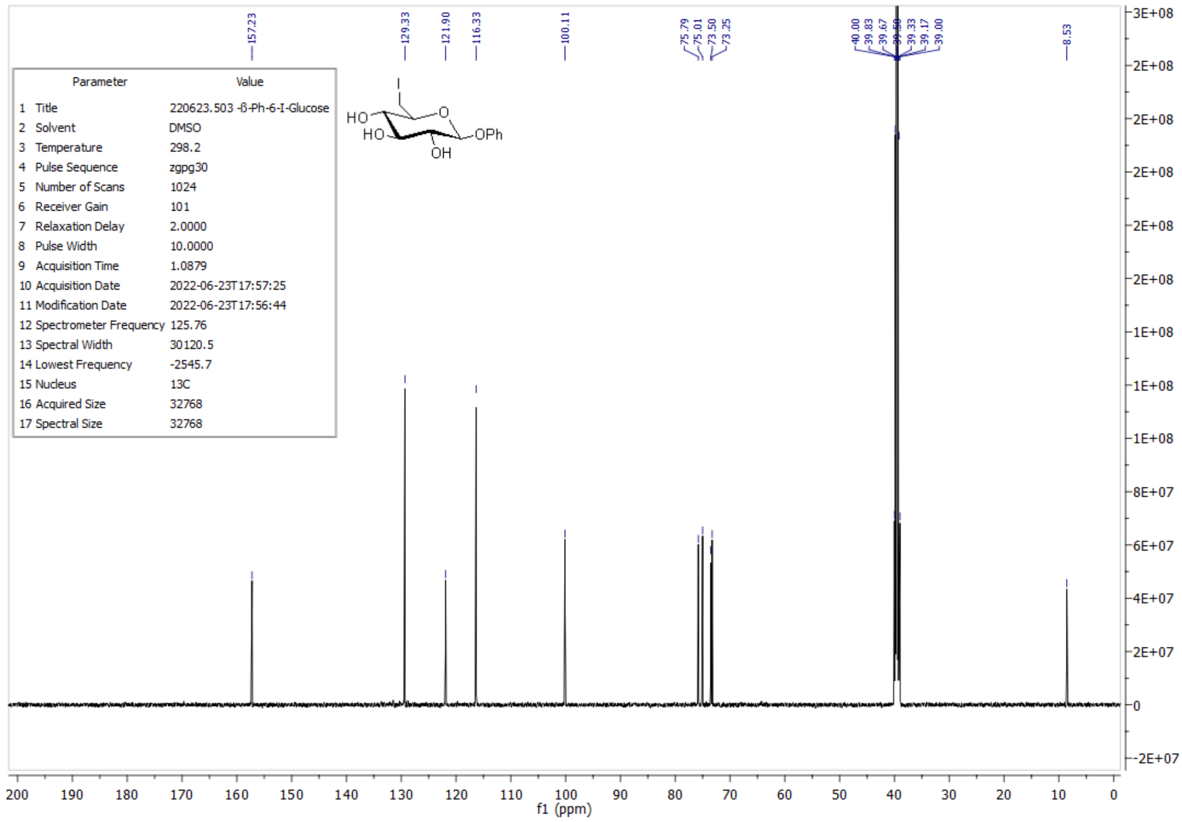

Figure S6. ^{13}C-NMR (DMSO) spectrum of compound Phenyl-6-iodo-ß-D-glucopyranoside **2c**.

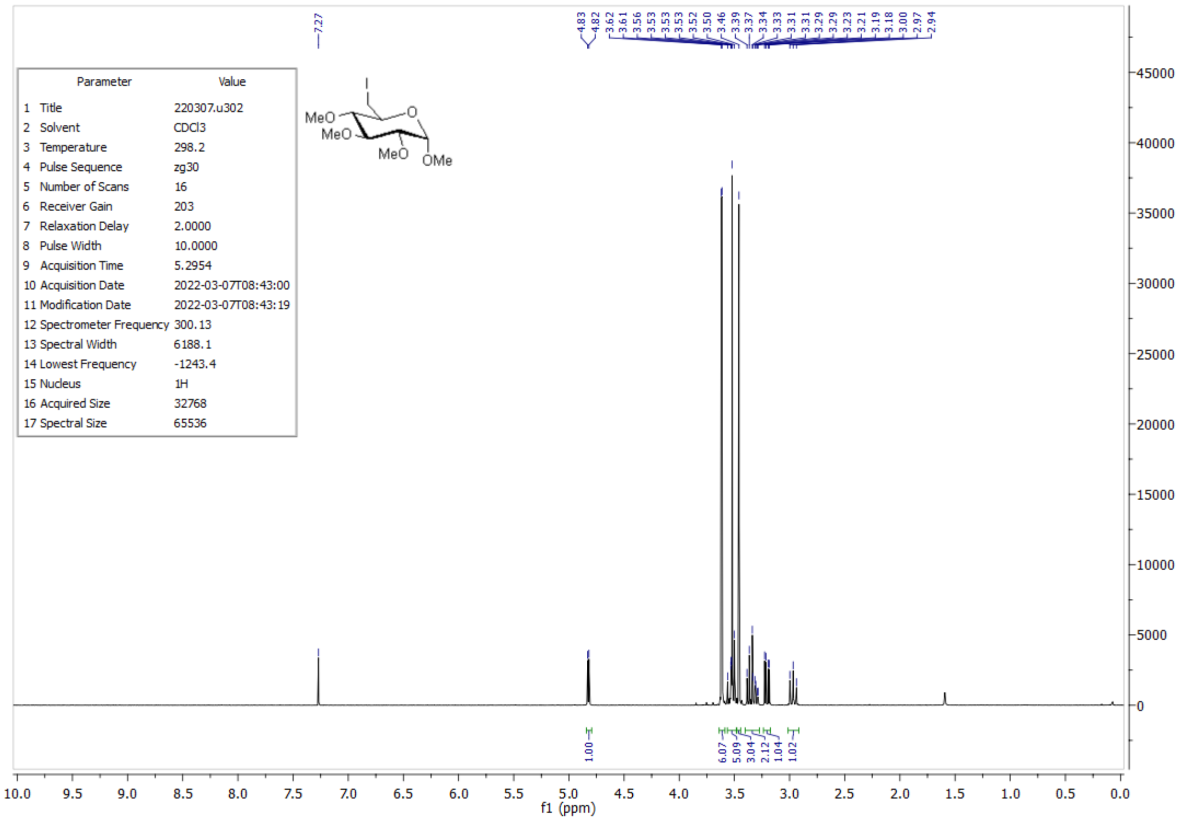

Figure S7. [1]H-NMR ($CDCl_3$) spectrum of compound Methyl-6-iodo-2,3,4-*O*-methyl-α-D-glucopyranoside **2d**.

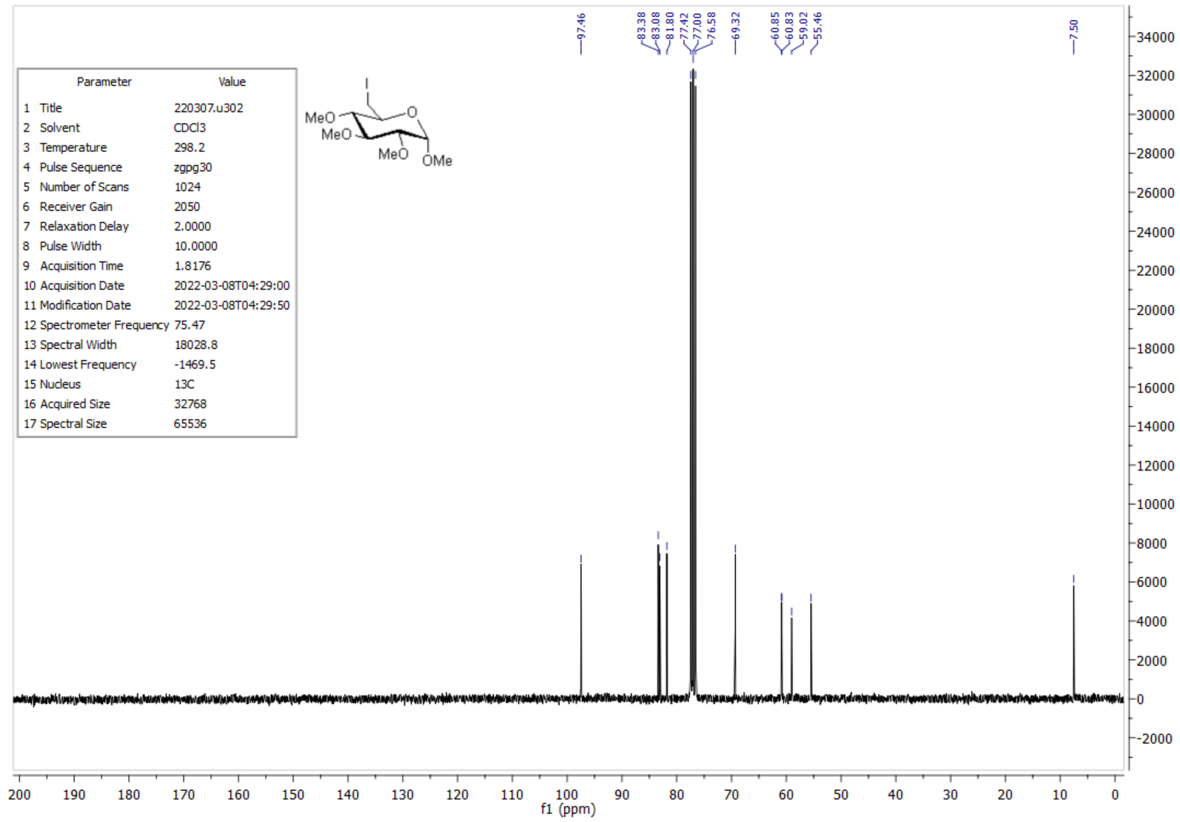

Figure S8. [13]C-NMR ($CDCl_3$) spectrum of compound Methyl-6-iodo-2,3,4-*O*-methyl-α-D-glucopyranoside **2d**.

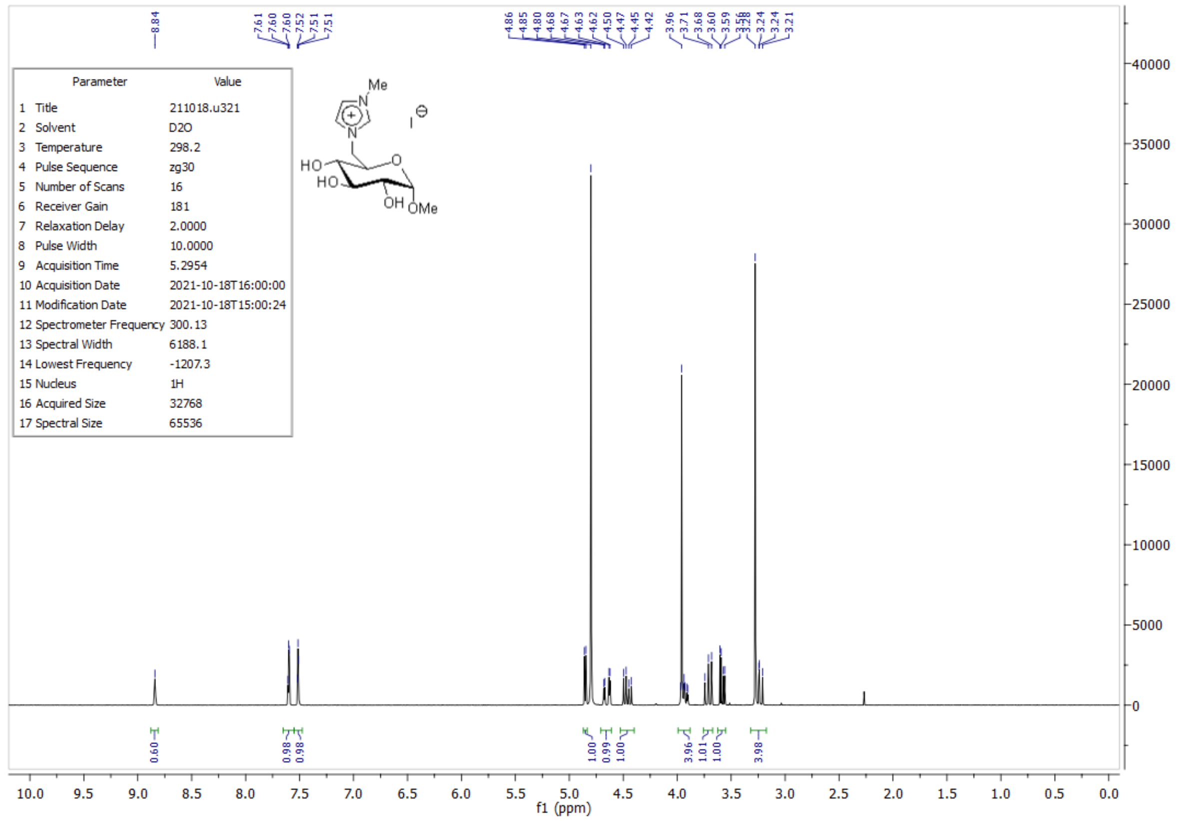

Figure S9. [1]H-NMR (D_2O) spectrum of compound 1-(Methyl-α-D-glucopyranosid-6-yl)-3-methylimidazolium iodide (GMIM-I) **3a.**

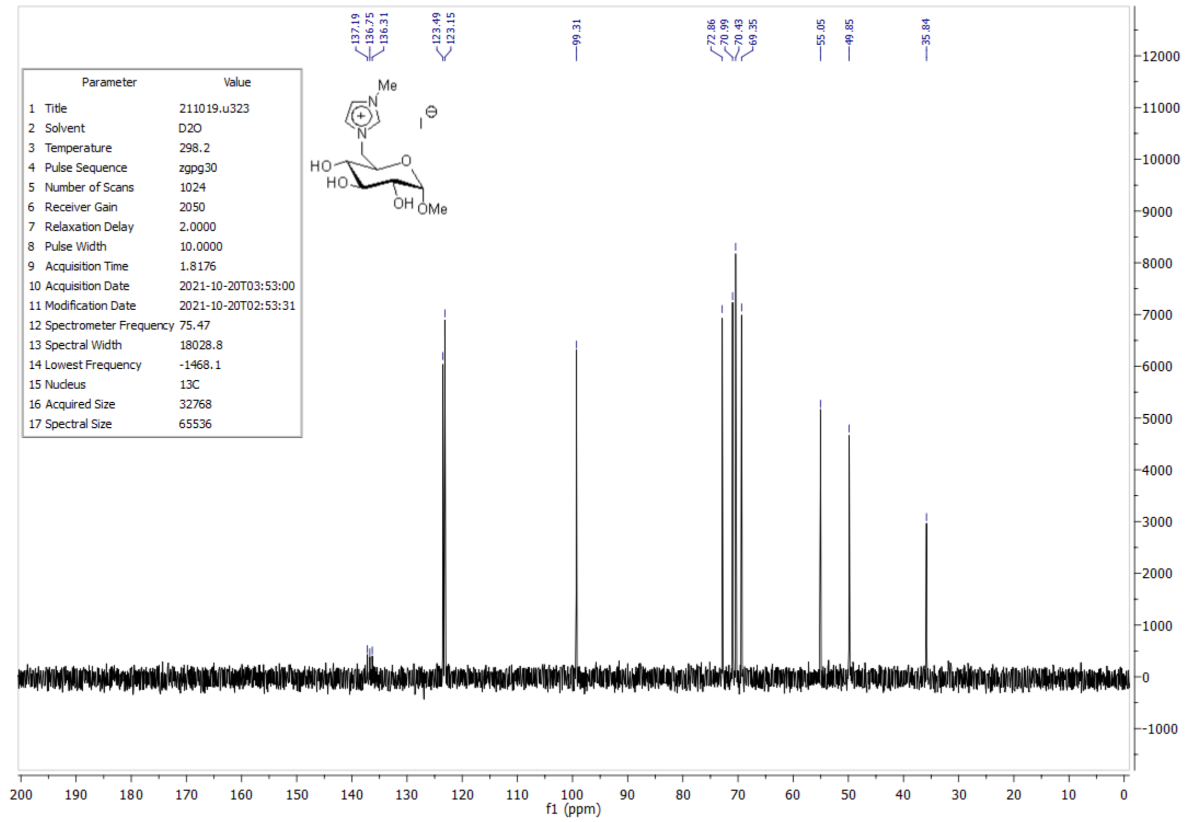

Figure S10. [13]C-NMR (D_2O) spectrum of compound 1-(Methyl-α-D-glucopyranosid-6-yl)-3-methylimidazolium iodide (GMIM-I) **3a.**

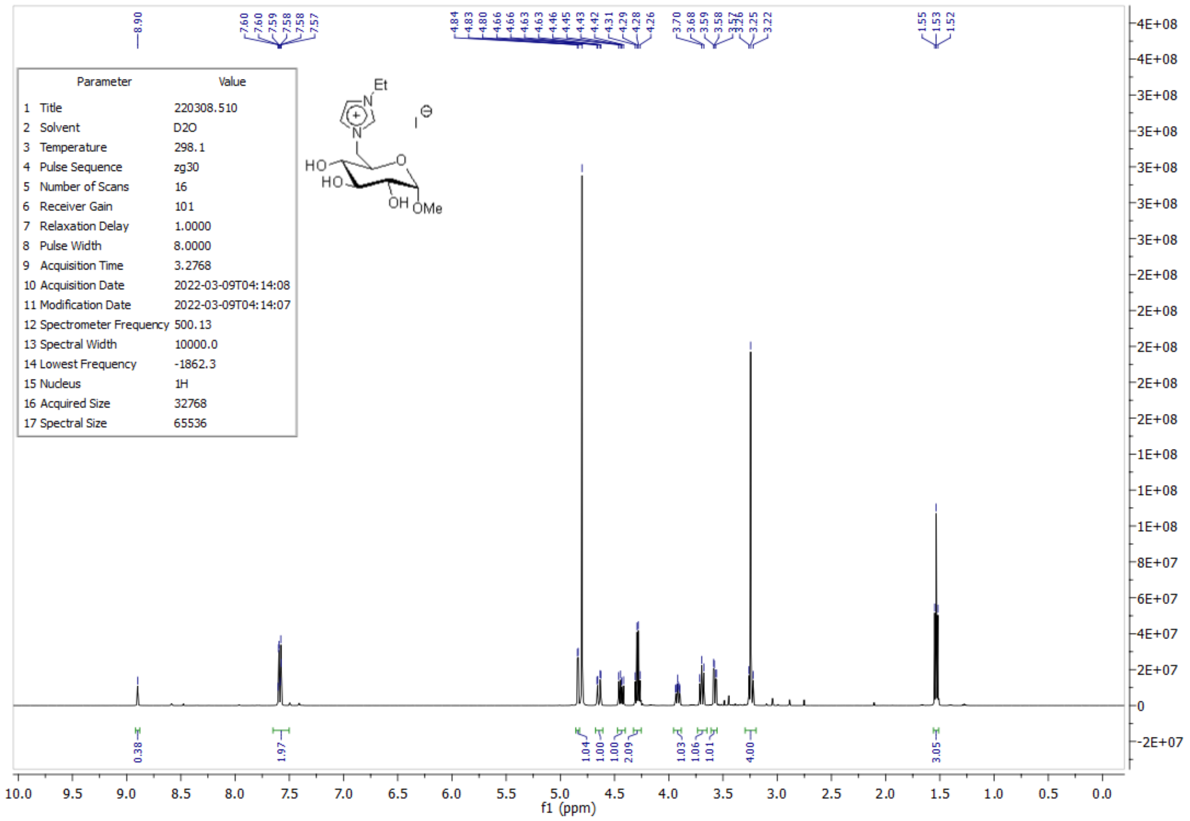

Figure S11. ^{1}H-NMR (D_2O) spectrum of compound 1-(Methyl-α-D-glucopyranosid-6-yl)-3-ethylimidazolium iodide (GEIM-I) **3b.**

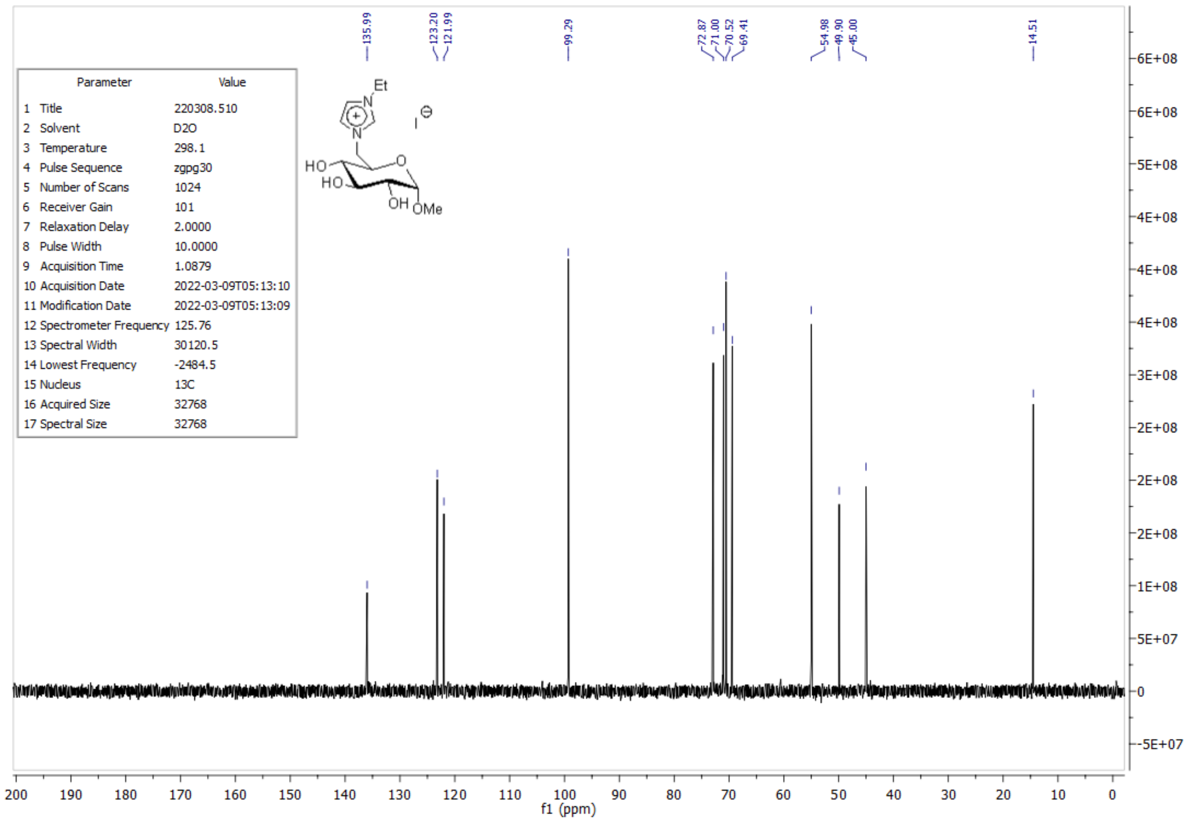

Figure S12. ^{13}C-NMR (D_2O) spectrum of compound 1-(Methyl-α-D-glucopyranosid-6-yl)-3-ethylimidazolium iodide (GEIM-I) **3b.**

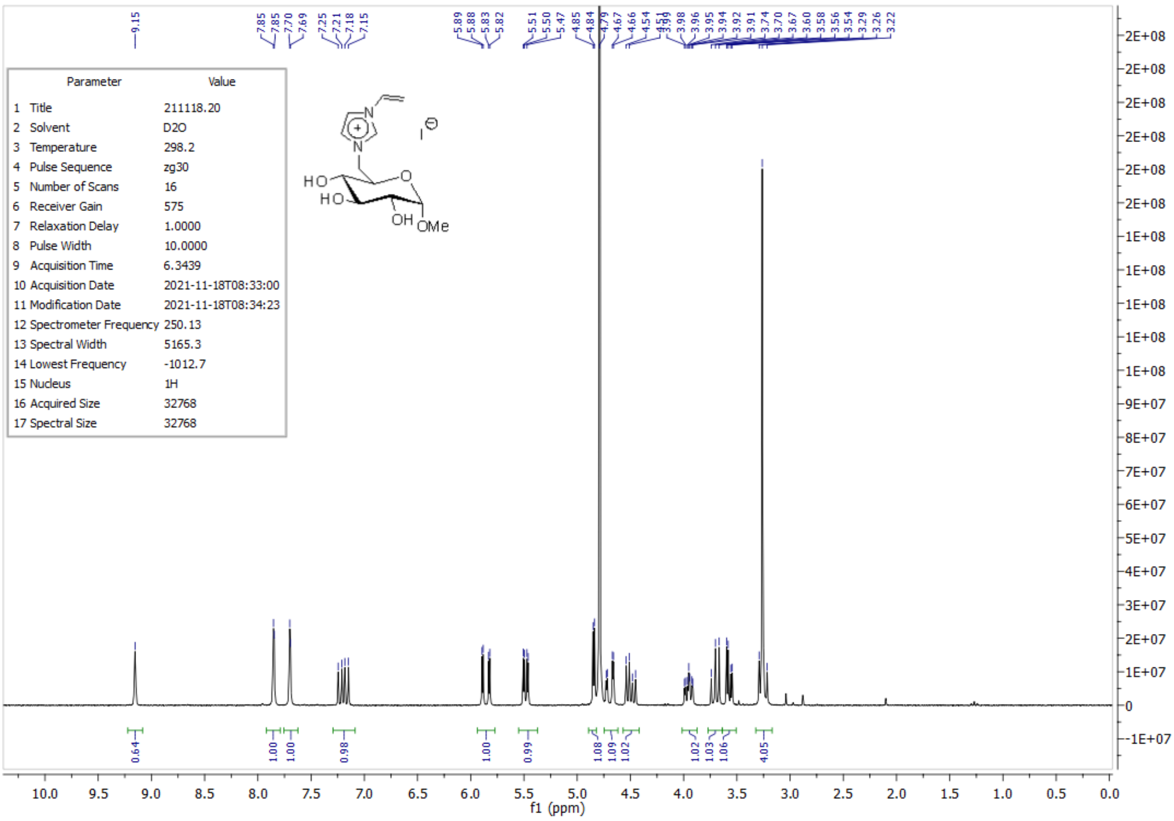

Figure S13. ^{1}H-NMR (D_2O) spectrum of compound 1-(Methyl-α-D-glucopyranosid-6-yl)-3-vinylimidazolium iodide (GVIM-I) **3c.**

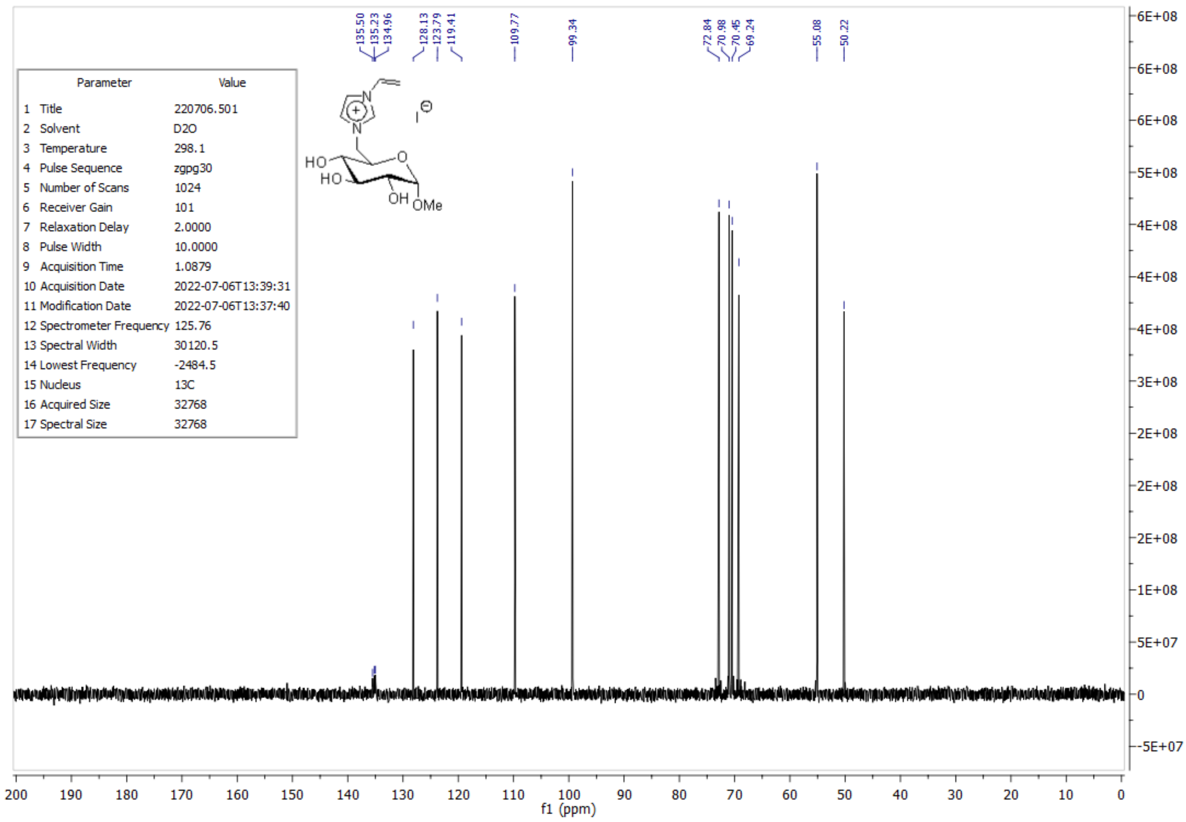

Figure S14. ^{13}C-NMR (D_2O) spectrum of compound 1-(Methyl-α-D-glucopyranosid-6-yl)-3-vinylimidazolium iodide (GVIM-I) **3c**.

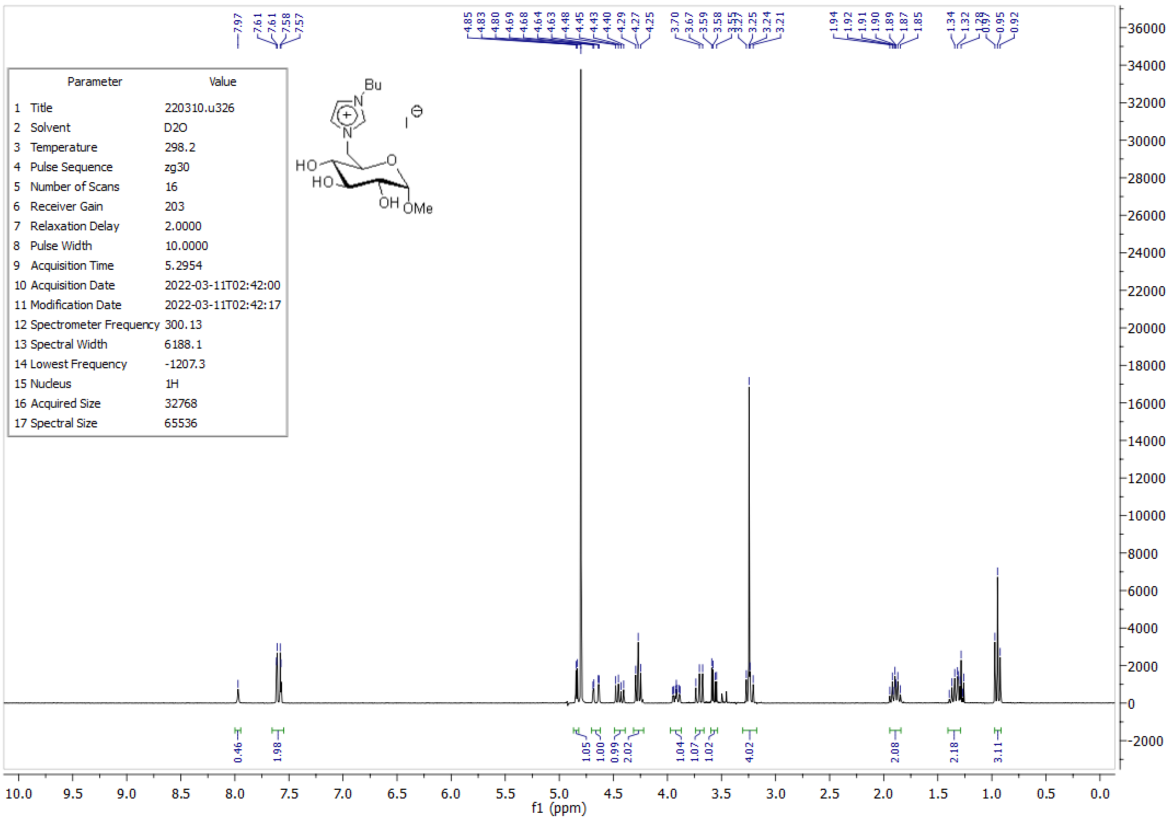

Figure S15. ^{1}H-NMR (D_2O) spectrum of compound 1-(Methyl-α-D-glucopyranosid-6-yl)-3-butylimidazolium iodide (GBIM-I) **3d**.

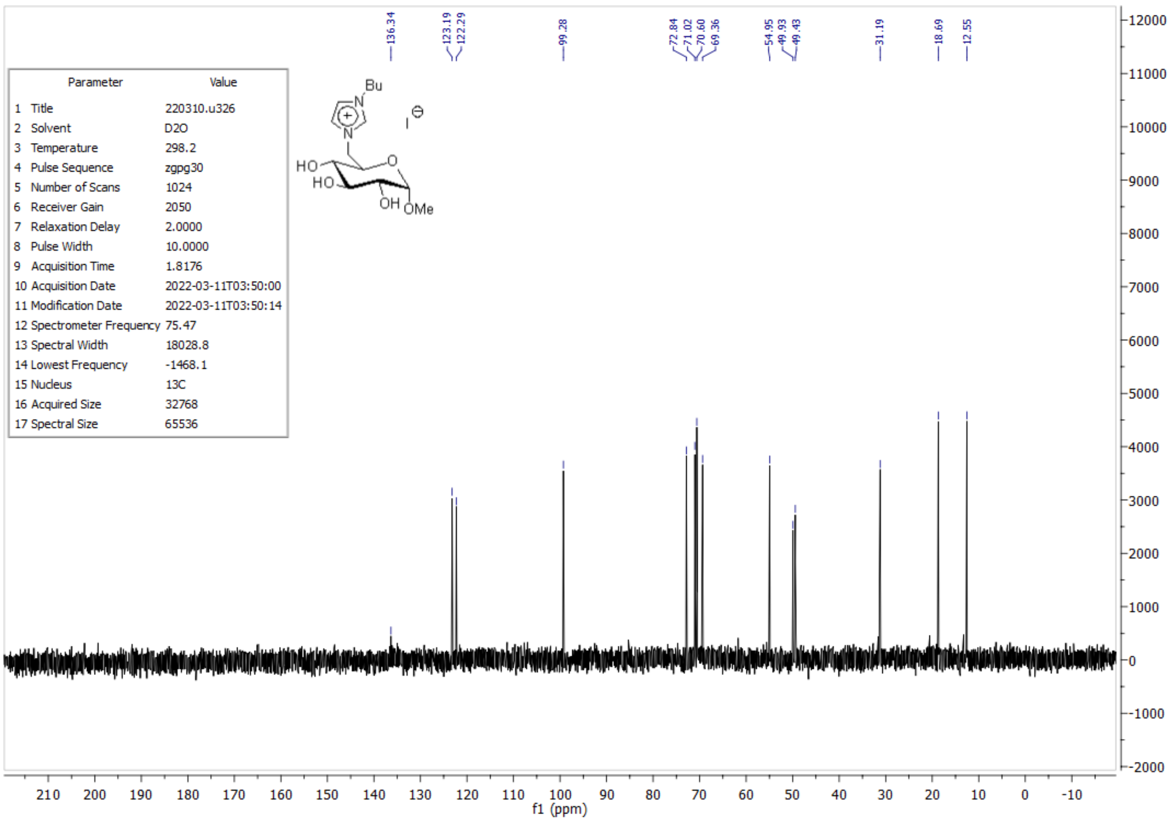

Figure S16. ^{13}C-NMR (D_2O) spectrum of compound 1-(Methyl-α-D-glucopyranosid-6-yl)-3-butylimidazolium iodide (GBIM-I) **3d**.

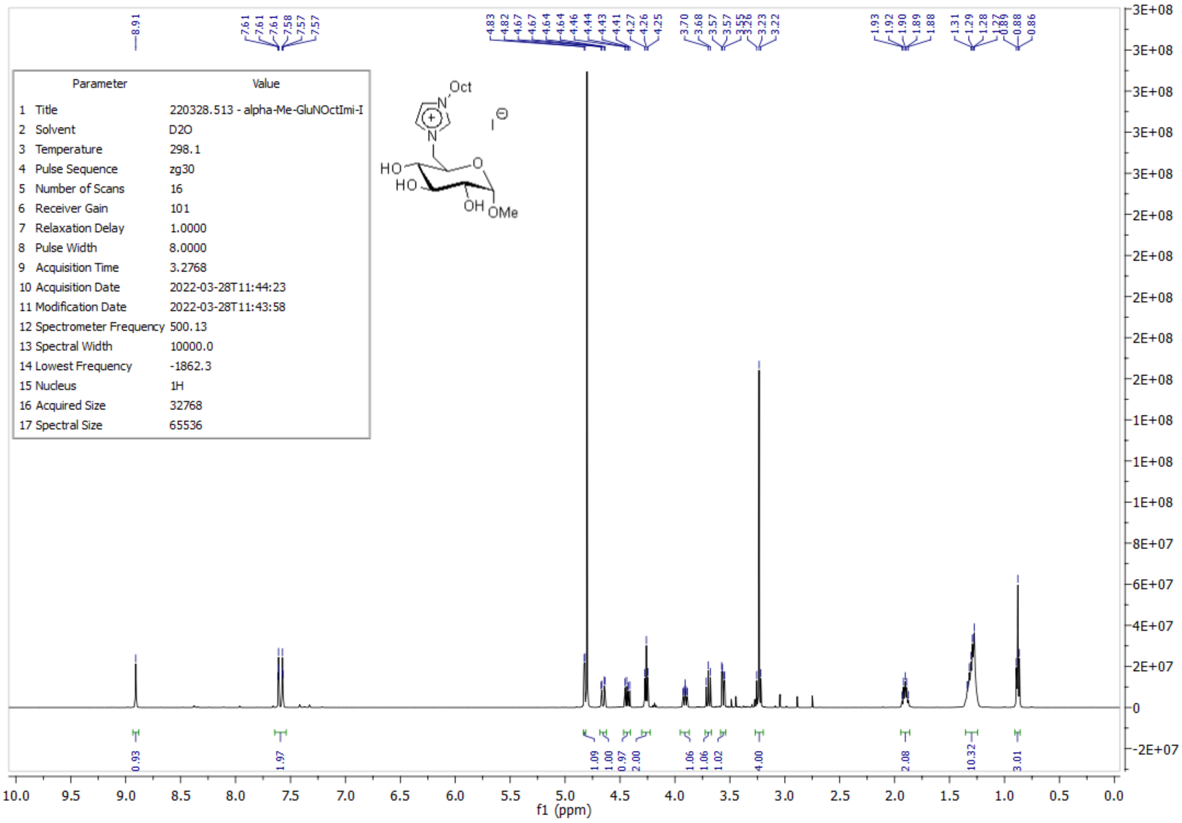

Figure S17. [1]H-NMR (D_2O) spectrum of compound 1-(Methyl-α-D-glucopyranosid-6-yl)-3-octylimidazolium iodide (GOIM-I) **3e**.

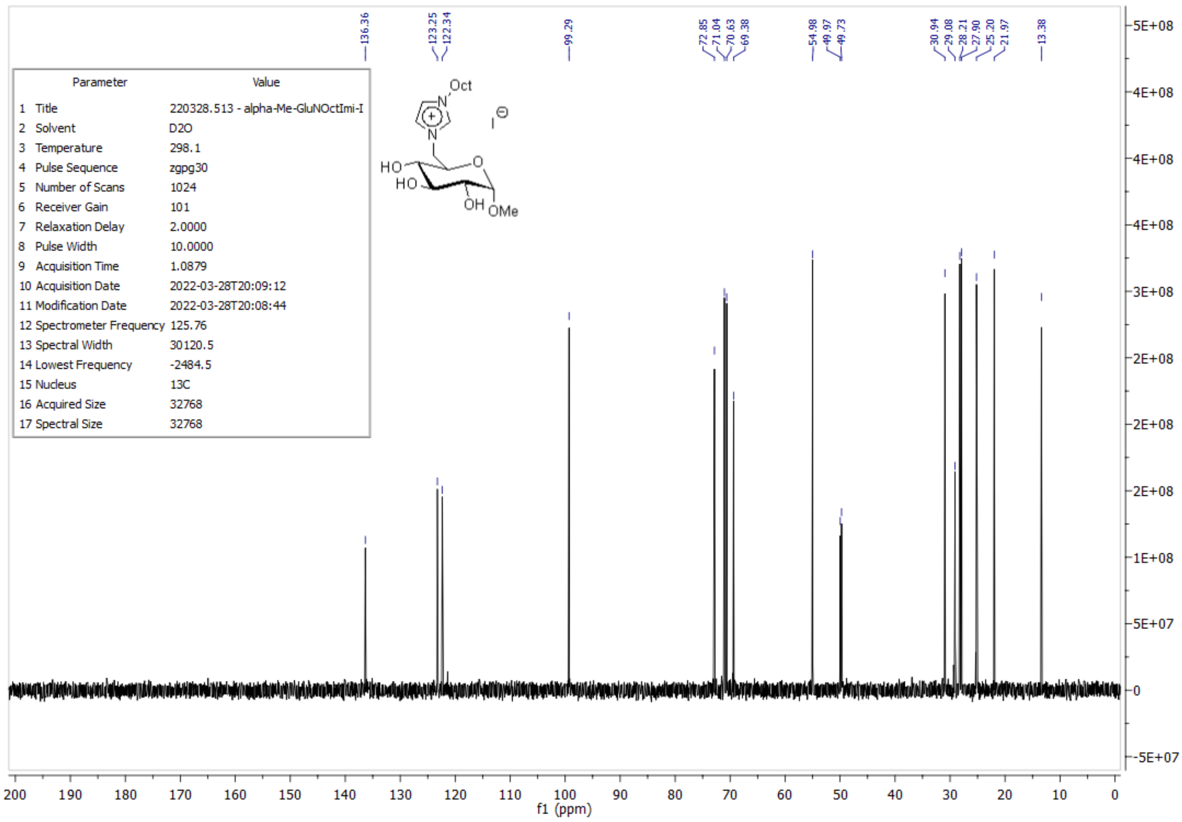

Figure S18. [13]C-NMR (D_2O) spectrum of compound 1-(Methyl-α-D-glucopyranosid-6-yl)-3-octylimidazolium iodide (GOIM-I) **3e**.

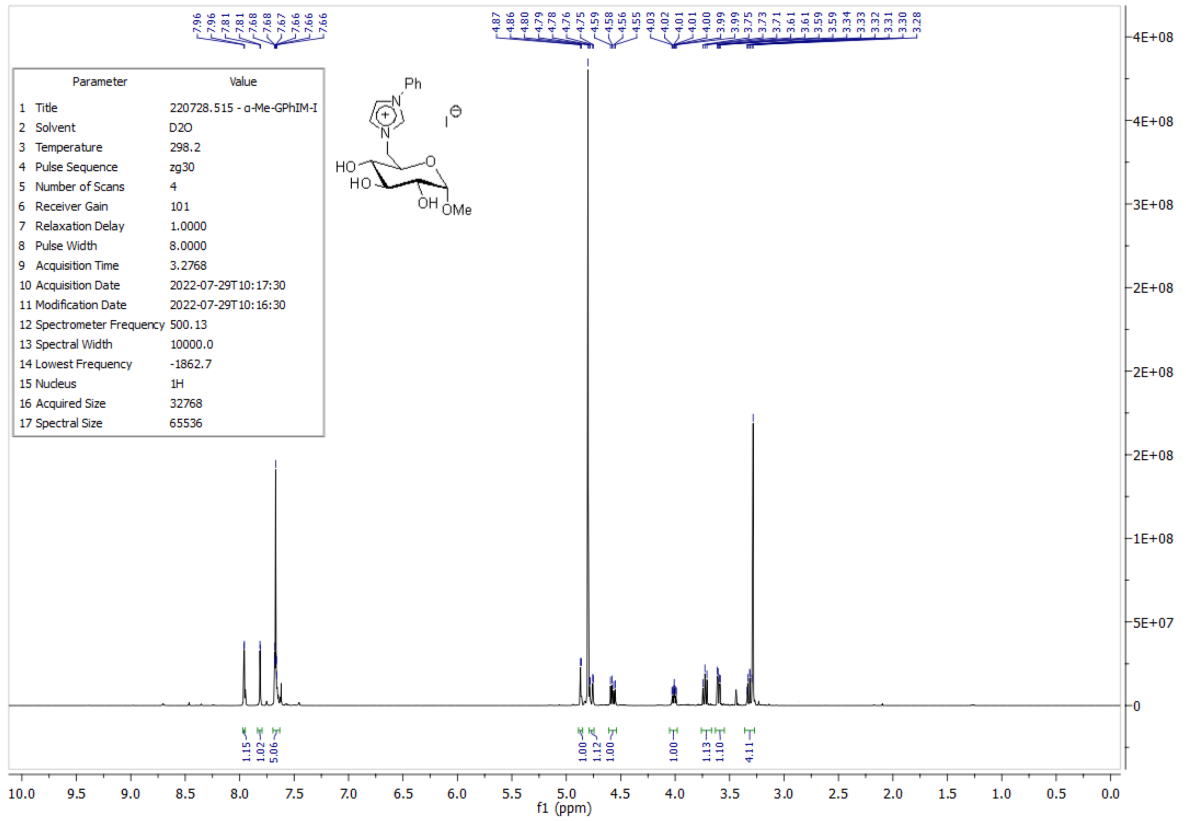

Figure S19. ^{1}H-NMR (D_2O) spectrum of compound 1-(Methyl-α-D-glucopyranosid-6-yl)-3-phenylimidazolium iodide (GPhIM-I) **3f**.

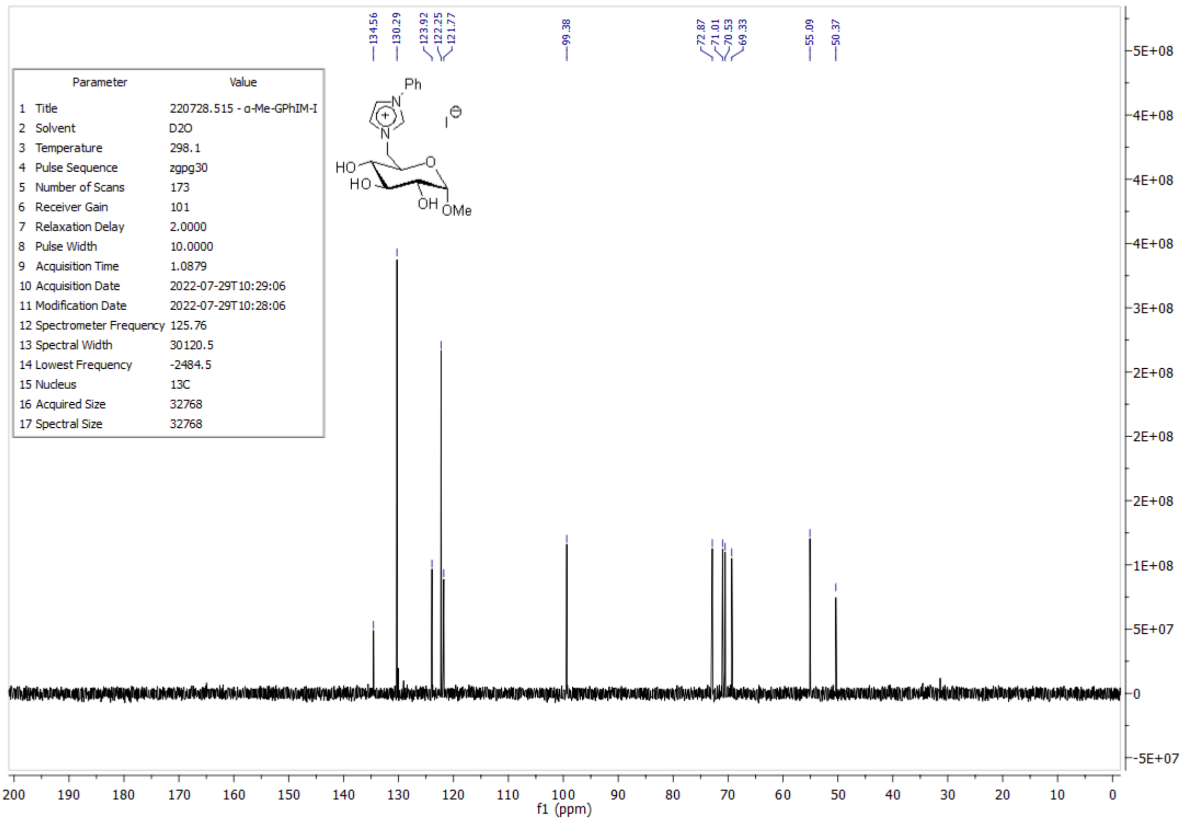

Figure S20. ^{13}C-NMR (D_2O) spectrum of compound 1-(Methyl-α-D-glucopyranosid-6-yl)-3-phenylimidazolium iodide (GPhIM-I) **3f**.

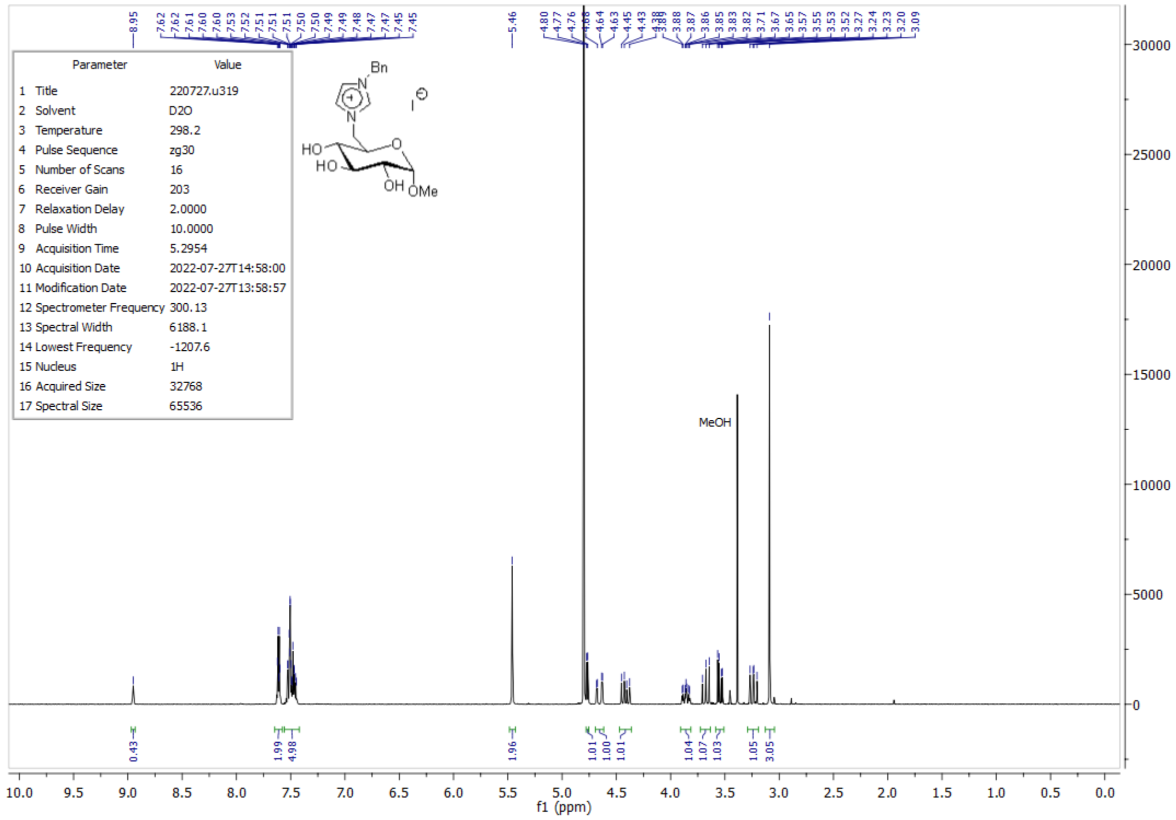

Figure S21. ^{1}H-NMR (D_2O) spectrum of compound 1-(Methyl-α-D-glucopyranosid-6-yl)-3-benzylimidazolium iodide (GBnIM-I) **3g.**

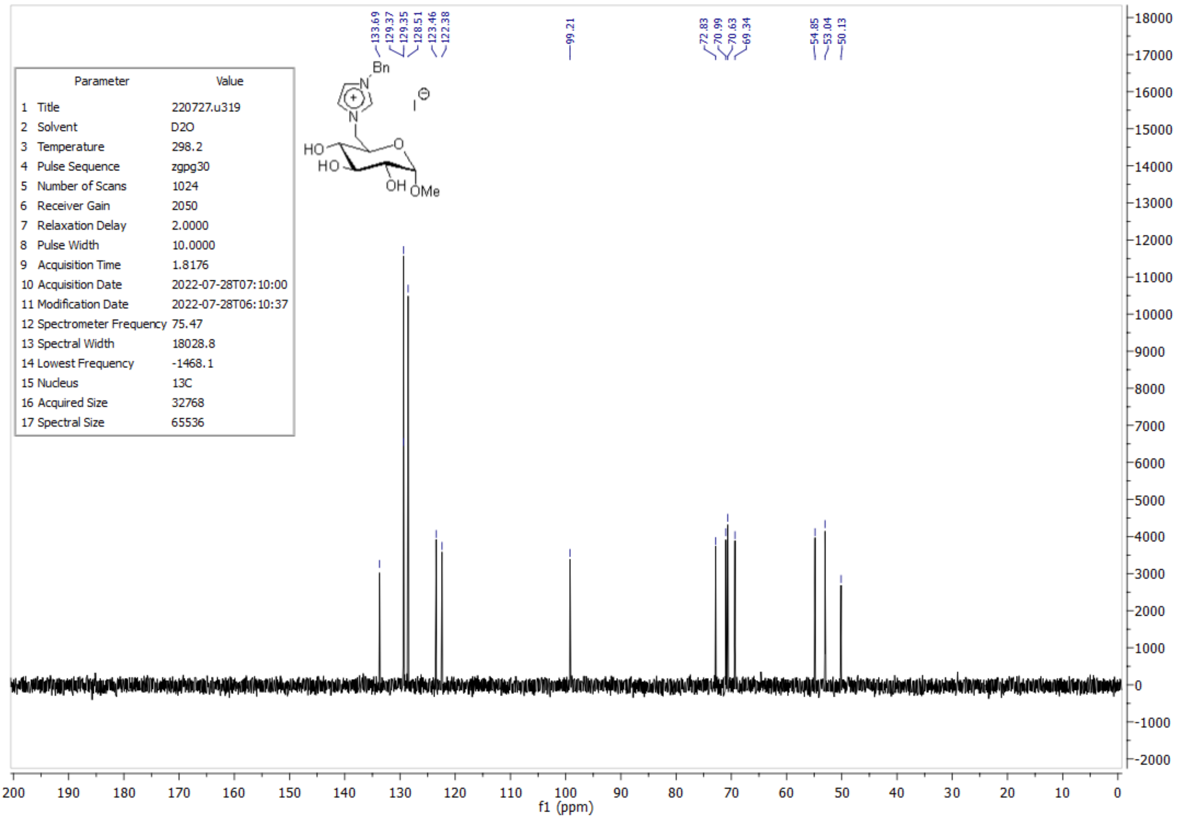

Figure S22. ^{13}C-NMR (D_2O) spectrum of compound 1-(Methyl-α-D-glucopyranosid-6-yl)-3-benzylimidazolium iodide (GBnIM-I) **3g.**

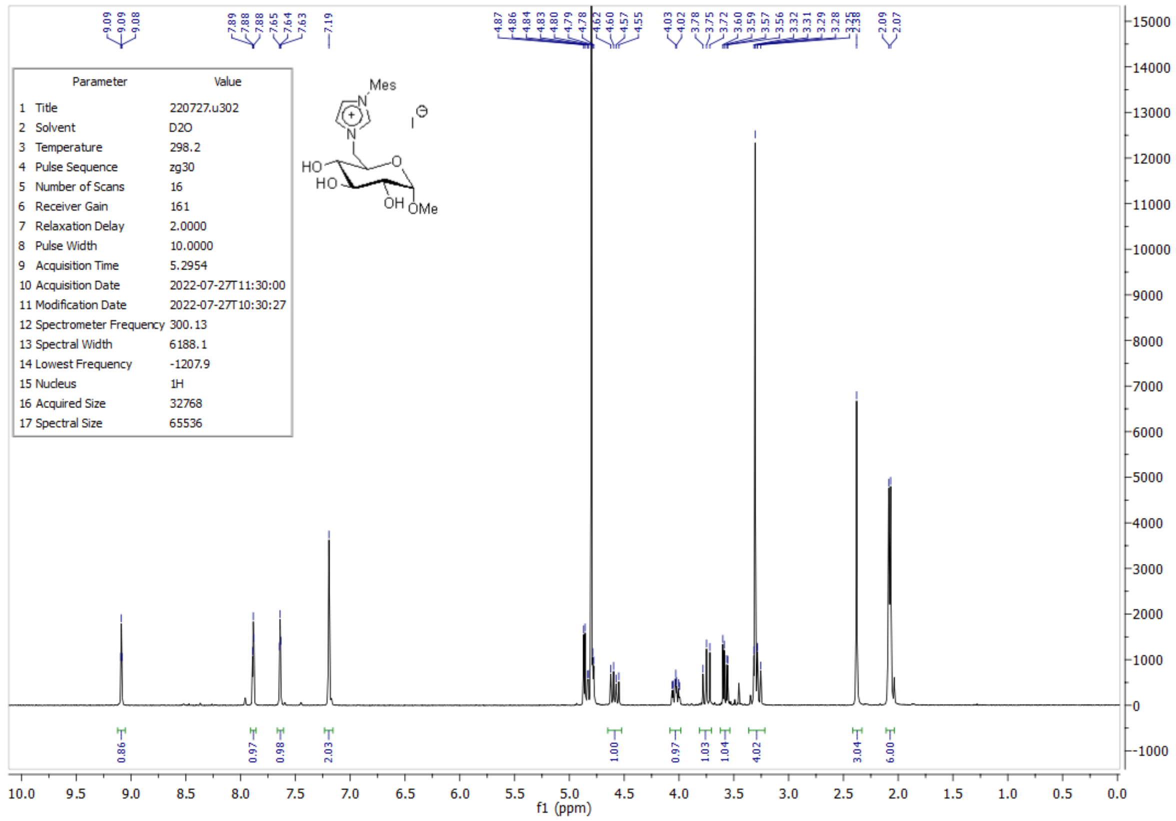

Figure S23. ^{1}H-NMR (D_2O) spectrum of compound 1-(Methyl-α-D-glucopyranosid-6-yl)-3-mesitylimidazolium iodide (GMEsIM-I) **3h.**

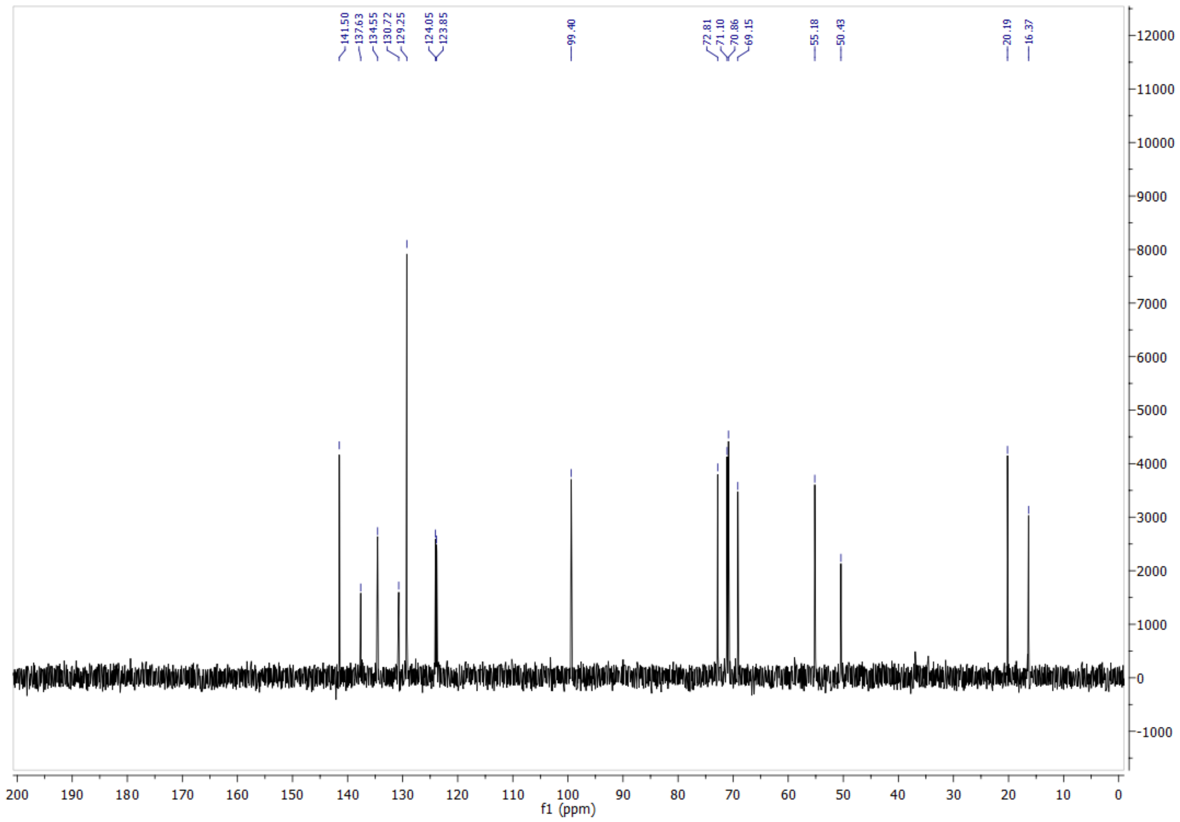

Figure S24. ^{13}C-NMR (D_2O) spectrum of compound 1-(Methyl-α-D-glucopyranosid-6-yl)-3-mesitylimidazolium iodide (GMEsIM-I) **3h.**

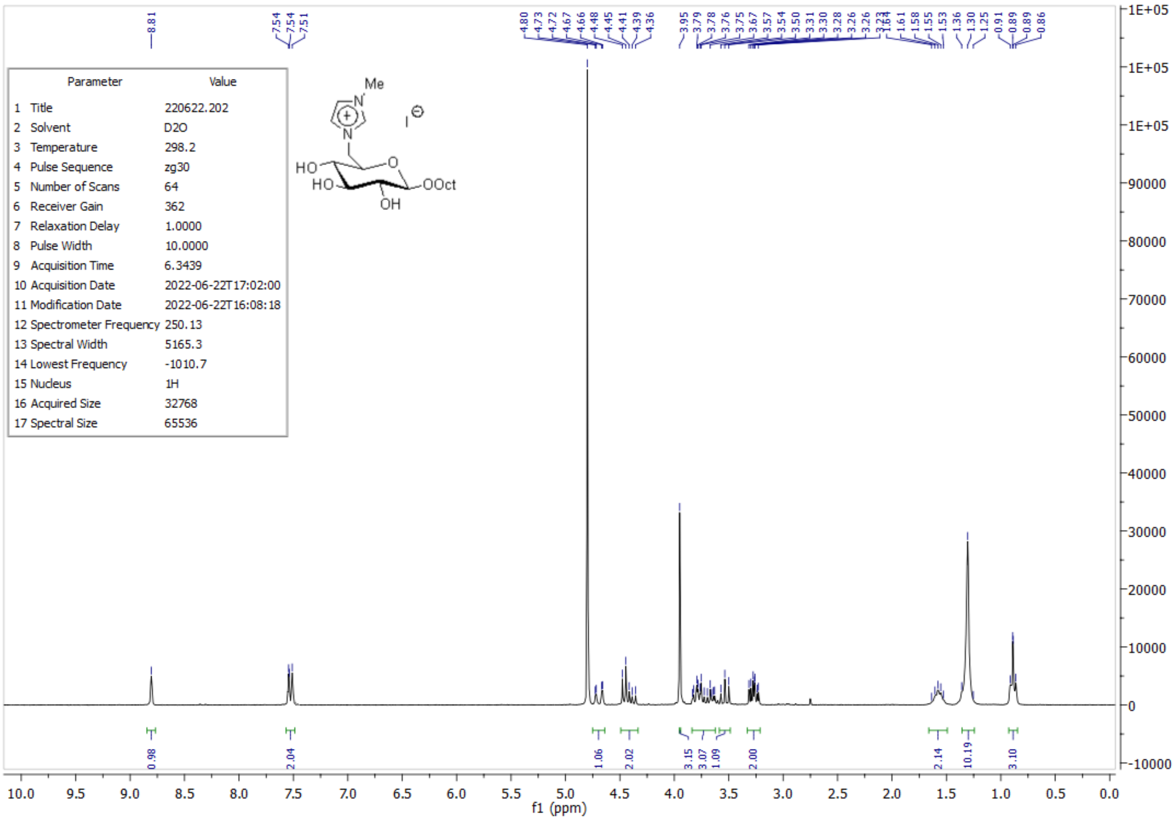

Figure S25. ^{1}H-NMR (D_2O) spectrum of compound 1-(*n*-Octyl-ß-D-glucopyranosid-6-yl)-3-methylimidazolium iodide (OctO-GMIM-I) **3i.**

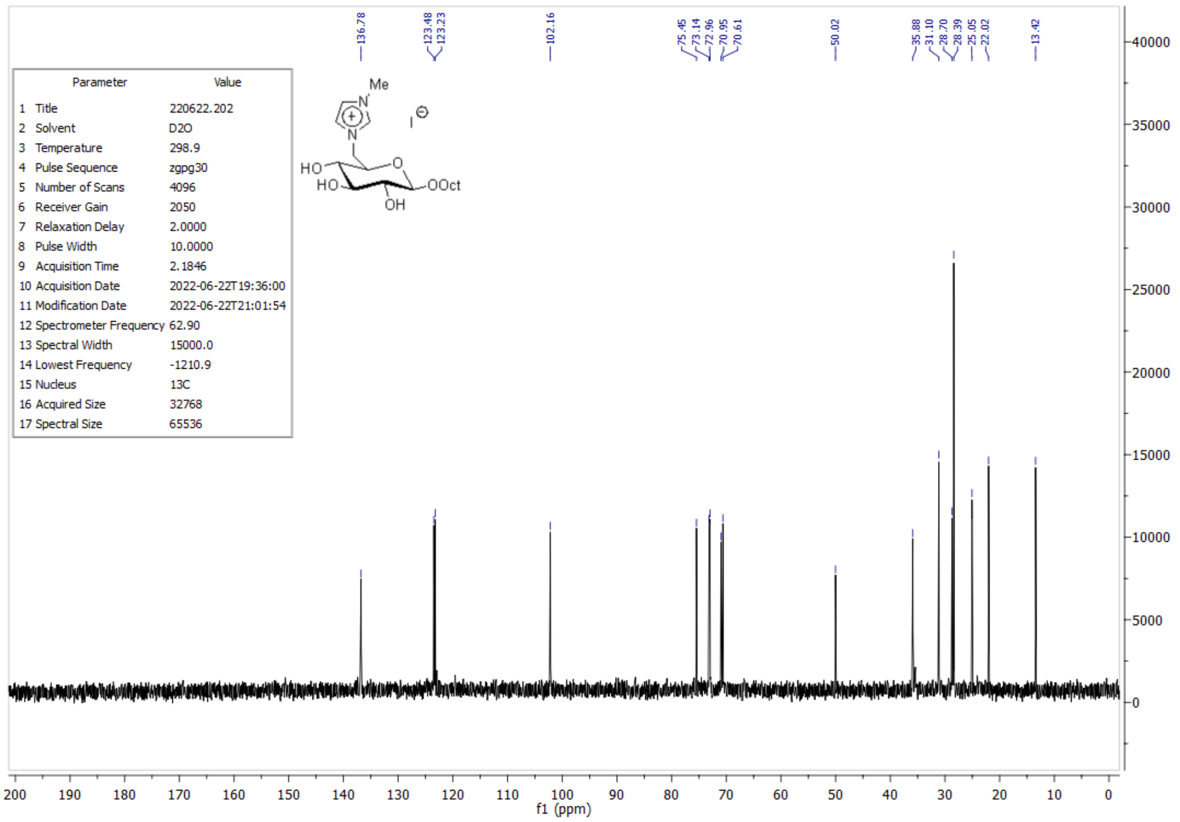

Figure S26. ^{13}C-NMR (D_2O) spectrum of compound 1-(*n*-Octyl-ß-D-glucopyranosid-6-yl)-3-methylimidazolium iodide (OctO-GMIM-I) **3i.**

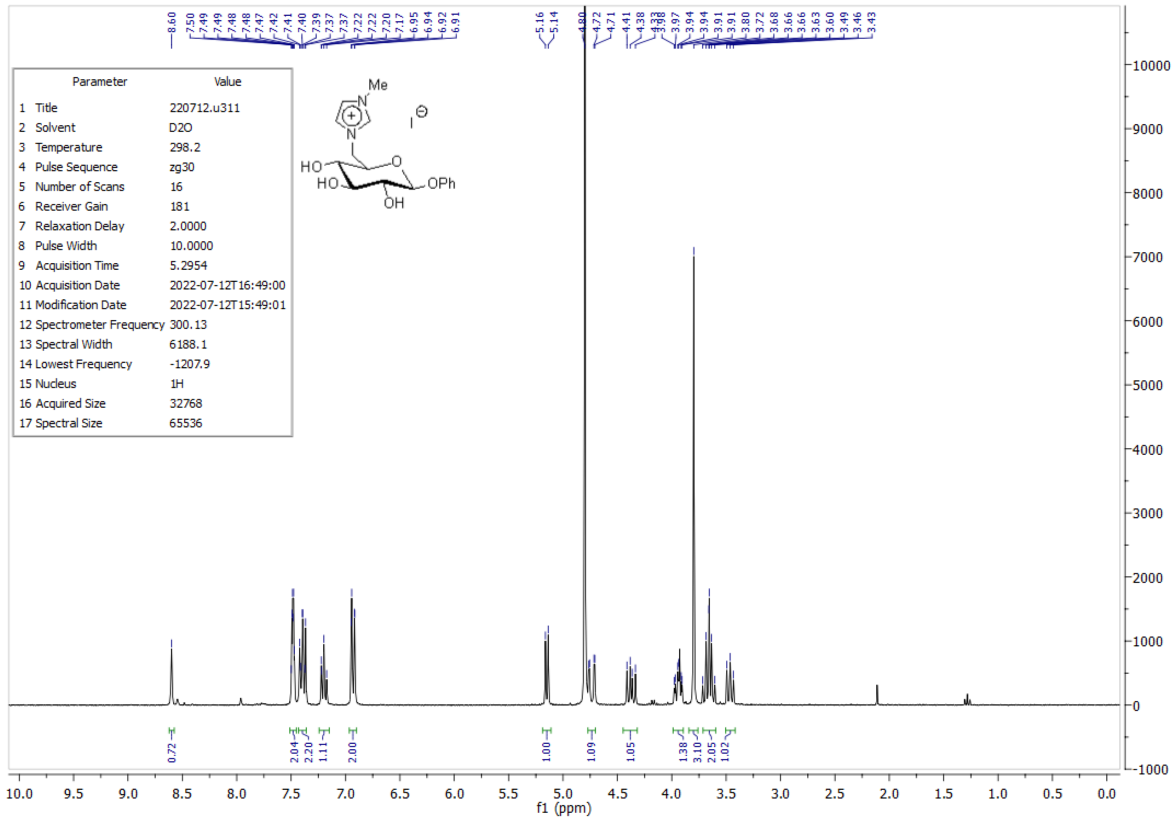

Figure S27. ^{1}H-NMR (D_2O) spectrum of compound 1-(Phenyl-ß-D-glucopyranosid-6-yl)-3-methylimidazolium iodide (PhO-GMIM-I) **3j.**

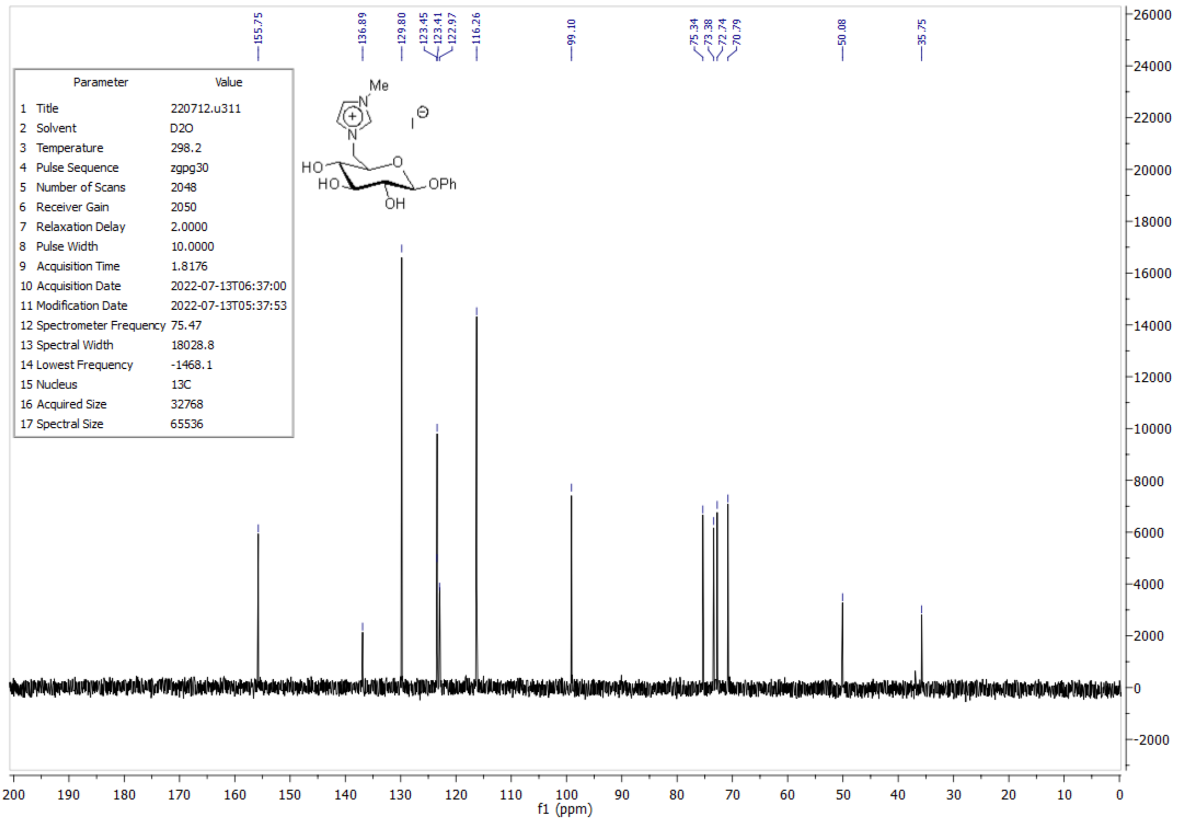

Figure S28. ^{13}C-NMR (D_2O) spectrum of compound 1-(Phenyl-ß-D-glucopyranosid-6-yl)-3-methylimidazolium iodide (PhO-GMIM-I) **3j.**

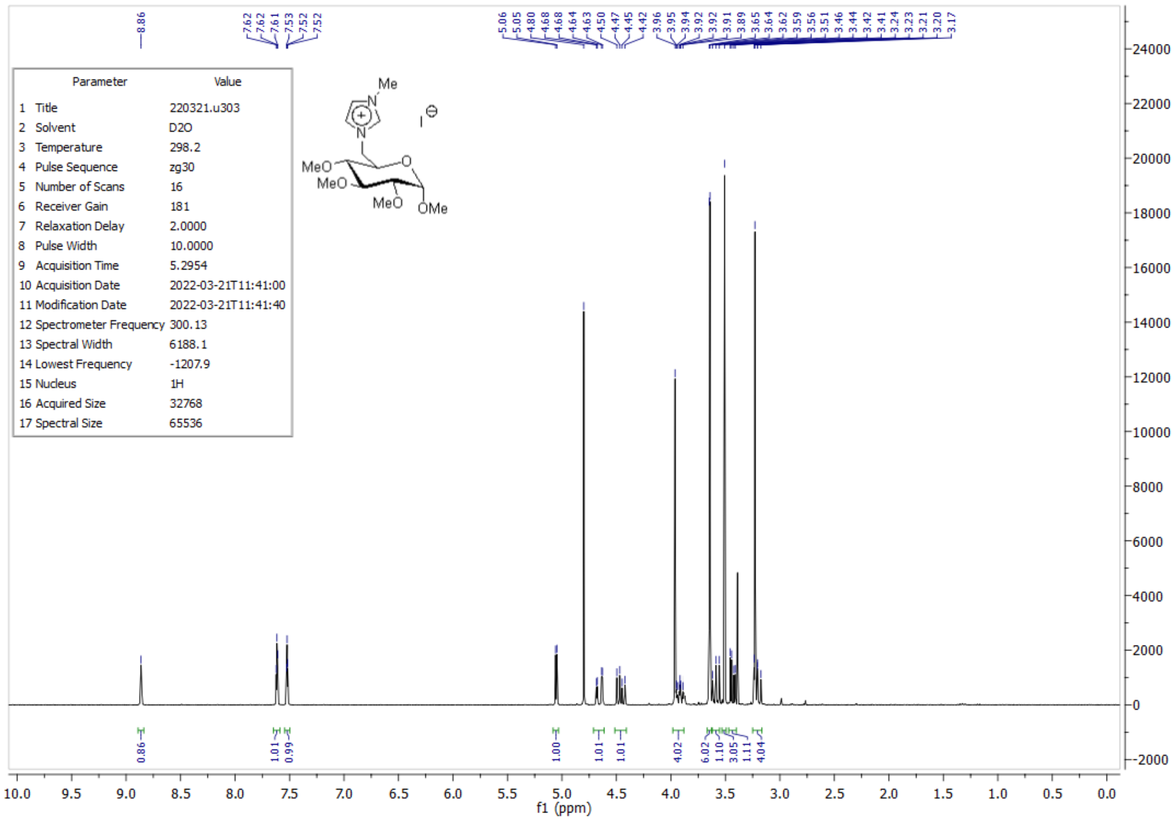

Figure S29. ^{1}H-NMR (D_2O) spectrum of compound 1-(Methyl-2,3,4-*O*-methyl-α-D-glucopyranosid-6-yl)-3-methylimidazolium iodide (PerMe-GMIM-I) **3k.**

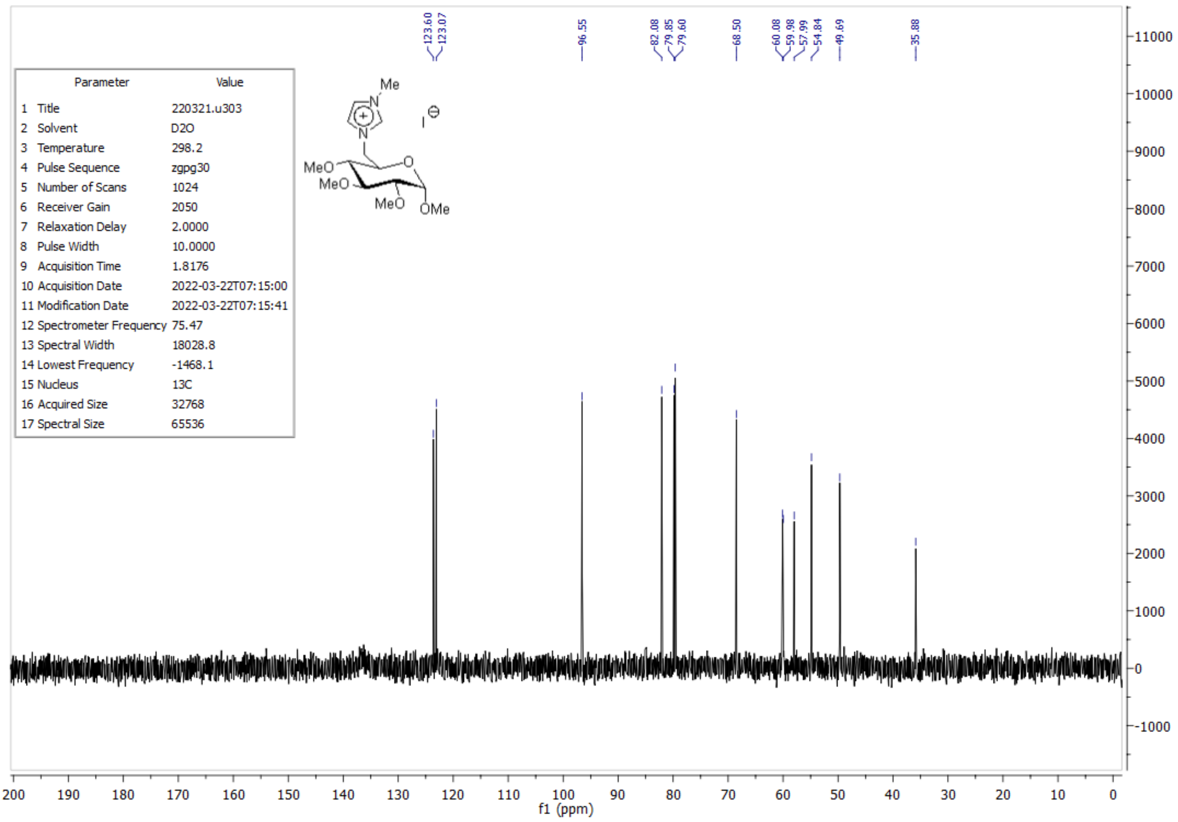

Figure S30. ^{13}C-NMR (D_2O) spectrum of compound 1-(Methyl-2,3,4-*O*-methyl-α-D-glucopyranosid-6-yl)-3-methylimidazolium iodide (PerMe-GMIM-I) **3k.**

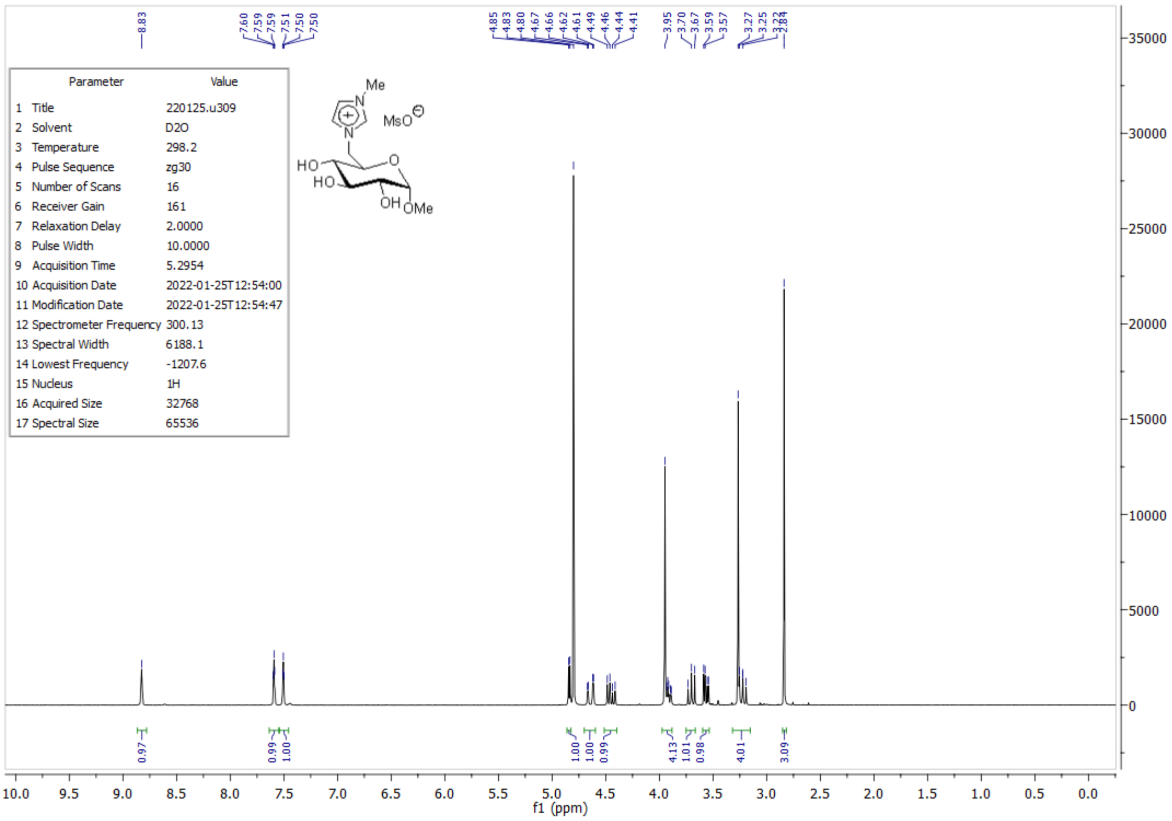

Figure S31. ^{1}H-NMR (D_2O) spectrum of compound 1-(Methyl-α-D-glucopyranosid-6-yl)-3-methylimidazolium methanesulfonate (GMIM-OMs) **4a.**

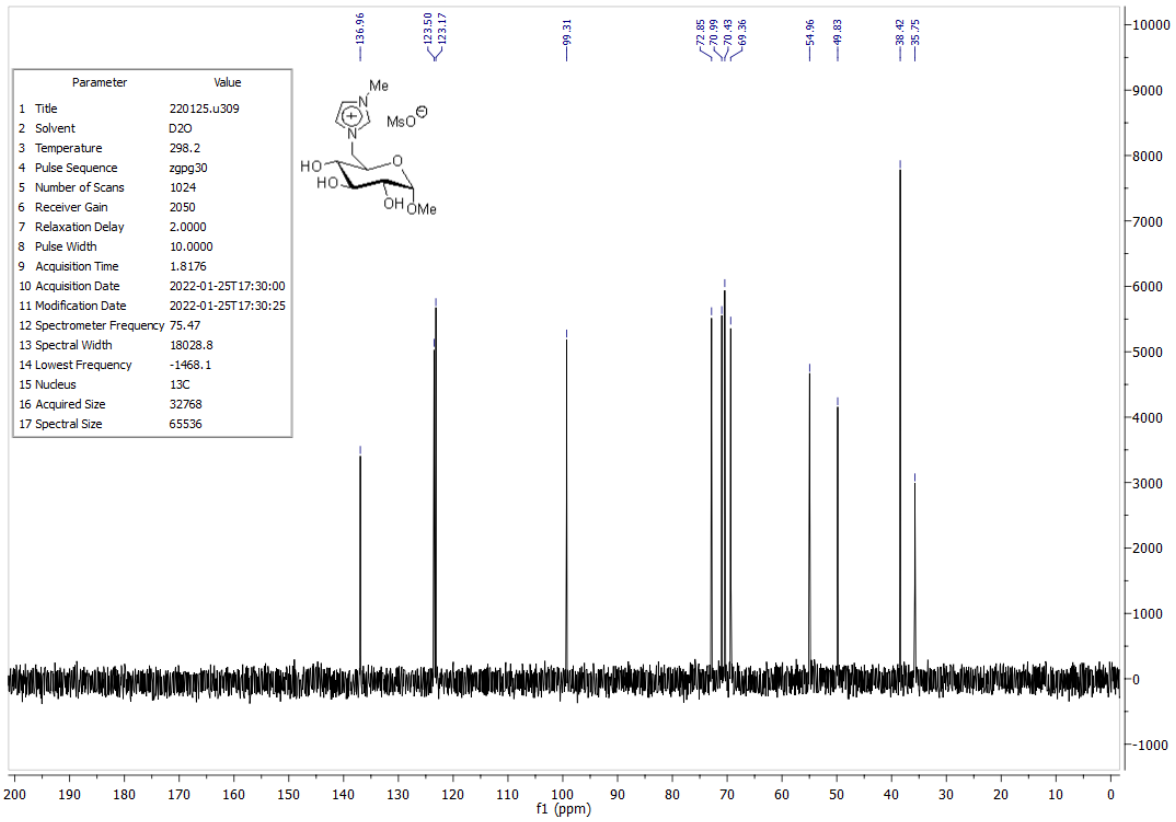

Figure S32. ^{13}C-NMR (D_2O) spectrum of compound 1-(Methyl-α-D-glucopyranosid-6-yl)-3-methylimidazolium methanesulfonate (GMIM-OMs) **4a.**

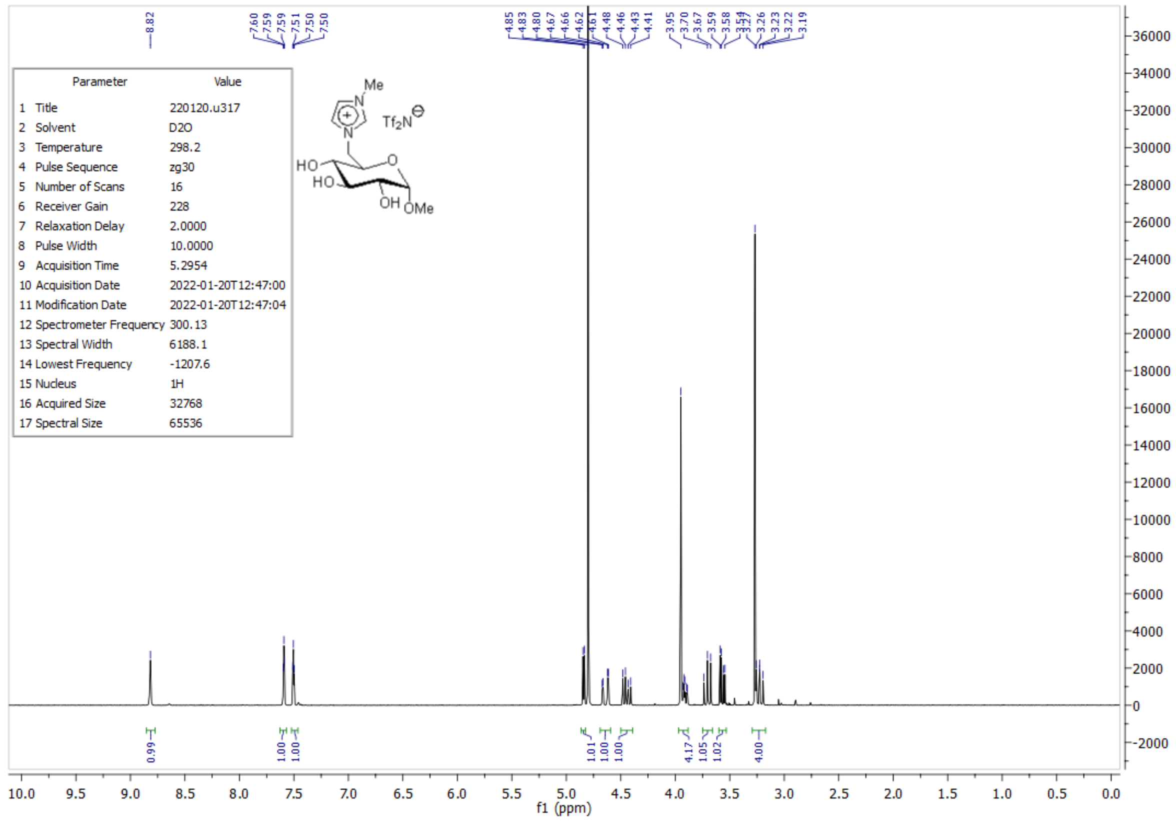

Figure S33. [1]H-NMR (D_2O) spectrum of compound 1-(Methyl-α-D-glucopyranosid-6-yl)-3-methylimidazolium bis-(trifluoromethanesulfonyl)-imide (GMIM-NTf_2) **4b.**

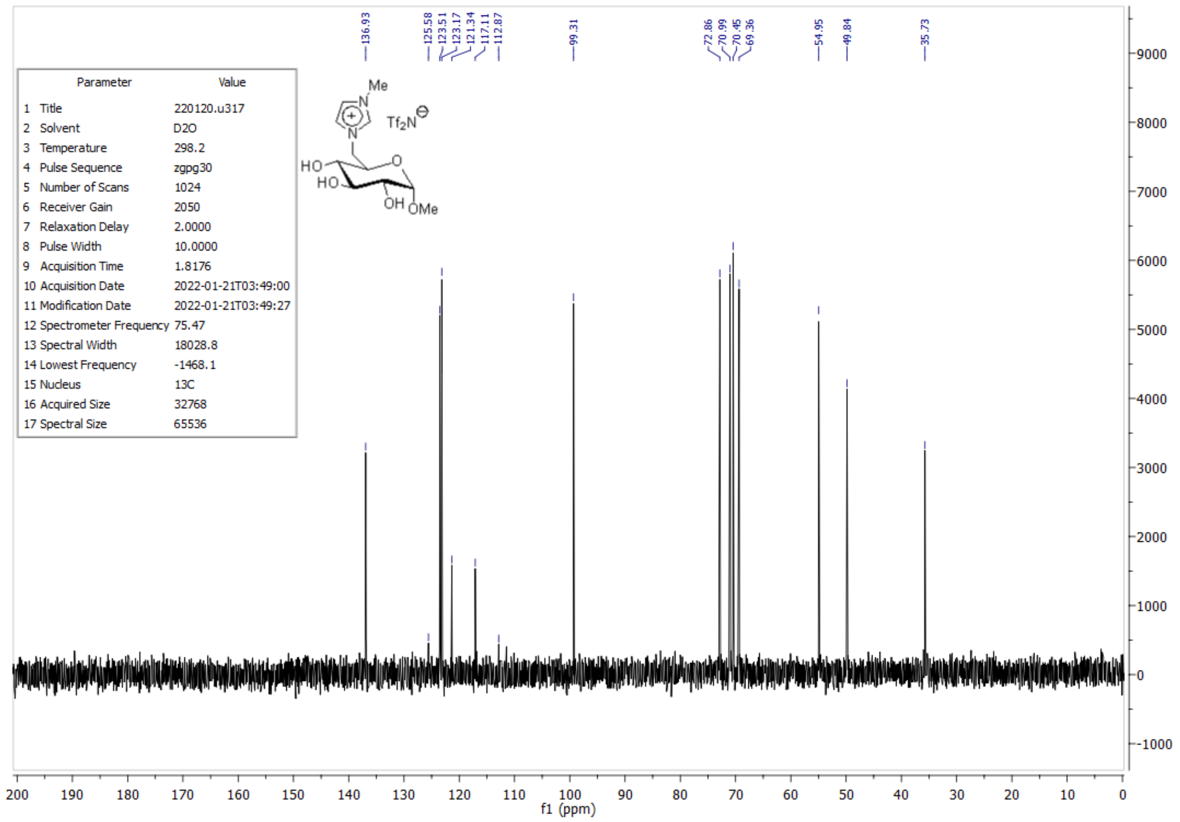

Figure S34. [13]C-NMR (D_2O) spectrum of compound 1-(Methyl-α-D-glucopyranosid-6-yl)-3-methylimidazolium bis-(trifluoromethanesulfonyl)-imide (GMIM-NTf_2) **4b.**

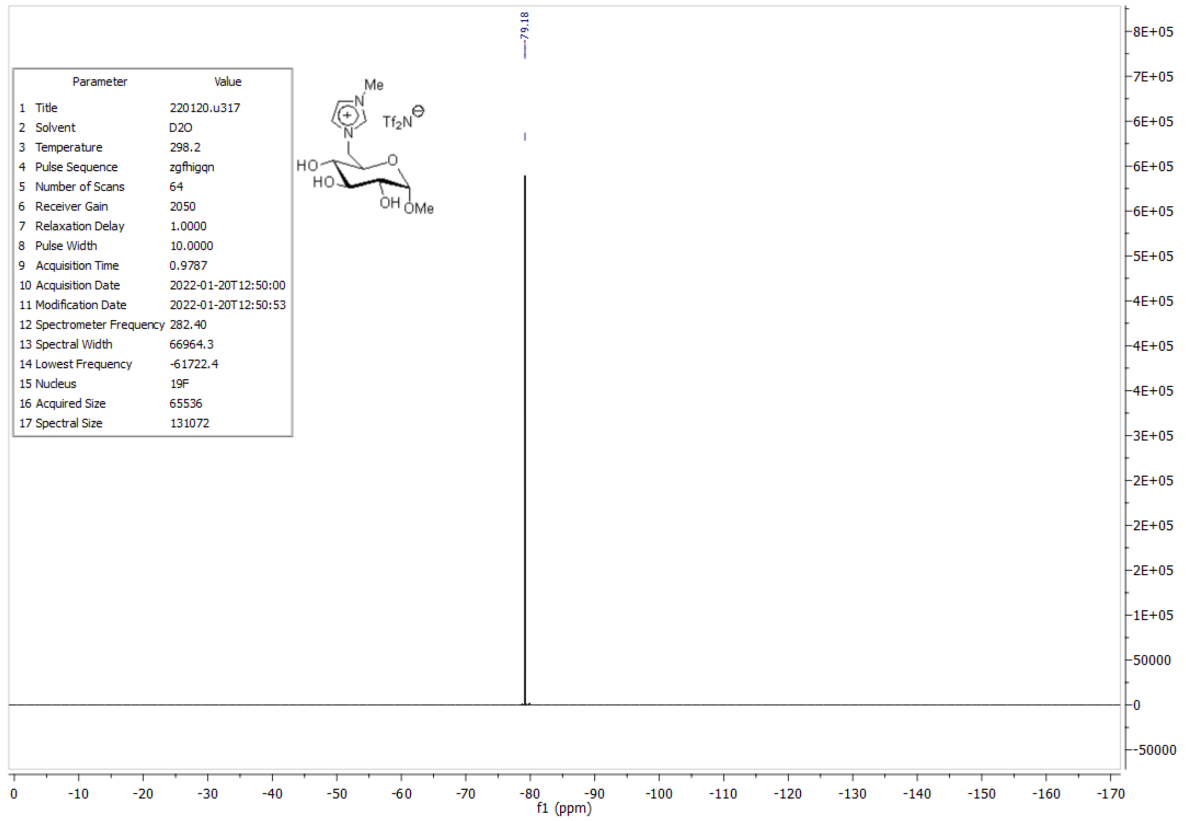

Figure S35. ^{19}F-NMR (D_2O) spectrum of compound 1-(Methyl-α-D-glucopyranosid-6-yl)-3-methylimidazolium bis-(trifluoromethanesulfonyl)-imide (GMIM-NTf_2) **4b.**

2. Cell viability of L929 cells - CellTiter blue (CTB) viability assay

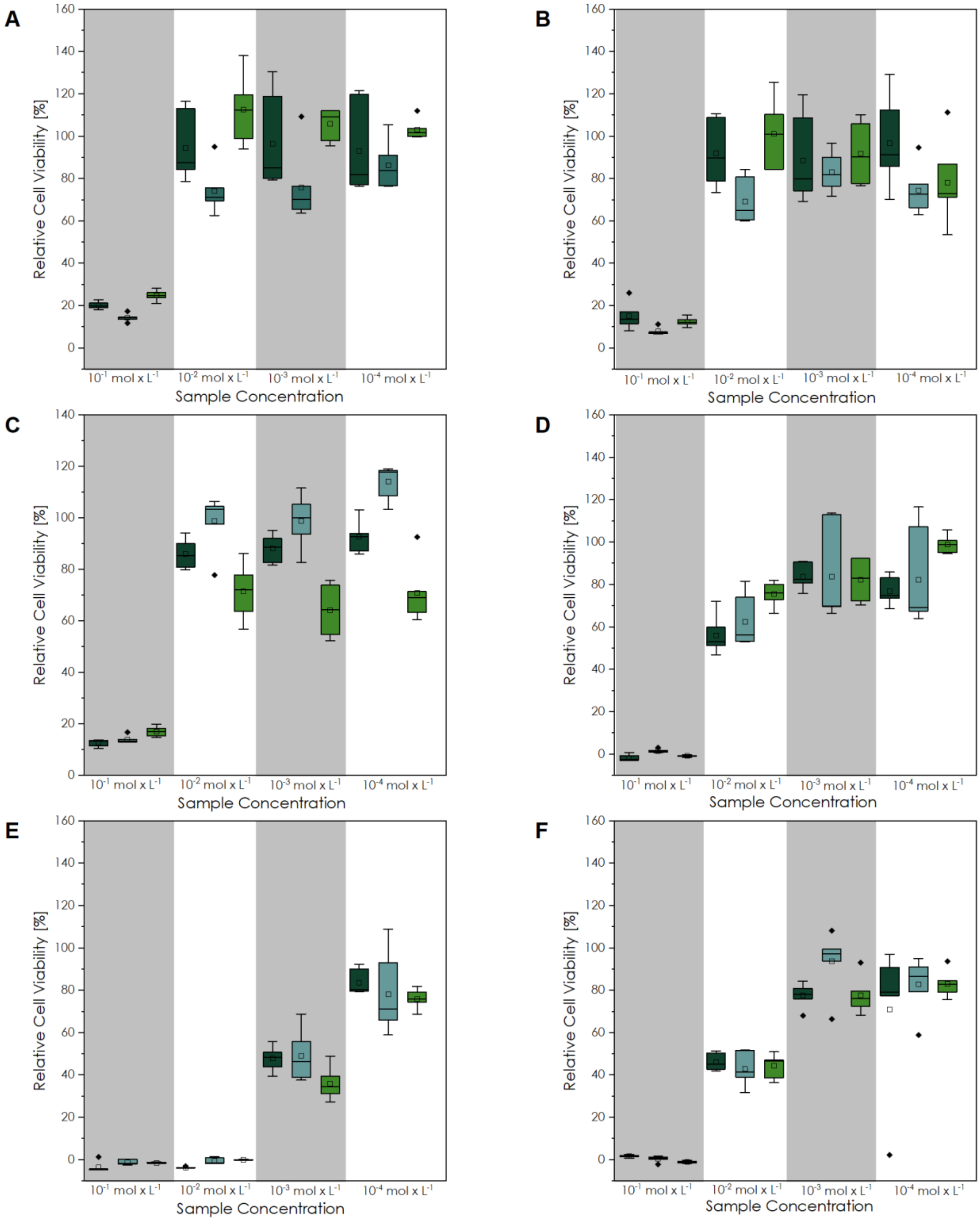

Figure S36. Cell viability after cultivation for 48 h of L929 cells in different concentrated (10^{-1} mol × L^{-1}; 10^{-2} mol × L^{-1}; 10^{-3} mol × L^{-1}; 10^{-4} mol × L^{-1}) CHIL solutions (**A** GMIM-I; **B** GEIM-I; **C** GVIM-I; **D** GBIM-I; **E** GOIM-I; **F** GPhIM-I) in the three different biological replicates (n = 6). The mean value of the wells without cells (background fluorescence) was subtracted from the fluorescence values of the rest of the wells, and the values of treated cultures were normalized to the mean fluorescence of the control cultures.

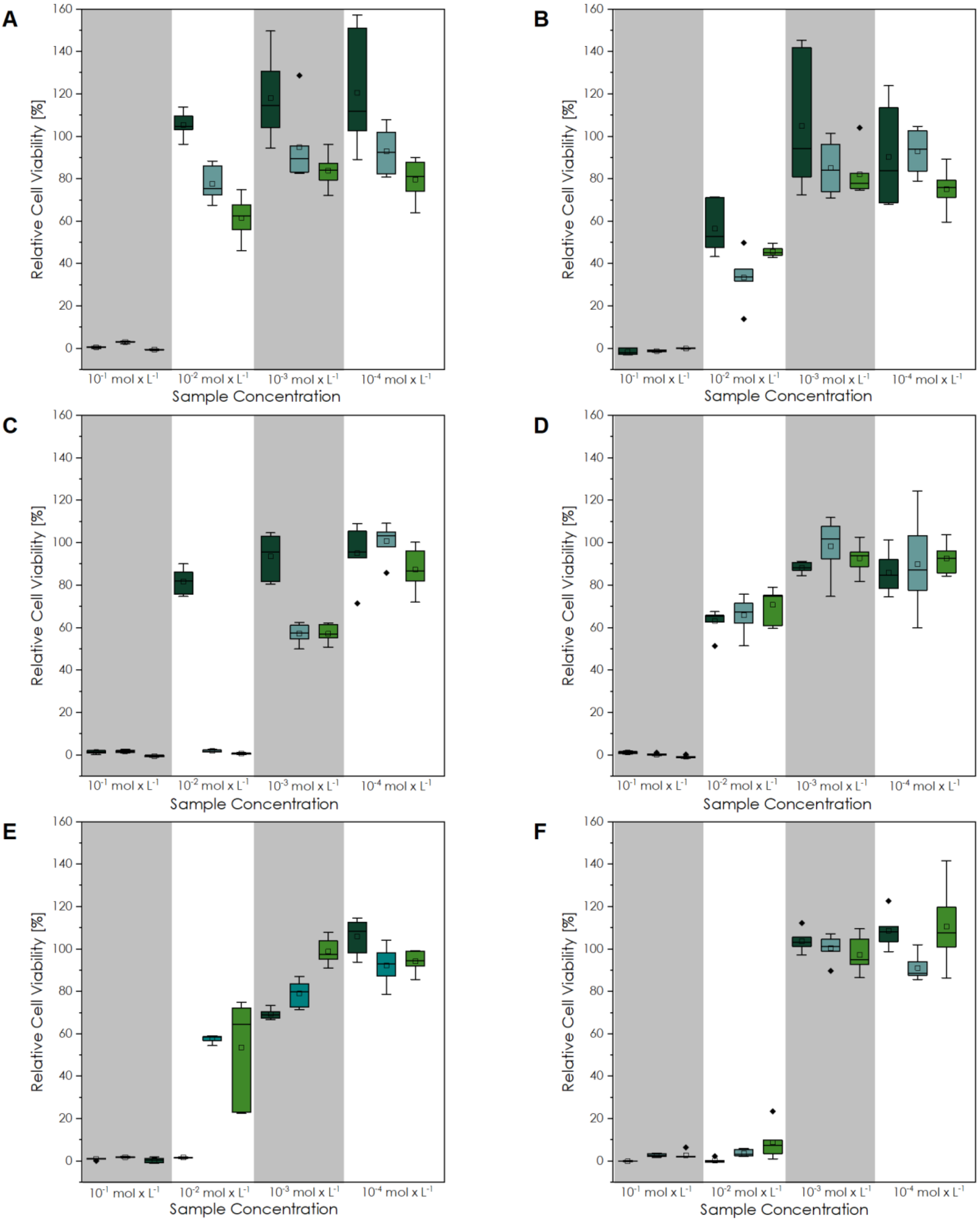

Figure S37. Cell viability after cultivation for 48 h of L929 cells in different concentrated (10^{-1} mol × L^{-1}; 10^{-2} mol × L^{-1}; 10^{-3} mol × L^{-1}; 10^{-4} mol × L^{-1}) CHIL solutions (**A** GBnIM-I; **B** GMesIM-I; **C** OctO-GMIM-I; **D** PhO-GMIM-I; **E** PerMe-GMIM-I; **F** GMIM-OMs) in the three different biological replicates (n = 6). The mean value of the wells without cells (background fluorescence) was subtracted from the fluorescence values of the rest of the wells, and the values of treated cultures were normalized to the mean fluorescence of the control cultures.

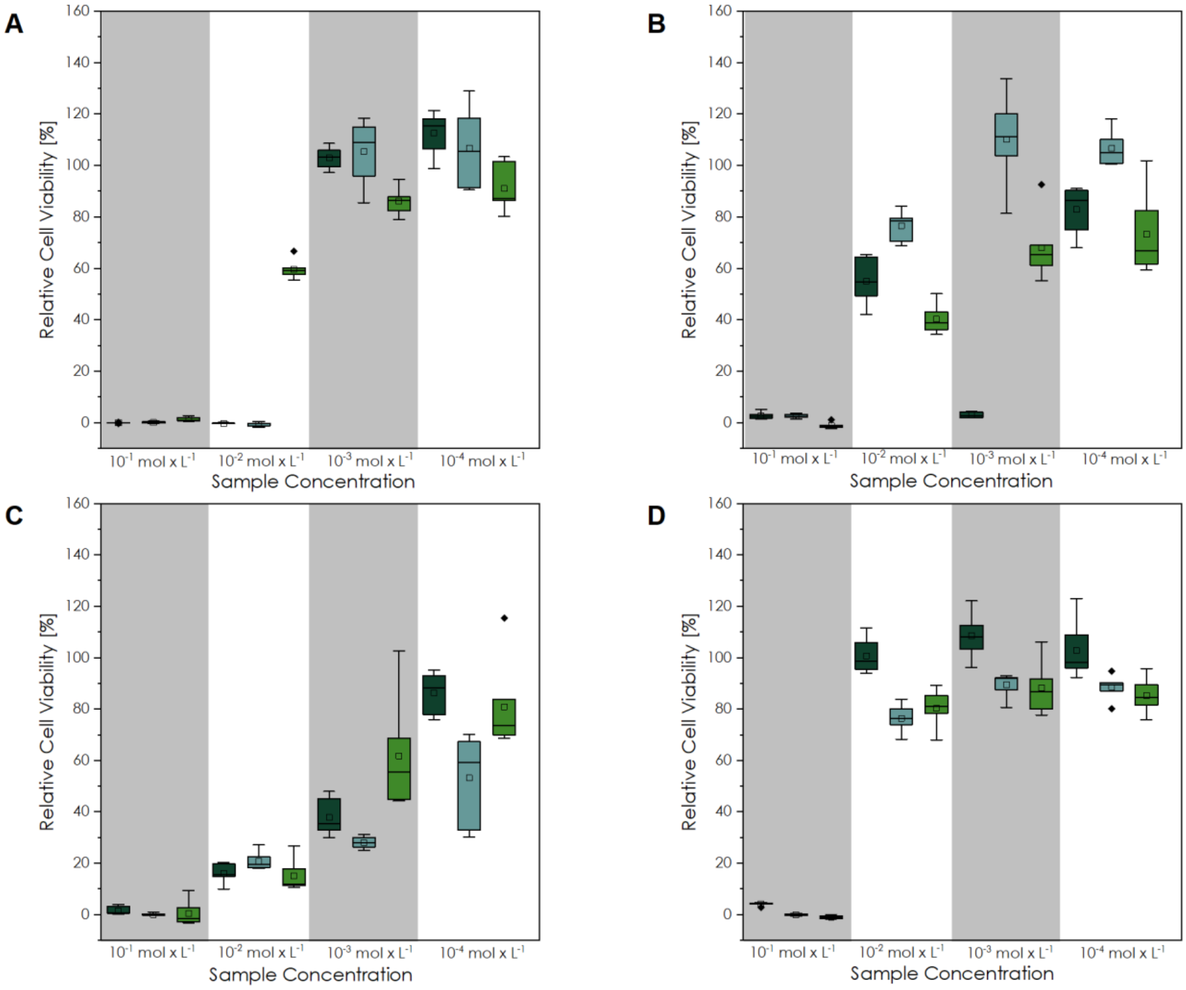

Figure S38. Cell viability after cultivation for 48 h of L929 cells in different concentrated (10^{-1} mol × L^{-1}; 10^{-2} mol × L^{-1}; 10^{-3} mol × L^{-1}; 10^{-4} mol × L^{-1}) CHIL solutions (**A** GMIM-NTf_2; **B** EMIM-I; **C** EMIM-NTf_2; **D** HO-EMIM-I) in the three different biological replicates (n = 6). The mean value of the wells without cells (background fluorescence) was subtracted from the fluorescence values of the rest of the wells, and the values of treated cultures were normalized to the mean fluorescence of the control cultures.

3. Microscopic analysis - Microscopic images of L929 cells

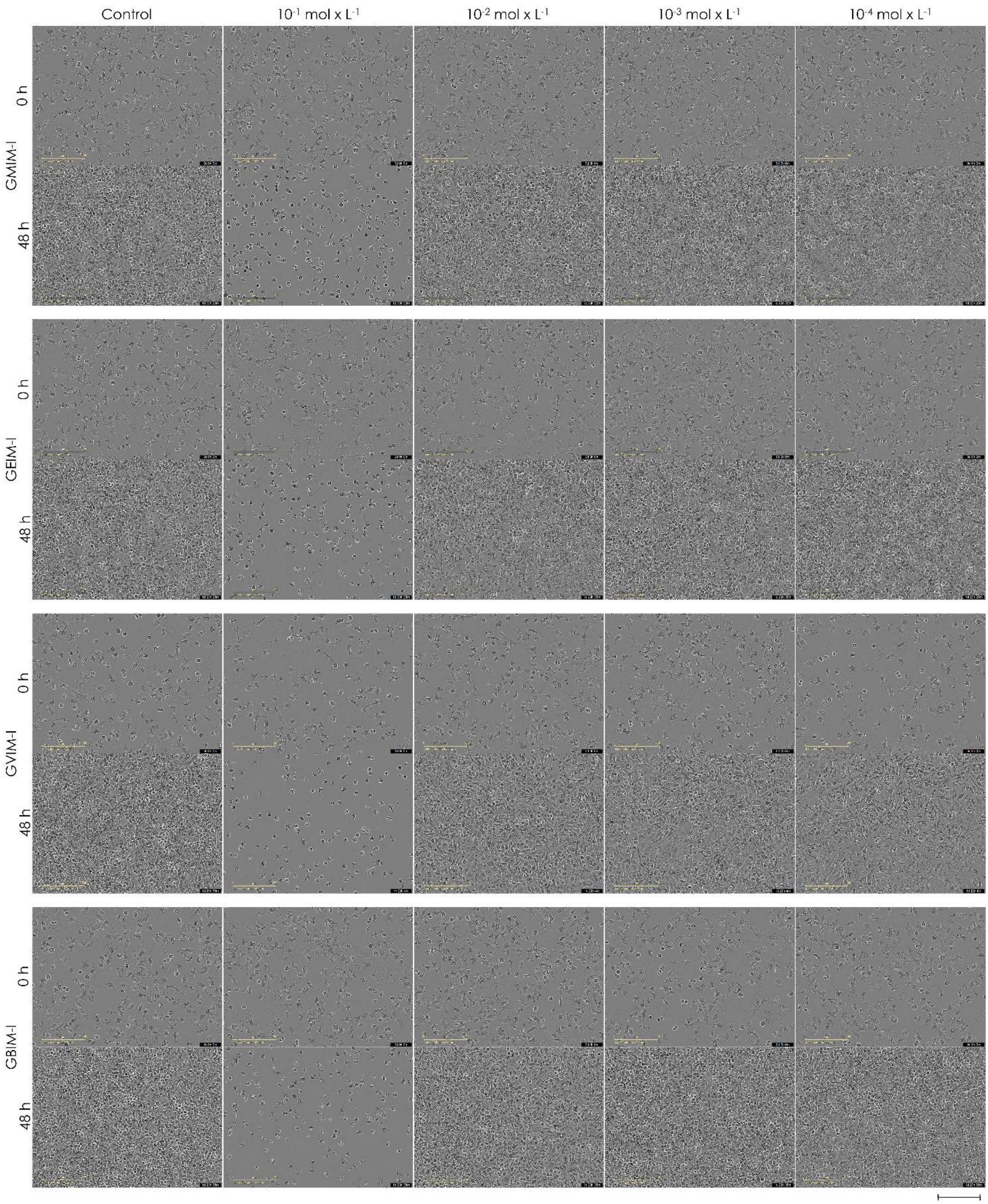

Figure S39. Microscopic brightfield images of L929 cells after 0 h and 48 h in different concentrated (10^{-1} mol × L^{-1}; 10^{-2} mol × L^{-1}; 10^{-3} mol × L^{-1}; 10^{-4} mol × L^{-1}) CHIL solutions (GMIM-I; GEIM-I; GVIM-I; GBIM-I) with variated alkyl chains. Scale bar 200 µm.

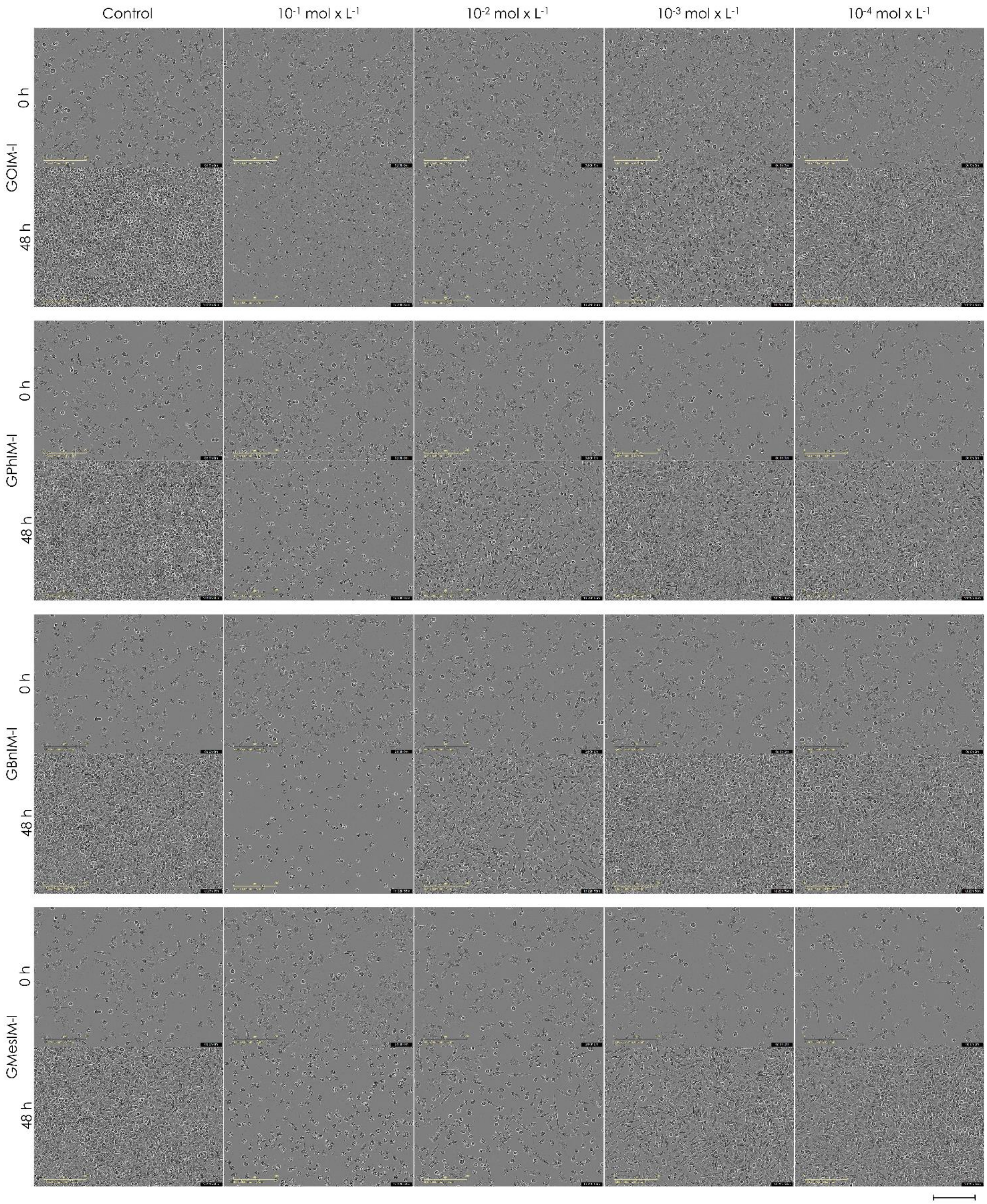

Figure S40. Microscopic brightfield images of L929 cells after 0 h and 48 h in different concentrated (10^{-1} mol × L^{-1}; 10^{-2} mol × L^{-1}; 10^{-3} mol × L^{-1}; 10^{-4} mol × L^{-1}) CHIL solutions (GOIM-I; GPhIM-I; GBnIM-I; GMesIM-I) with variated alkyl chains. Scale bar 200 µm.

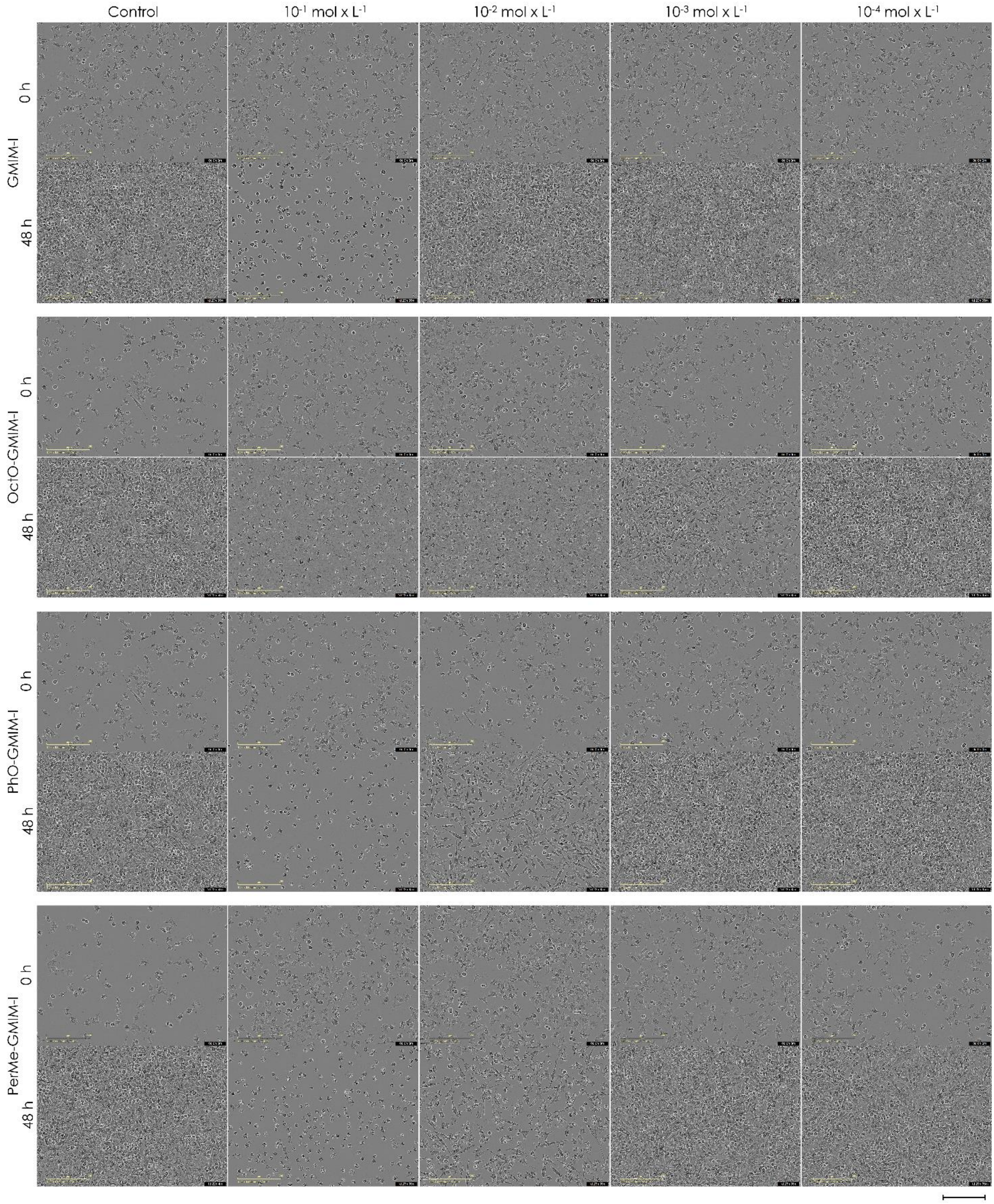

Figure S41. Microscopic images of L929 cells after 0 h and 48 h in different concentrated (10^{-1} mol × L^{-1}; 10^{-2} mol × L^{-1}; 10^{-3} mol × L^{-1}; 10^{-4} mol × L^{-1}) CHIL solutions (GMIM-I; OctO-GMIM-I; PhO-GMIM-I; PerMe-GMIM-I) with variated alkyl chains. Scale bar 200 µm.

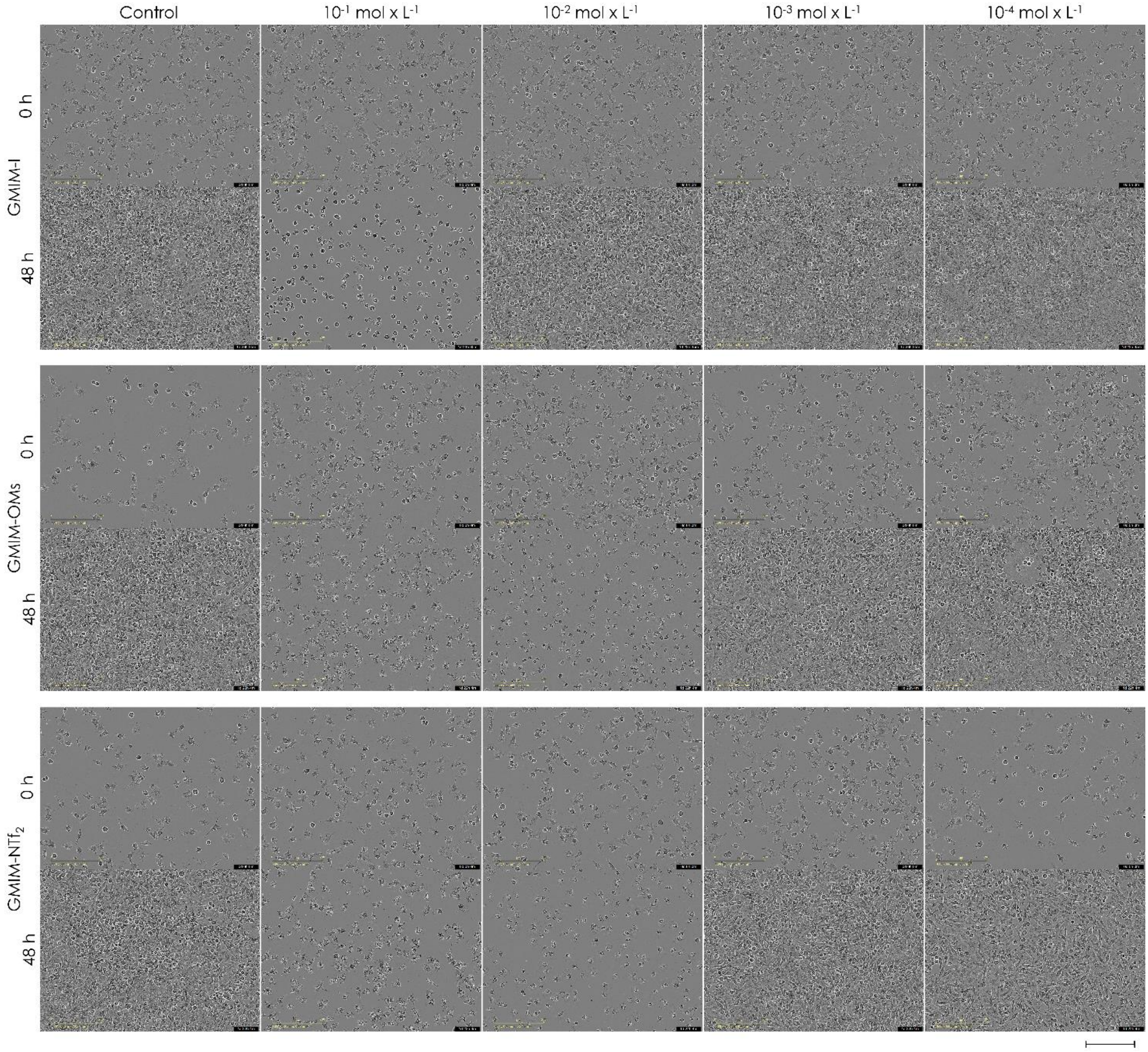

Figure S42. Microscopic images of L929 cells after 0 h and 48 h in different concentrated (10^{-1} mol × L^{-1}; 10^{-2} mol × L^{-1}; 10^{-3} mol × L^{-1}; 10^{-4} mol × L^{-1}) CHIL solutions (GMIM-I; GMIM-OMs; GMIM-NTf_2) with different counter ions. Scale bar 200 µm.

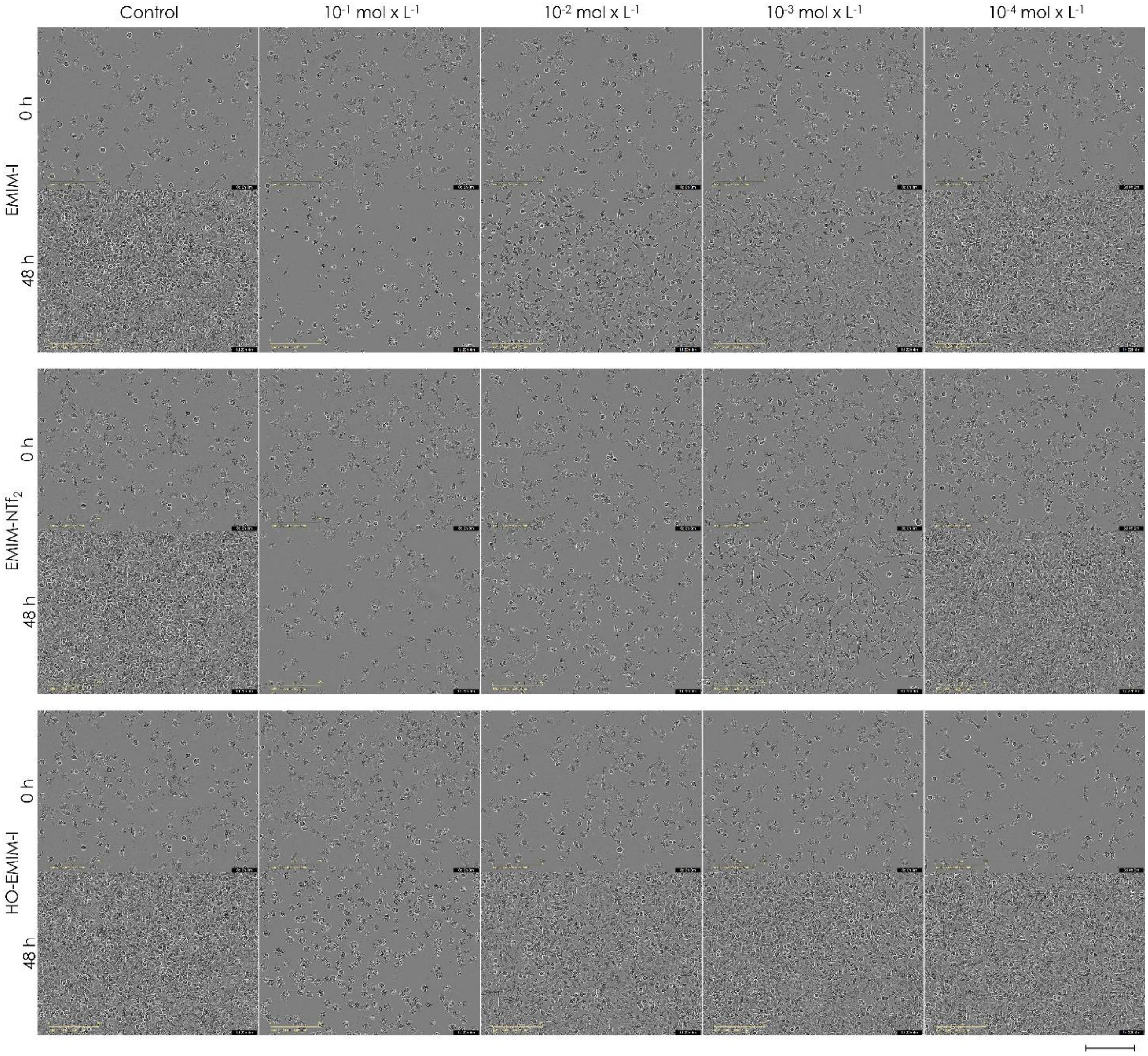

Figure S43. Microscopic images of L929 cells after 0 h and 48 h in different concentrated (10^{-1} mol × L^{-1}; 10^{-2} mol × L^{-1}; 10^{-3} mol × L^{-1}; 10^{-4} mol × L^{-1}) CHIL solutions. Scale bar 200 µm.

4. Cell staining (live/dead assay) - Calcein-AM/PI staining

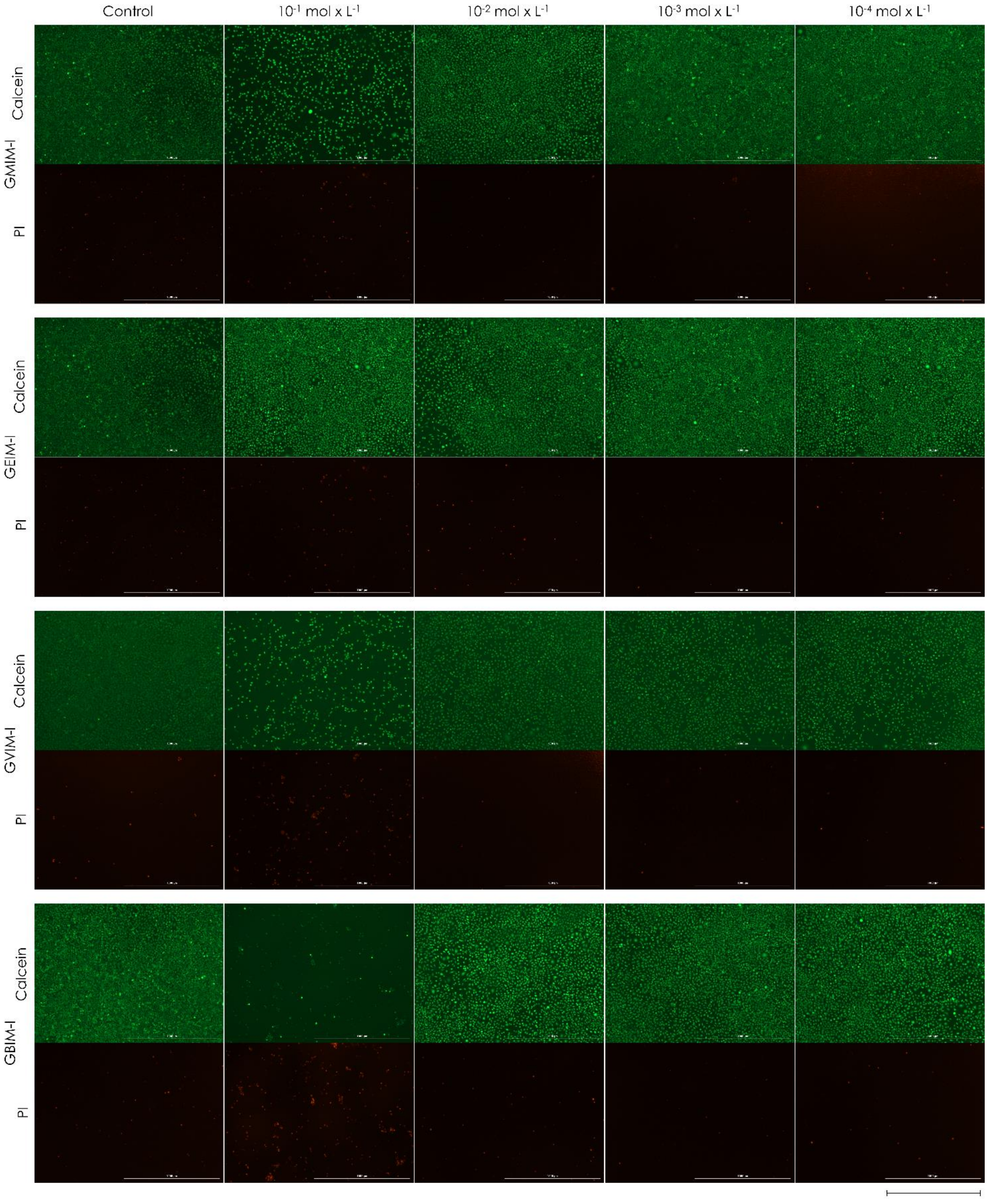

Figure S44. Calcein-AM/PI staining of L929 cells exposed for 48 h to different concentrated (10^{-1} mol × L^{-1}; 10^{-2} mol × L^{-1}; 10^{-3} mol × L^{-1}; 10^{-4} mol × L^{-1}) CHIL solutions (GMIM-I; GEIM-I; GVIM-I; GBIM-I). Scale bar 1000 µm.

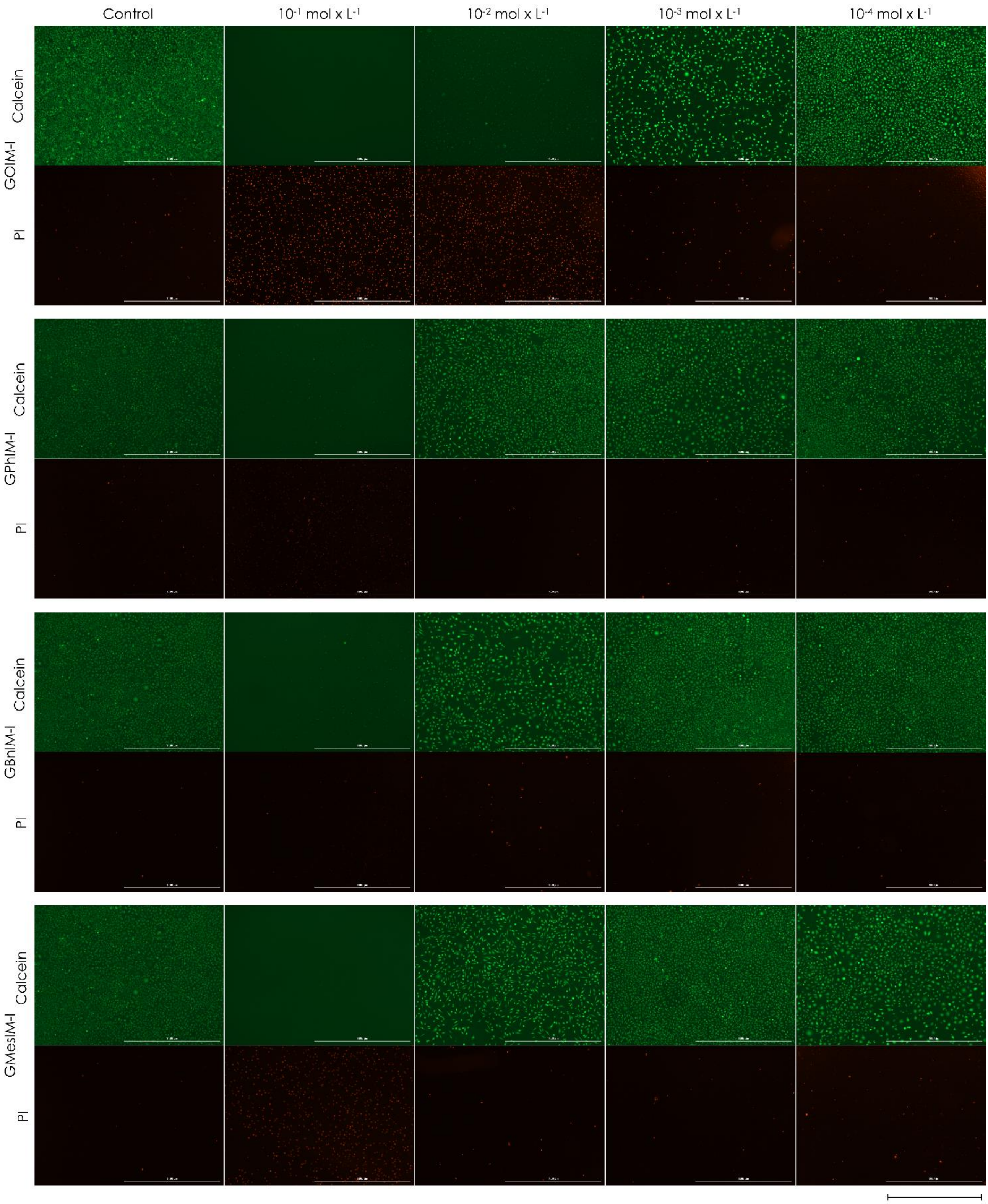

Figure S45. Calcein-AM/PI staining of L929 cells exposed for 48 h to different concentrated (10^{-1} mol × L^{-1}; 10^{-2} mol × L^{-1}; 10^{-3} mol × L^{-1}; 10^{-4} mol × L^{-1}) CHIL solutions (GOIM-I; GPhIM-I; GBnIM-I; GMesIM-I). Scale bar 1000 µm.

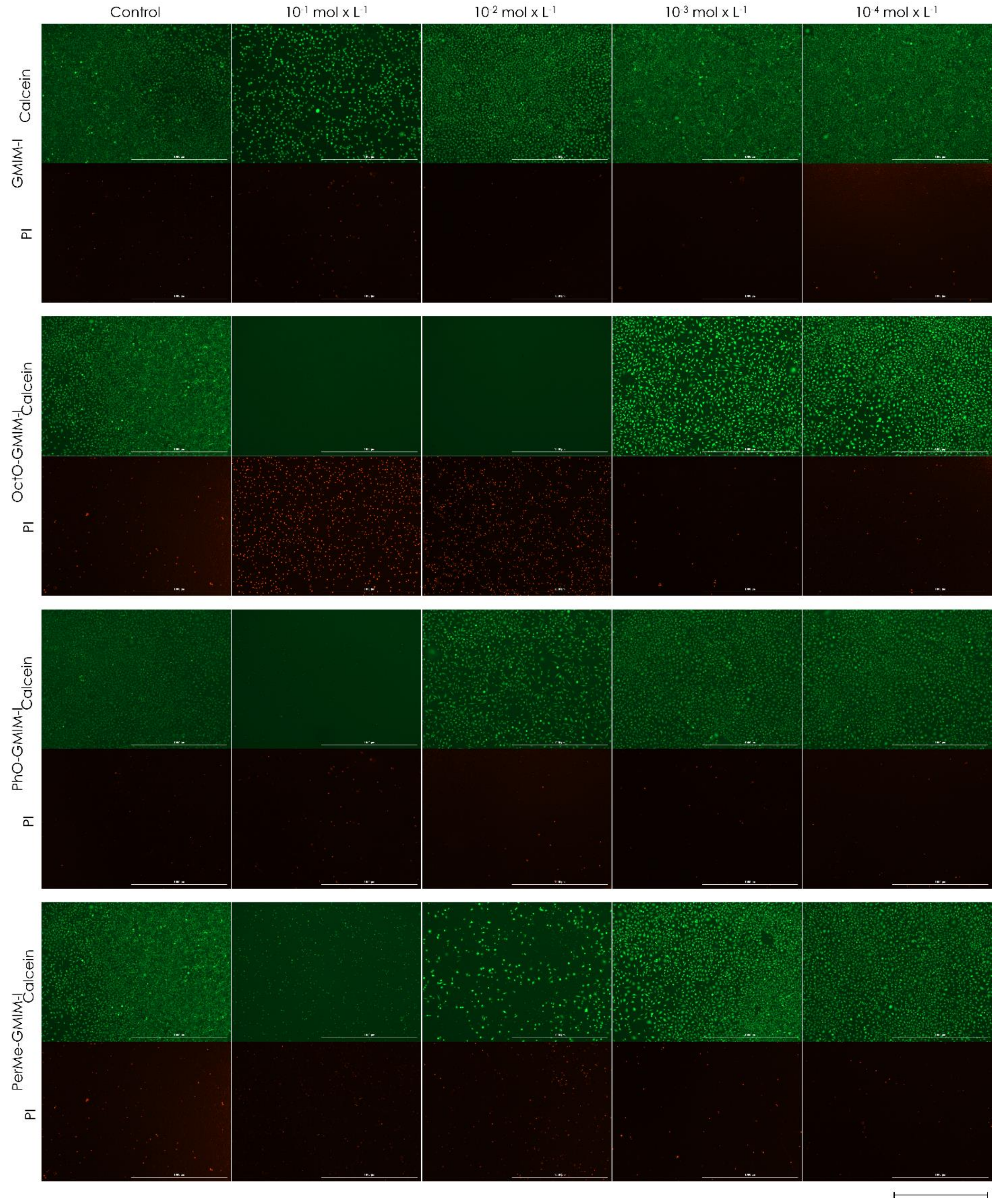

Figure S46. Calcein-AM/PI staining of L929 cells exposed for 48 h to different concentrated (10^{-1} mol × L^{-1}; 10^{-2} mol × L^{-1}; 10^{-3} mol × L^{-1}; 10^{-4} mol × L^{-1}) CHIL solutions (GMIM-I; OctO-GMIM-I; PhO-GMIM-I; PerMe-GMIM-I). Scale bar 1000 µm.

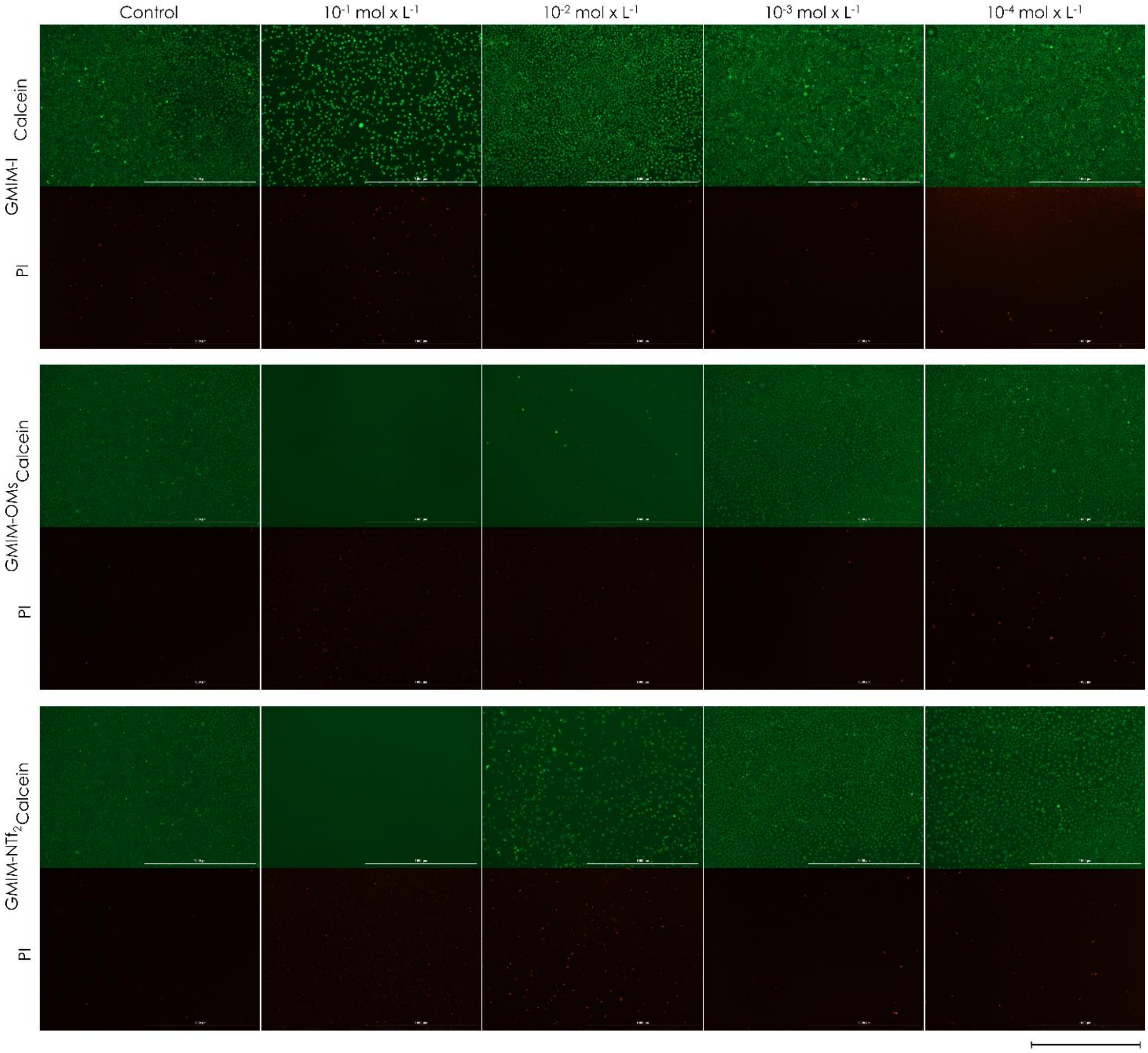

Figure S47. Calcein-AM/PI staining of L929 cells exposed for 48 h to different concentrated (10^{-1} mol × L^{-1}; 10^{-2} mol × L^{-1}; 10^{-3} mol × L^{-1}; 10^{-4} mol × L^{-1}) CHIL solutions (GMIM-I; GMIM-OMs; GMIM-NTf_2). Scale bar 1000 µm.

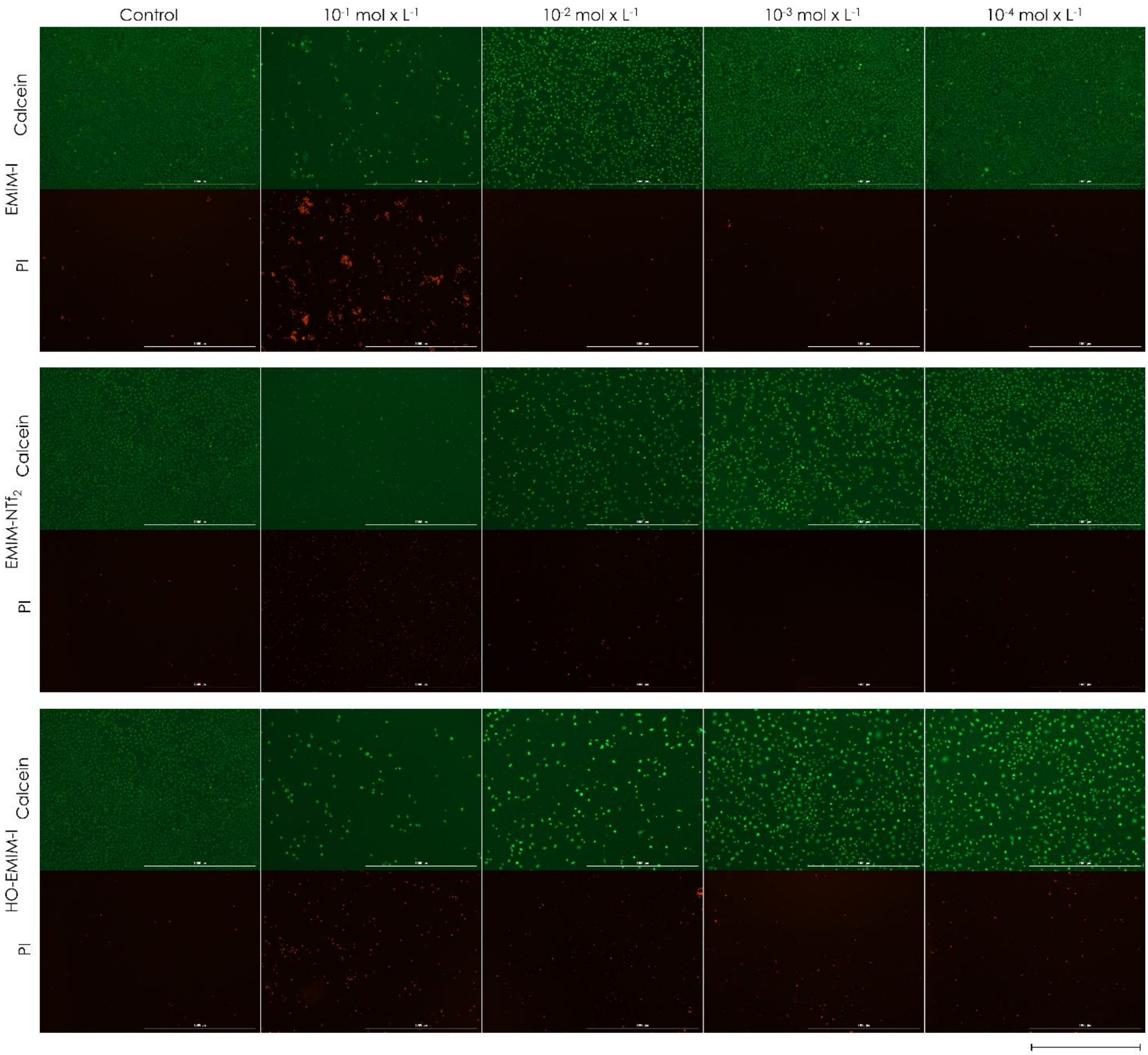

Figure S48. Calcein-AM/PI staining of L929 cells exposed for 48 h to different concentrated (10^{-1} mol × L^{-1}; 10^{-2} mol × L^{-1}; 10^{-3} mol × L^{-1}; 10^{-4} mol × L^{-1}) IL representatives (EMIM-I; EMIM-NTf_2; HO-EMIM-I). Scale bar 1000 µm.

5. Antimicrobial Activity – Disk Diffusion Method

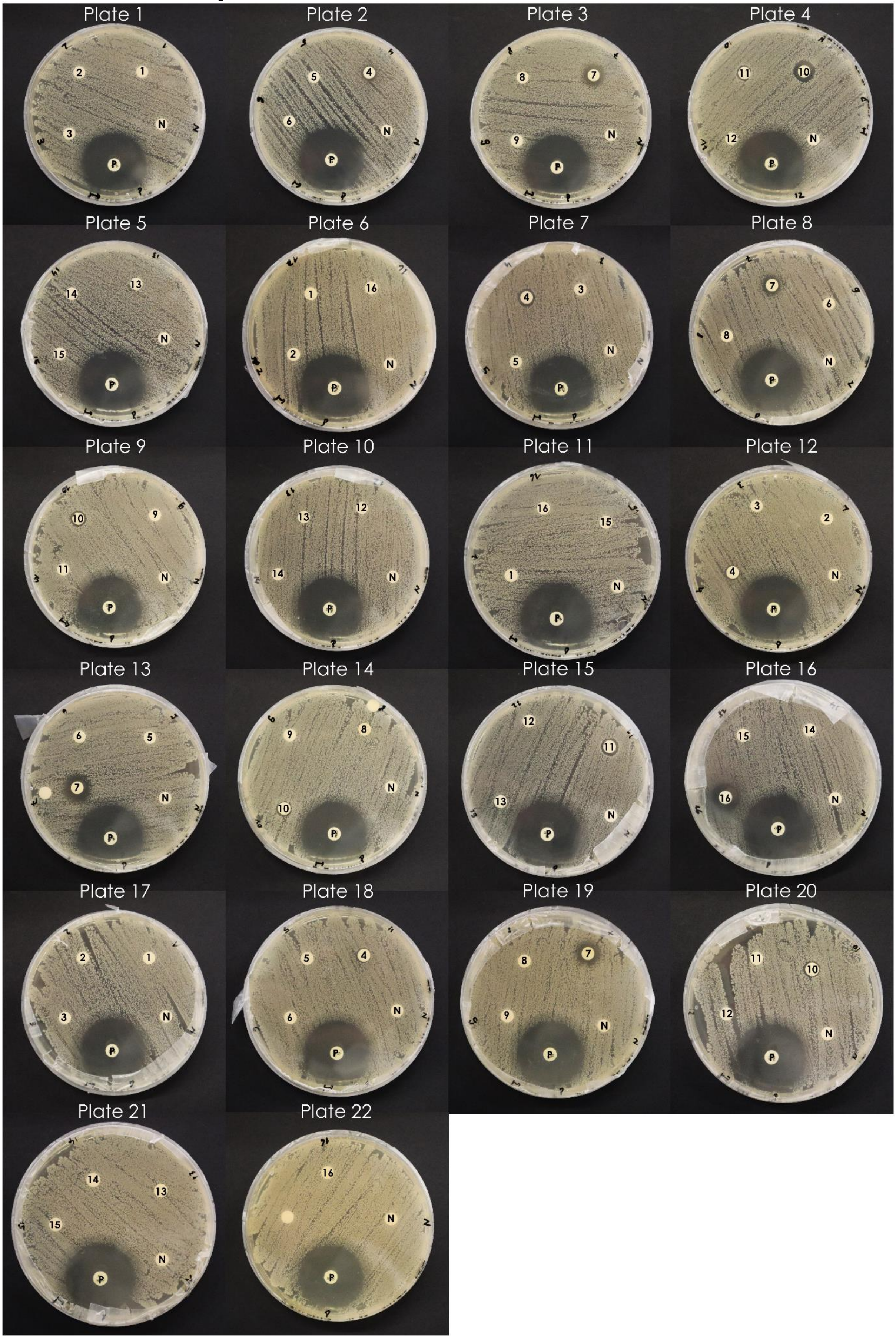

Figure S49. Overview of the disk diffusion tests against *B. subtilis* (**P** positive control Gentamicin; **N** negative control H_2O; **1** GMIM-I; **2** GEIM-I; **3** GBIM-I; **4** GOIM-I; **5** GVIM-I; **6** GPhIM-I; **7** OctO-GMIM-I; **8** PhO-GMIM-I; **9** PerMe-GMIM-I; **10** GMIM-NTf_2; **11** GMIM-OMs; **12** GBnIM-I; **13** GMesIM-I; **14** EMIM-I; **15** EMIM-NTf_2 and **16** HO-EMIM-I).

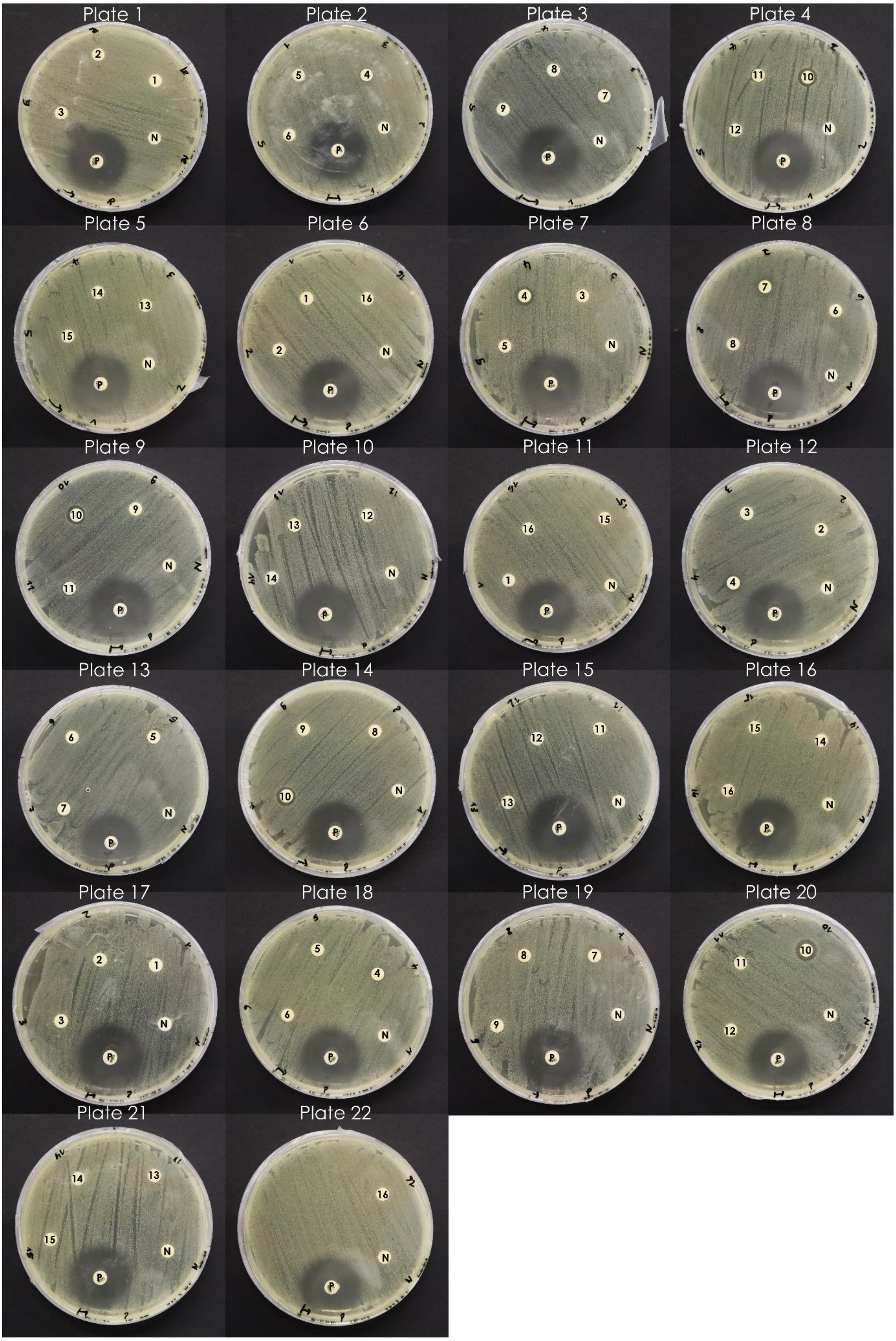

Figure S50. Overview of the disk diffusion tests against *E. coli* (**P** positive control Gentamicin; **N** negative control H_2O; **1** GMIM-I; **2** GEIM-I; **3** GBIM-I; **4** GOIM-I; **5** GVIM-I; **6** GPhIM-I; **7** OctO-GMIM-I; **8** PhO-GMIM-I; **9** PerMe-GMIM-I; **10** GMIM-NTf_2; **11** GMIM-OMs; **12** GBnIM-I; **13** GMesIM-I; **14** EMIM-I; **15** EMIM-NTf_2 and **16** HO-EMIM-I).

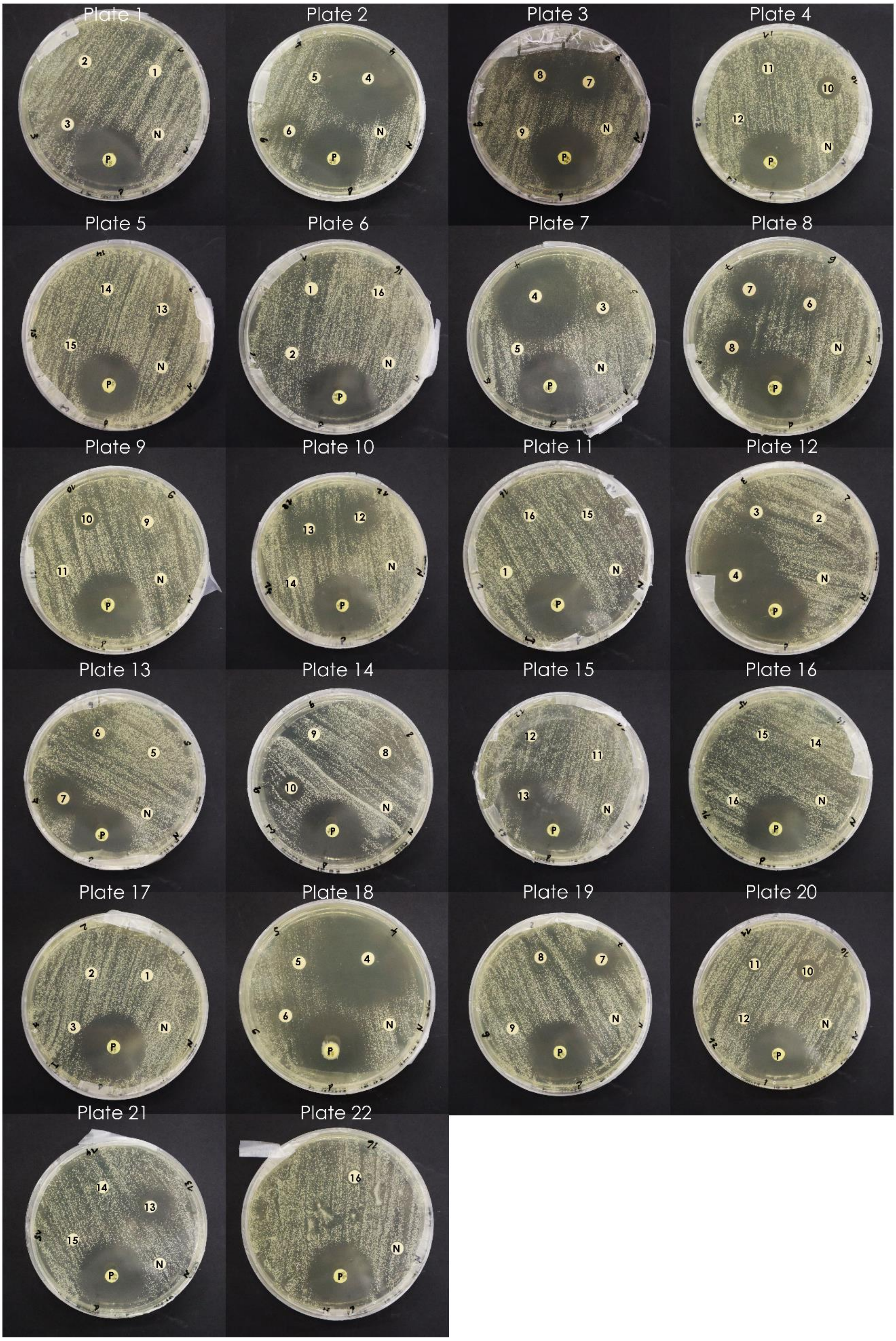

Figure S51. Overview of the disk diffusion tests against *C. auris* (**P** positive control Gentamicin; **N** negative control H_2O; **1** GMIM-I; **2** GEIM-I; **3** GBIM-I; **4** GOIM-I; **5** GVIM-I; **6** GPhIM-I; **7** OctO-GMIM-I; **8** PhO-GMIM-I; **9** PerMe-GMIM-I; **10** GMIM-NTf_2; **11** GMIM-OMs; **12** GBnIM-I; **13** GMesIM-I; **14** EMIM-I; **15** EMIM-NTf_2 and **16** HO-EMIM-I).

6. SEM-EDX of GMIM-OMs 4a and GMIM-NTf$_2$ 4b

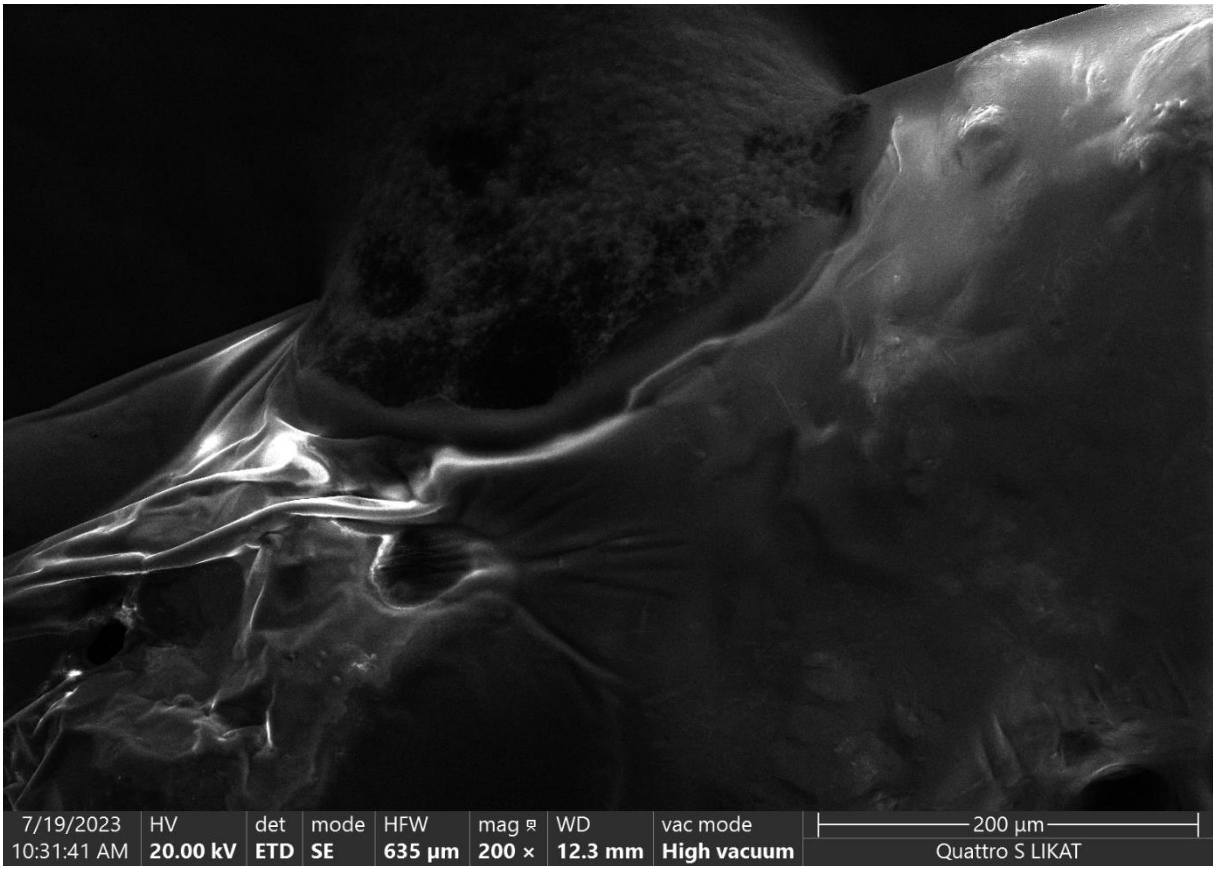

Figure S52. First SEM image of GMIM-OMs **4a**.

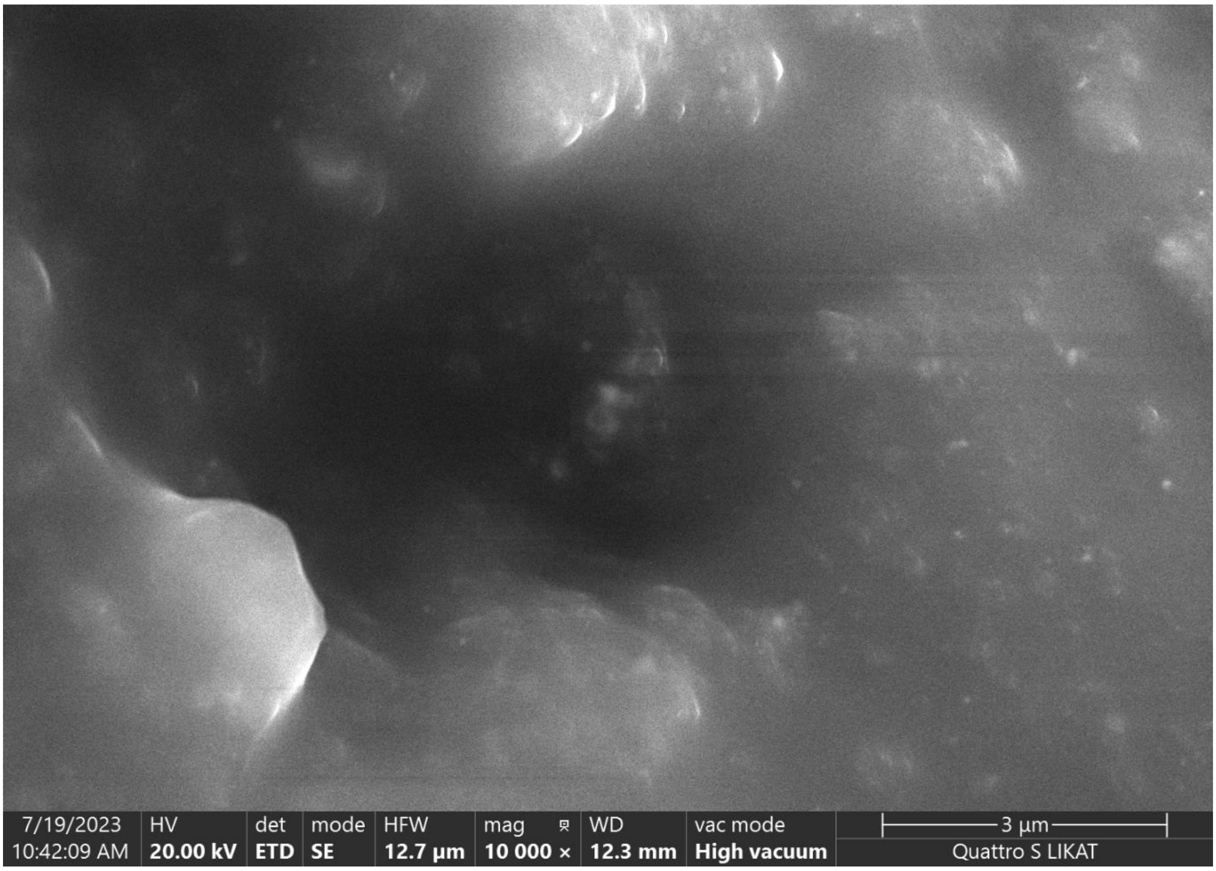

Figure S53. Second SEM image of GMIM-OMs **4a**.

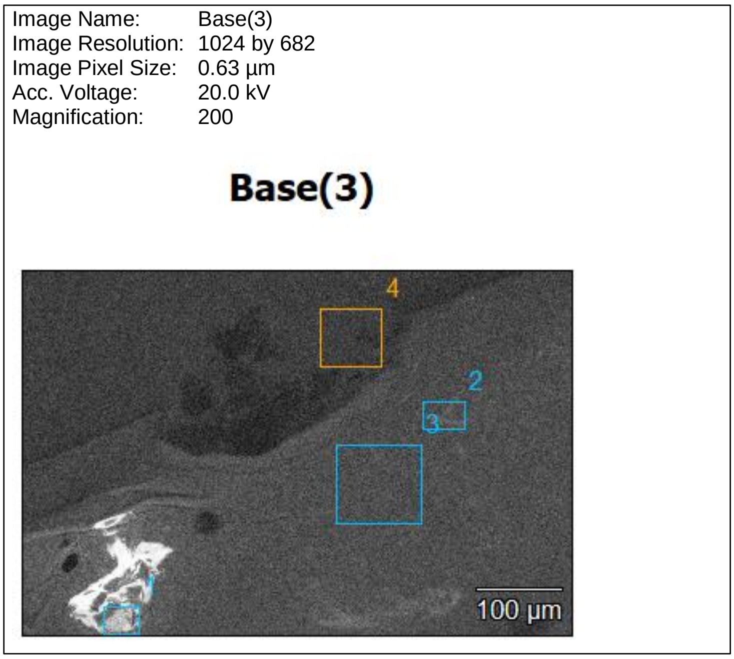
Image Name: Base(3)
Image Resolution: 1024 by 682
Image Pixel Size: 0.63 µm
Acc. Voltage: 20.0 kV
Magnification: 200
Base(3)
4
2
3
100 µm

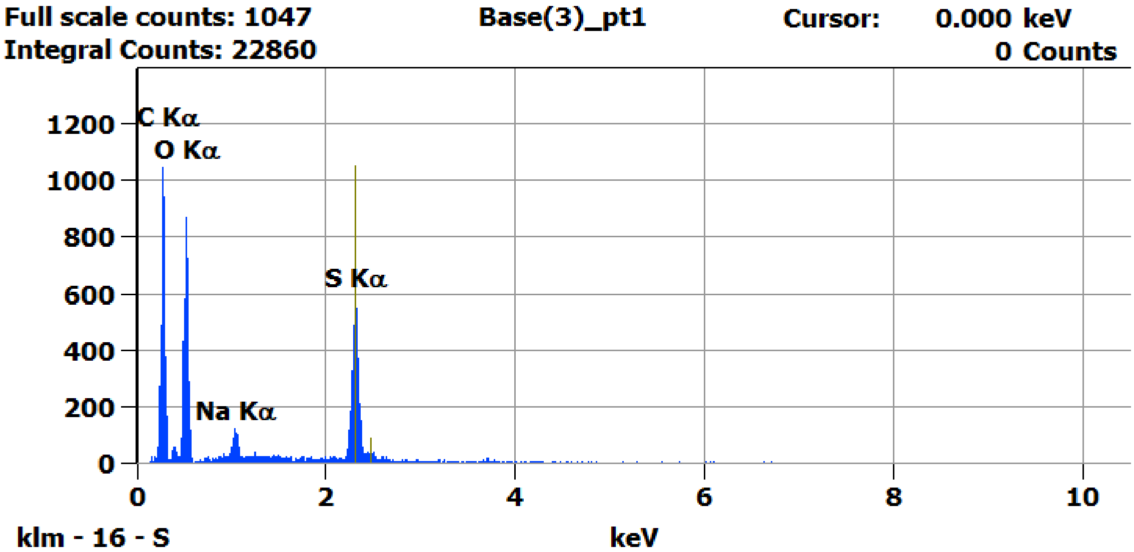
Full scale counts: 1047
Integral Counts: 22860
Base(3)_pt1
Cursor: 0.000 keV
0 Counts
C Kα
O Kα
S Kα
Na Kα
klm - 16 - S
keV

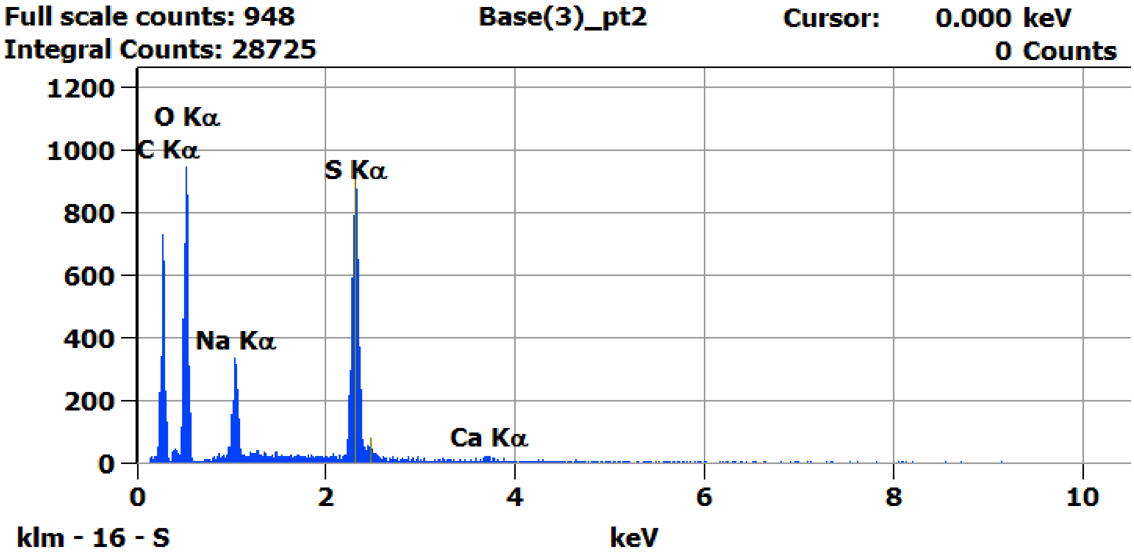
Full scale counts: 948
Integral Counts: 28725
Base(3)_pt2
Cursor: 0.000 keV
0 Counts
O Kα
C Kα
S Kα
Na Kα
Ca Kα
klm - 16 - S
keV

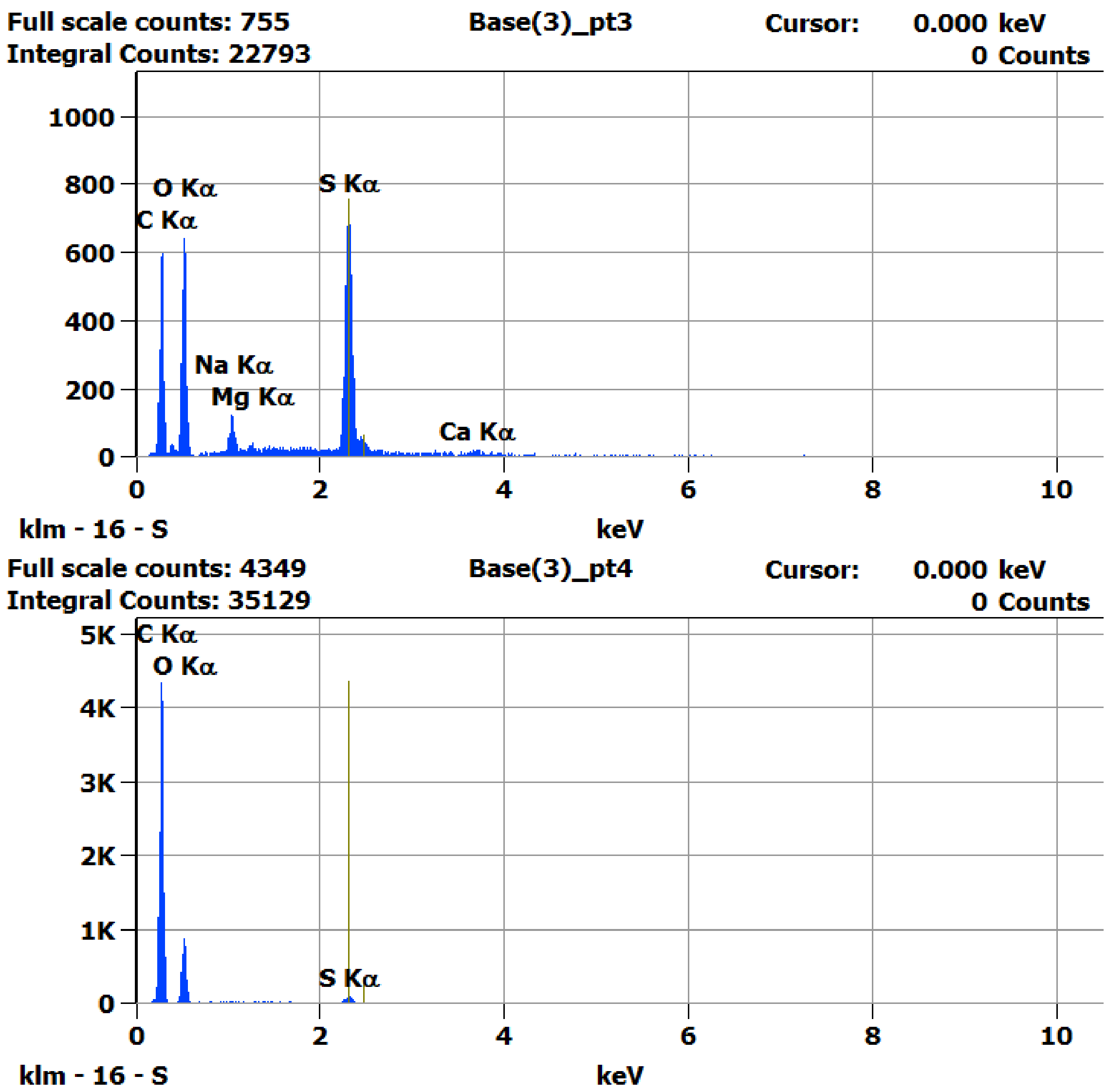

Figure S54. EDX of the first REM image of **4a** with Base(3)_pt1, Base(3)_pt2 and Base(3)_pt3 and Base(3)_pt4 showing different areas of the sample **4a**. All expected elements (C,N,O,S) are found and no silver is present. Sodium, magnesium and calcium may be present in traces in **4a** due to water as reaction solvent.

Image Name: Base(4)
Image Resolution: 1024 by 682
Image Pixel Size: 0.01 µm
Acc. Voltage: 20.0 kV
Magnification: 10000

Base(4)

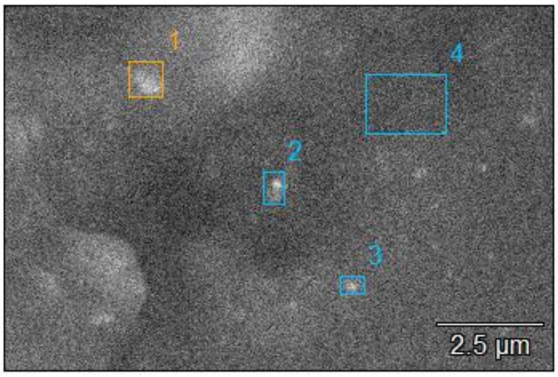

Full scale counts: 713 **Base(4)_pt1** **Cursor: 0.000 keV**
Integral Counts: 13072 **0 Counts**

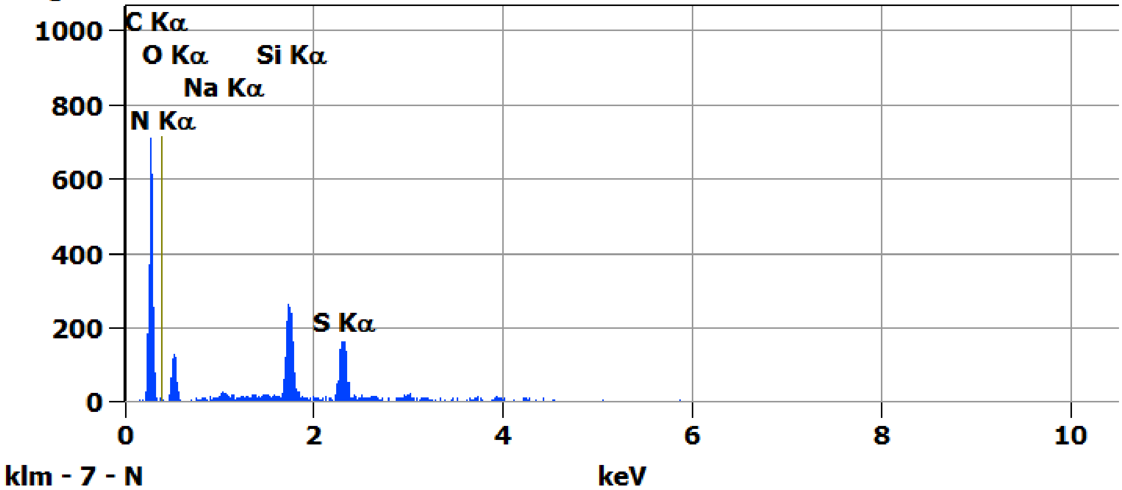

Full scale counts: 574 **Base(4)_pt2** **Cursor: 0.000 keV**
Integral Counts: 11446 **0 Counts**

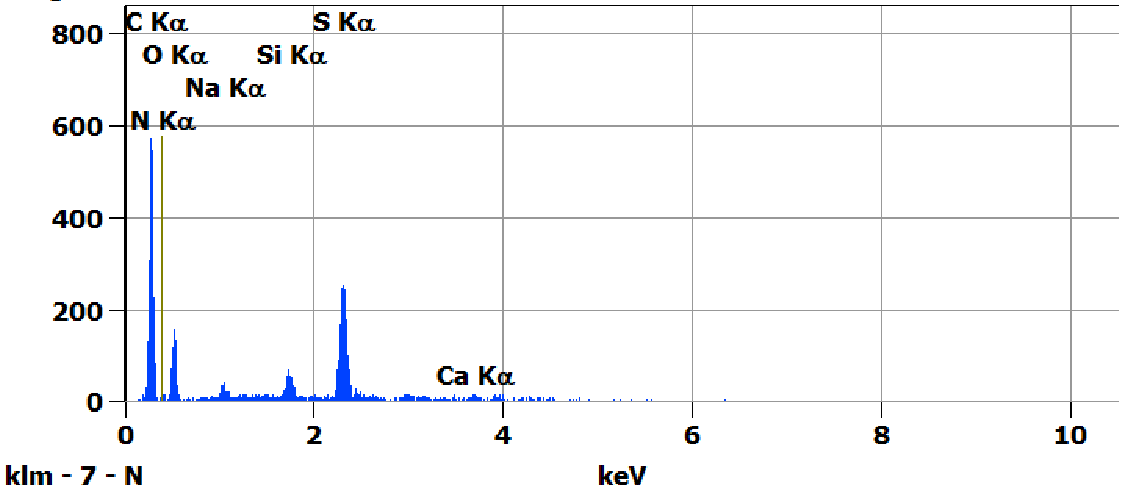

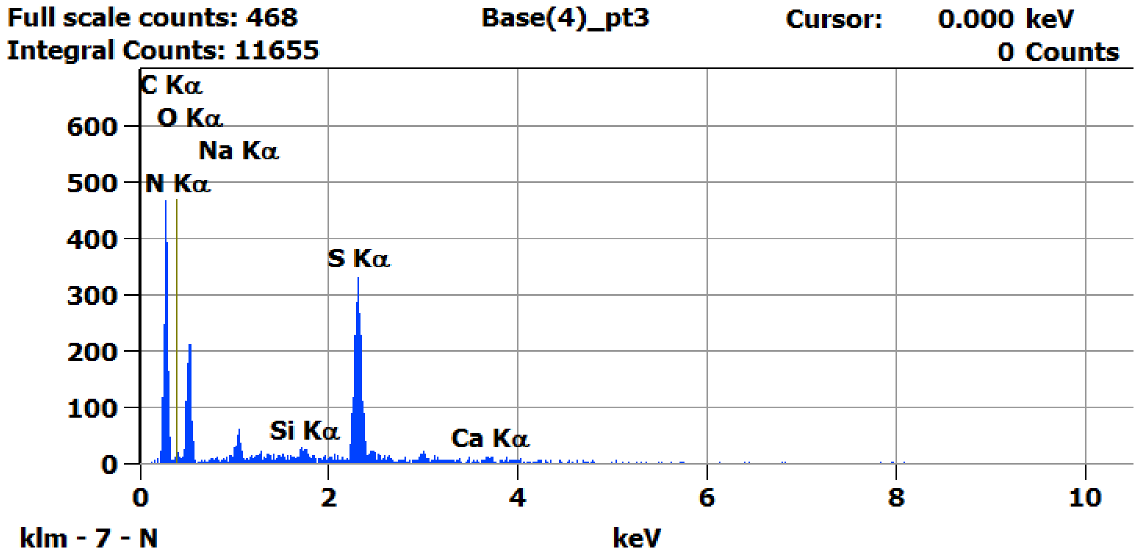

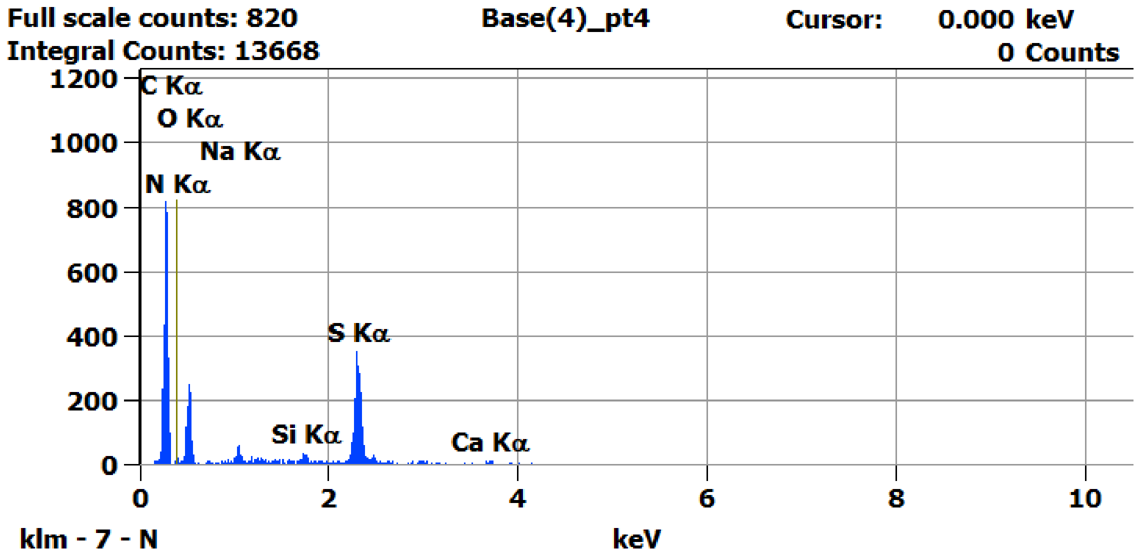

Figure S55. EDX of the second REM image of **4a** with Base(4)_pt1, Base(4)_pt2 and Base(4)_pt3 and Base(4)_pt4 showing different areas of the sample **4a**. All expected elements (C,N,O,S) are found and no silver is present. The small particles found in these areas were identified as silicon, most likely remaining from silica gel column chromatography.

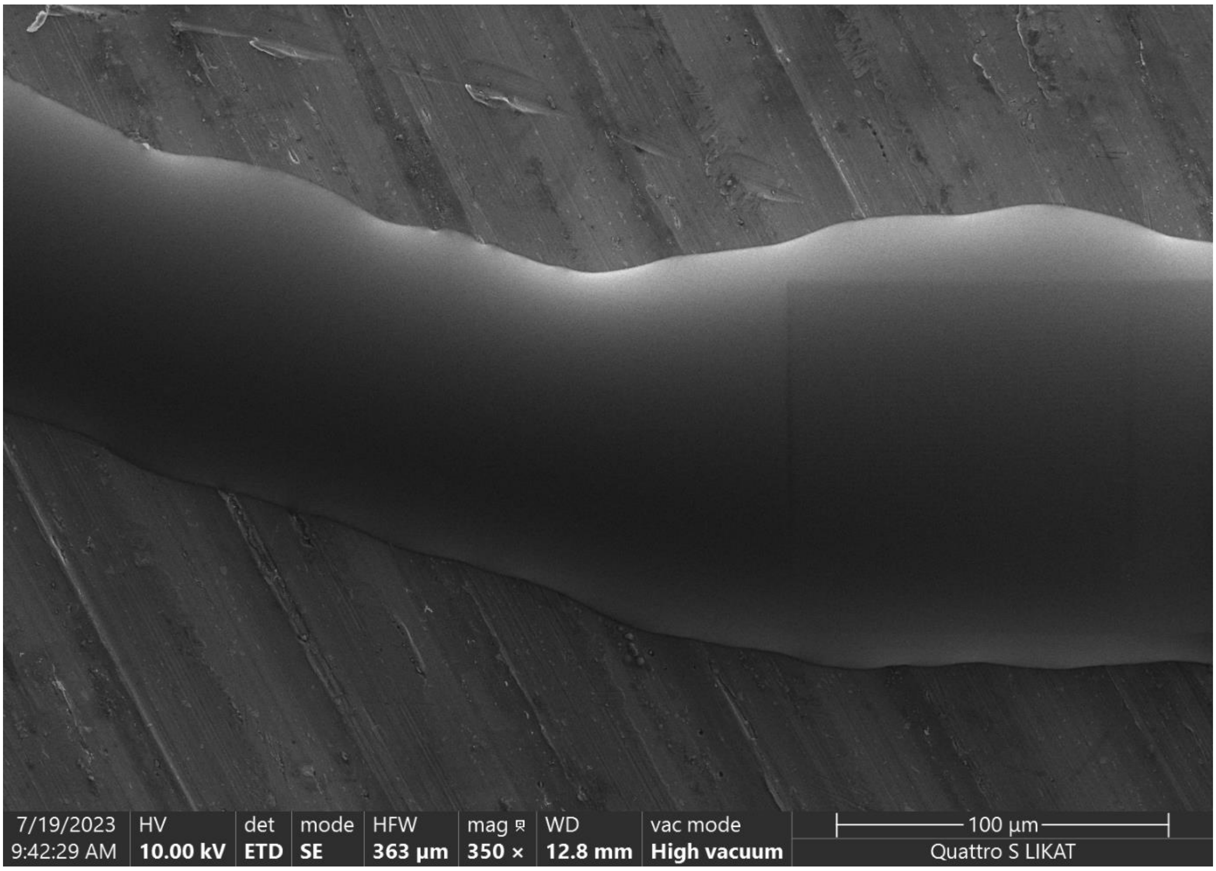

Figure S56. First SEM image of GMIM-NTf_2 **4b**.

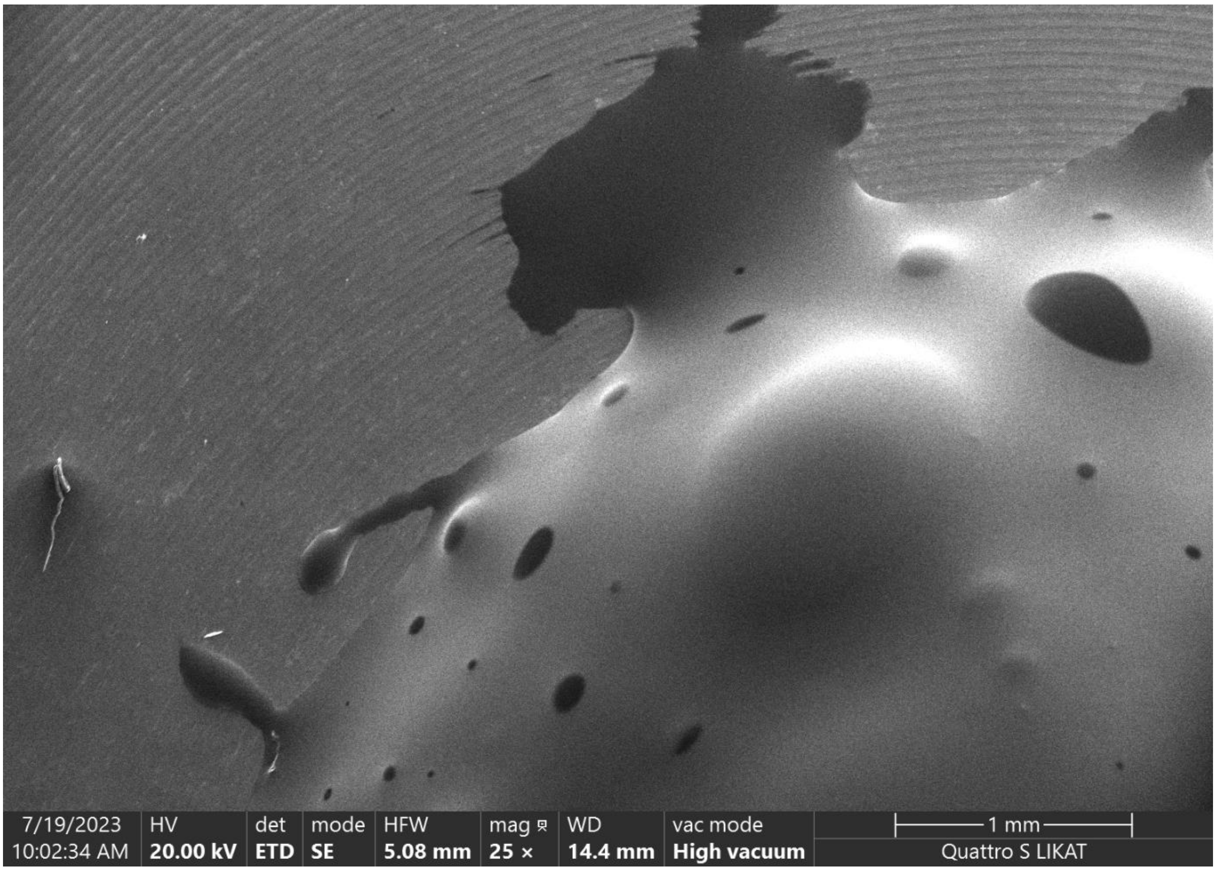

Figure S57. Second SEM image of GMIM-NTf_2 **4b**.

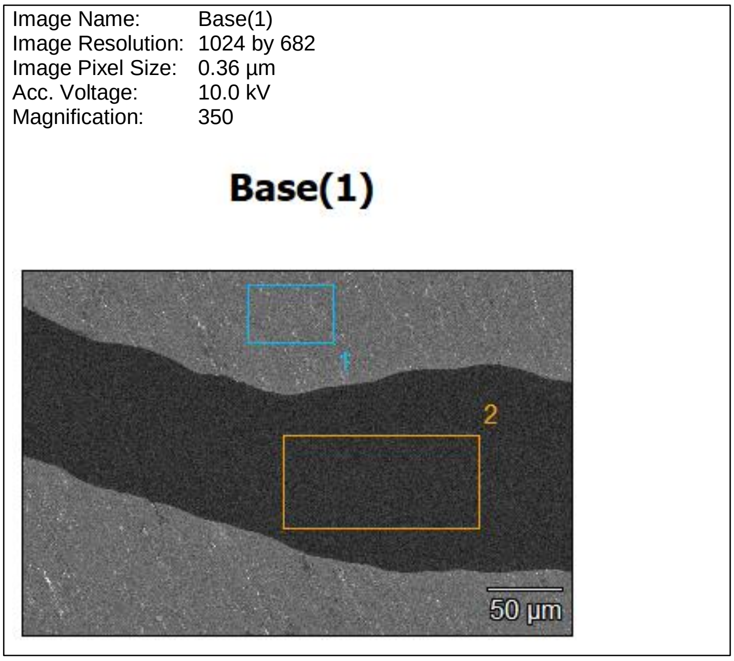

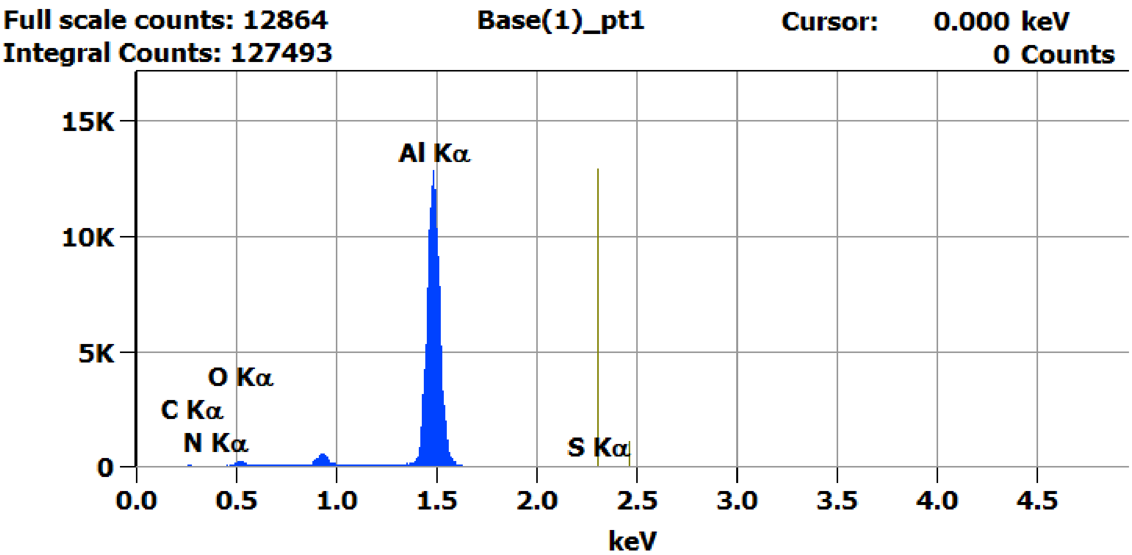

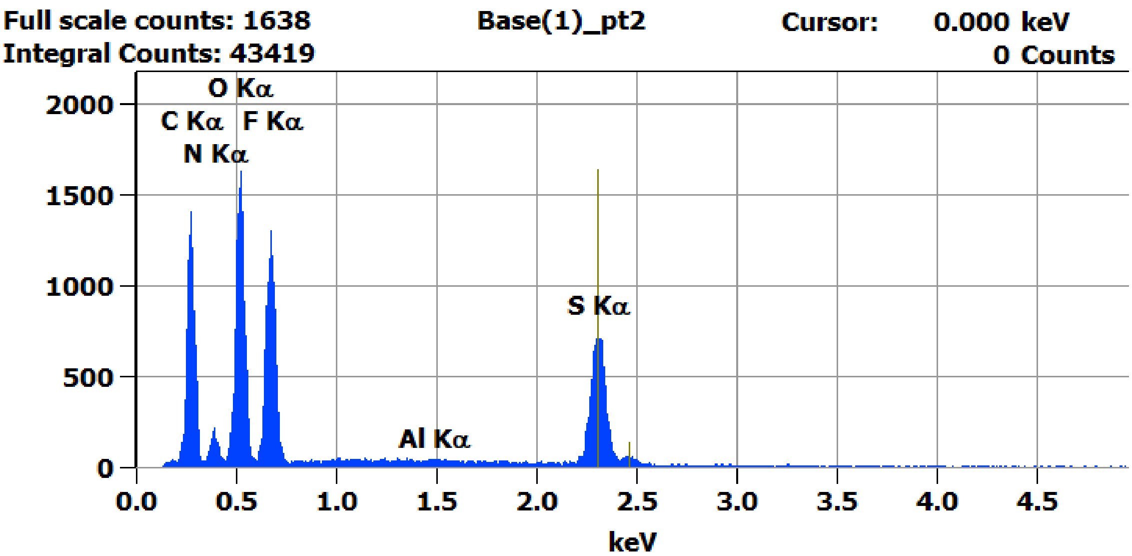

Figure S58. EDX of the first REM image of **4b** with Base(1)_pt1 showing the aluminum background and Base(1)_pt2 showing the sample **4b**. All expected elements (C,N,O,F,S) are found and no silver is present.

Image Name: Base(2)
Image Resolution: 1024 by 682
Image Pixel Size: 5.03 µm
Acc. Voltage: 20.0 kV
Magnification: 25

Base(2)

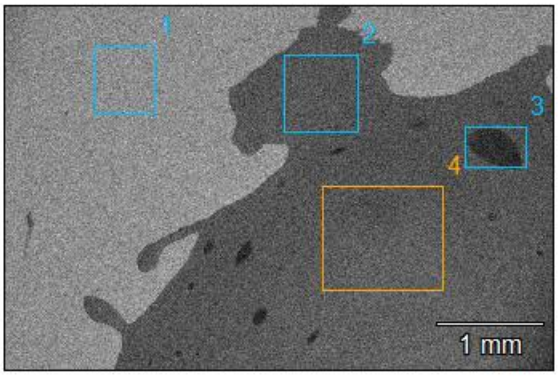

Full scale counts: 10409 **Base(2)_pt1** **Cursor: 0.000 keV**
Integral Counts: 98233 **0 Counts**

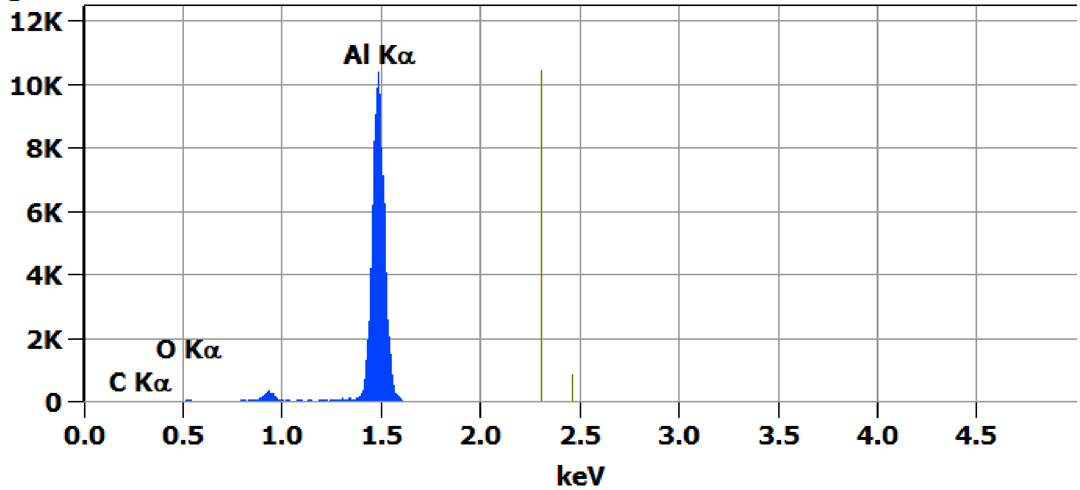

Full scale counts: 870 **Base(2)_pt2** **Cursor: 0.000 keV**
Integral Counts: 26748 **0 Counts**

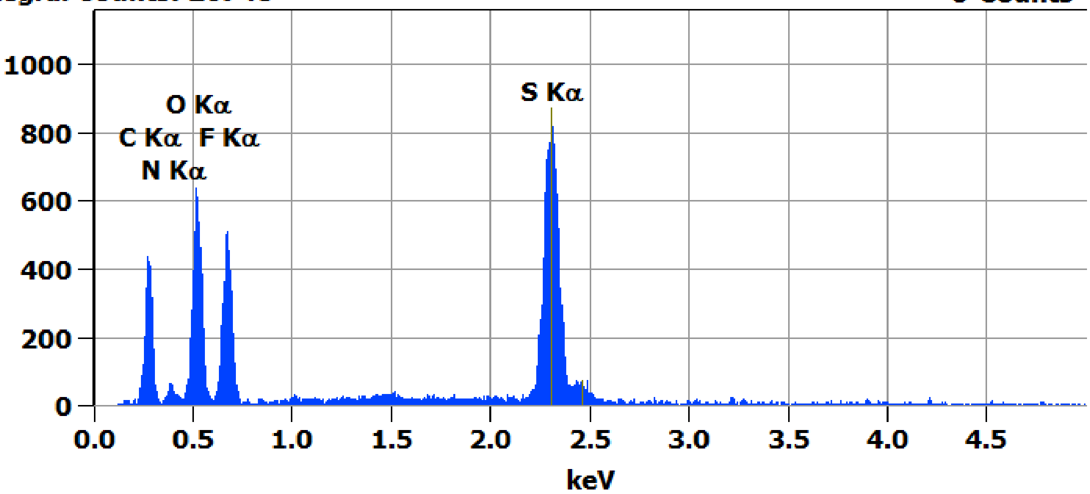

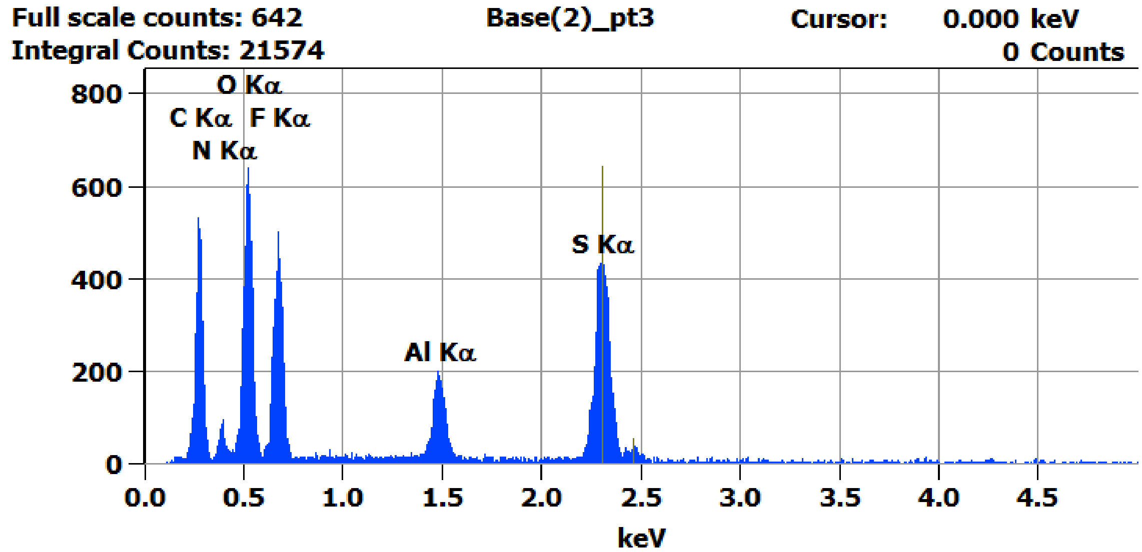

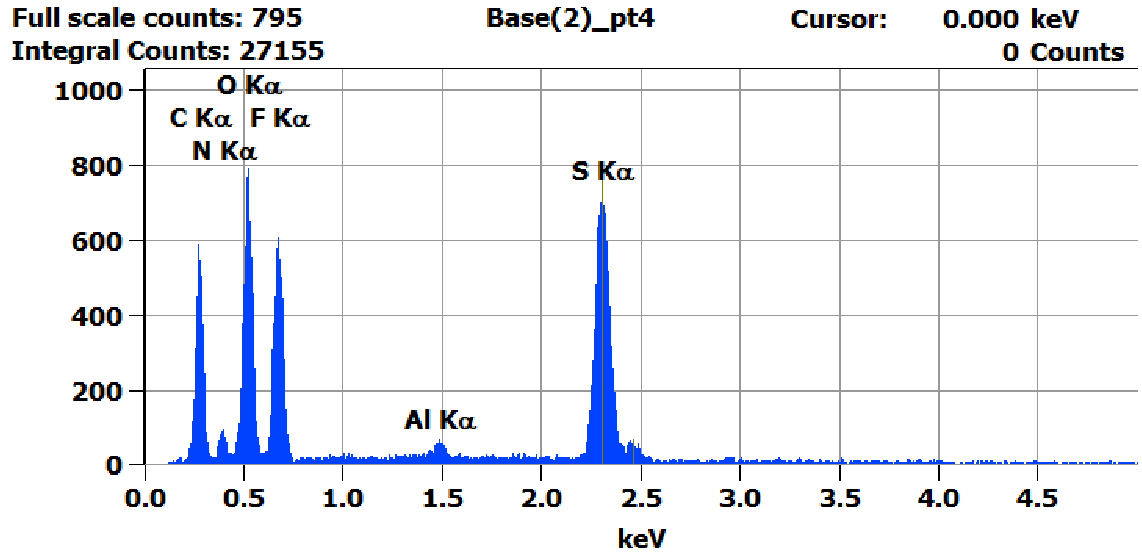

Figure S59. EDX of the second REM image of **4b** with Base(2)_pt1 showing the aluminum background and Base(2)_pt2, Base(2)_pt3 and Base(2)_pt4 showing different areas of the sample **4b**. All expected elements (C,N,O,F,S) are found and no silver is present.

7. ICP-OES of GMIM-OMs 4a and GMIM-NTf$_2$ 4b

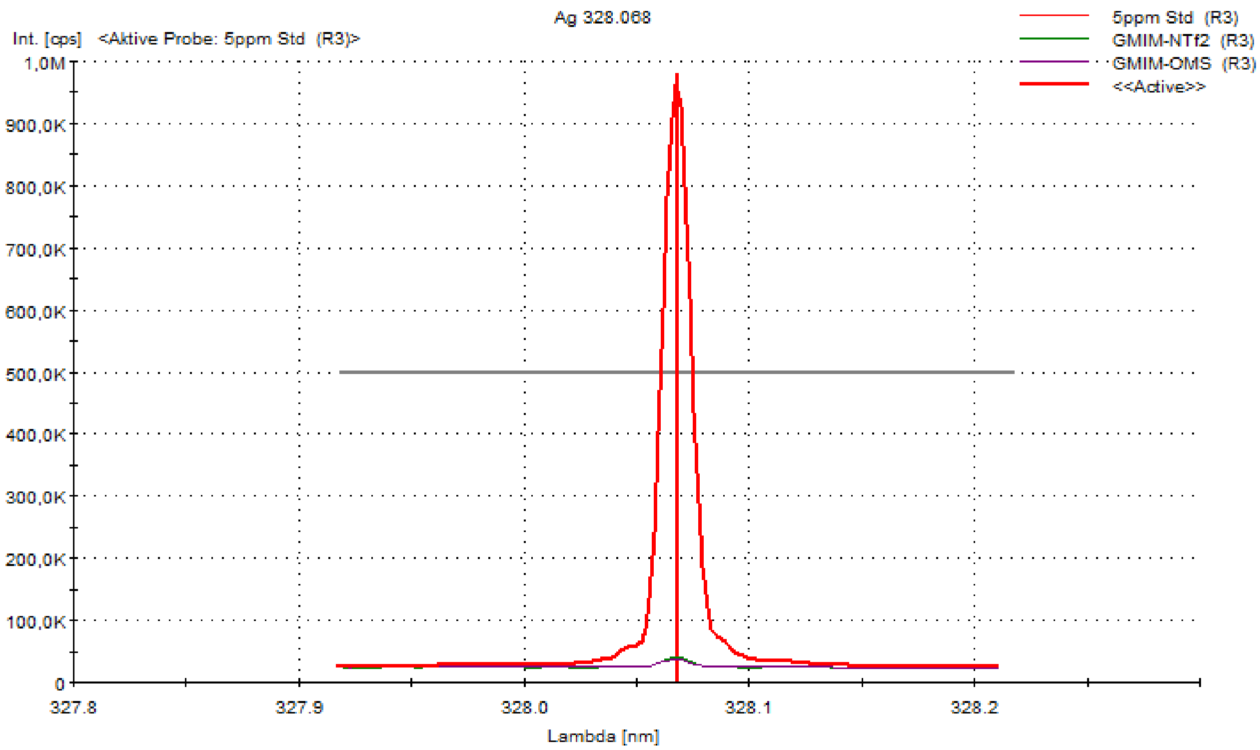

Figure S60. ICP-OES of GMIM-OMs **4a** and GMIM-NTf2 **4b** in comparison to a 5 ppm silver standard. No silver was found in these ionic liquids.